Cdc2-like kinases represent evolutionarily adapted temperature-sensors, which globally control alternative splicing and gene expression

Inaugural Dissertation

to obtain the academic degree

Doctor rerum naturalium (Dr. rer. nat)

submitted to the Department of Biology, Chemistry and Pharmacy
of Freie Universität Berlin

by

Tom Haltenhof

2019

Selbstständigkeitserklärung

Gem. § 7 Abs. 4 der Promotionsordnung basierend auf den Mitteilungen im Amtsblatt der Freien Universität Berlin Nr. 52/2007 vom 04.09.2007 und Nr. 04/2008 vom 07.02.2008 und Nr. 02/2012 vom 18.02. 2012.

Hierdurch versichere ich, dass ich die vorliegende Dissertation selbstständig und ohne unerlaubte Hilfe angefertigt habe.

Hierdurch versichere ich, dass meine Dissertation nicht auf meiner Masterarbeit aufbaut bzw. nicht daraus erwachsen ist.

Hierdurch versichere ich, dass ich meine Dissertation im Einvernehmen mit meinem Betreuer Prof. Dr. Florian Heyd in Teilen veröffentlicht habe. Die Publikationen sind Bestandteil der kumulativen Dissertation.

Declaration

This work was carried out in the period between September 2015 and September 2019 under the supervision of Prof. Dr. Florian Heyd at the Institute of Chemistry and Biochemistry, Freie Universität Berlin, Germany.

First reviewer:

Prof. Dr. Florian Heyd
RNA Biochemistry
Institute for Chemistry and Biochemistry
Freie Universität Berlin
Takustraße 6
14195 Berlin, Germany

Second reviewer:

Prof. Sutapa Chakrabarti, Ph.D.
mRNA metabolism
Institute for Chemistry and Biochemistry
Freie Universität Berlin
Takustraße 6
14195 Berlin, Germany

Date of defense: 13.12.2019

Abstract

Alternative pre-mRNA splicing allows the generation of multiple mRNA isoforms from one precursor. Translation of these isoforms drastically increases the structural and functional space of the proteome. Besides the expansion of protein diversity, alternative splicing creates an additional layer of gene expression regulation, as it influences several steps of the mRNA maturation process. Alternative splicing is a very fast process and therefore represents an ideal mechanism for cells to quickly respond to changed internal or external conditions.

Temperature is an omnipresent external clue, influencing basically every aspect of life. The ability of organisms to sense potentially noxious temperatures is a fundamental requirement to survive. Homeothermic organisms are able to keep their core body temperature constant, which makes them resilient to even strongly fluctuating external temperatures. However, the core body temperature itself also slightly oscillates in a time of the day dependent manner.

Within this thesis we showed that these subtle core body temperature oscillations are sufficient and necessary to control time of the day dependent alternative splicing of a large and functionally related group of genes in a concerted manner. We further demonstrated that this splicing program is controlled by temperature-dependent phosphorylation of SR proteins. Overexpression and knockdown experiments suggested a role of Cdc2-like kinases (CLKs), a family of SR protein specific kinases, in the regulation of temperature-dependent SR protein phosphorylation. In in vitro kinase assays we showed that activity of human and mouse CLKs reacts extremely sensitive to temperature changes within a physiological relevant temperature range with higher activity at lower temperatures, therefore matching the in vivo phosphorylation state of SR proteins. The temperature dependence is an inherent feature of the kinase domain and is caused by slight conformational changes within the activation segment, as shown by molecular dynamics simulations and biochemical assays. Furthermore, CLK temperature dependence is specific, as activity of a member of the other family of SR protein kinases, namely SRPK1, was stable in the contemplated temperature range.

We further investigated the role of CLKs as in vivo thermometers by using RNA-sequencing and demonstrated that inhibition with the specific CLK inhibitor TG003 results in an almost complete loss of temperature-dependent alternative splicing in HEK293 cells. Additionally, temperature-dependent gene expression was markedly reduced upon CLK inhibition.

CLKs are conserved throughout eukaryotic evolution, which is why we focused on the thermo-sensing ability of CLK homologs from different species. All tested homologs

exhibited a temperature profile exactly fitting the respective living temperatures with a drop of activity at the upper limit. Furthermore, the dynamic temperature range of reptilian CLK homologs suggests a role in temperature-dependent sex determination. Lastly, we focused on a CLK homolog from *Cyanidioschyzon merolae* (LIK), a red algae inhabiting hot springs. The temperature activity optimum of the LIK kinase domain also exactly fell into the preferred living temperature of *C. merolae* with a maximum activity at 48 °C and a subsequent drop of activity at the upper temperature limit. We further sought to crystallize its kinase domain and were able to obtain a structure at 2.5 Å resolution. We identified a salt bridge, which directly contributes to heat-stability and temperature-dependent activity of the kinase, as shown by mutational analysis, in vitro kinase assays and CD spectroscopy.

In summary, this thesis offers comprehensive insights of how subtle changes in body or ambient temperatures are sensed and integrated into altered alternative splicing and gene expression programs by CLKs.

Zusammenfassung

Alternatives Spleißen von prä-mRNA führt zur Bildung mehrerer mRNA Isoformen aus einem Vorläufer. Die Translation dieser Isoformen erweitert die strukturelle und funktionelle Breite des Proteoms drastisch. Neben der Erweiterung der Protein Diversität, schafft alternatives Spleißen eine zusätliche Ebene der Genexpressionsregulation, da es diverse Prozesse der mRNA Reifung beeinflussen kann. Alternatives Spleißen ist ein sehr schneller Prozess und somit ein idealer Mechanismus der Zellen um rasch auf sich ändernde innere oder äußere Bedingungen zu reagieren.
Temperatur ist ein omnipräsenter äußerer Faktor, der jegliche Aspekte des Lebens beeinflusst. Die Fähigkeit von Organismen potentiell schädliche Temperaturen wahrzunehmen, ist eine Grundbedingung um zu überleben. Homeotherme Organismen können ihre Körpertemperatur konstant halten, womit Sie relativ belastbar gegenüber sich stark ändernden äußeren Temperaturen sind. Allerdings schwankt auch die Körpertemperatur in Abhängigkeit von der Tageszeit.

In der vorliegenden Arbeit konnten wir zeigen, dass diese Körpertemperatur-schwankungen ausreichend und notwendig sind, um tageszeitabhängiges alternatives Spleißen einer großen Gruppe von Genen, die funktionell miteinander verwandt sind, koordiniert zu kontrollieren. Weiterhin konnten wir demonstrieren, dass dies durch die temperaturabhängige Phosphorylierung von SR Proteinen kontrolliert wird. Überexpressions und *knock down* Experimente deuteten auf eine Rolle von Cdc2-like Kinasen (CLKs), einer Familie SR Protein spezifischer Kinasen, bei der Regulierung von temperaturabhängiger SR Protein Phosphorylierung hin. In in vitro Kinase *Assays* konnten wir zeigen, dass die Aktivität von aufgereinigten CLKs aus Maus und Mensch extrem sensitiv auf Temperaturänderungen in einem physiologisch relevantem Bereich reagiert und die Aktivität bei niedrigeren Temperaturen erhöht ist, was in vivo Beobachtungen entspricht. Die Temperaturabhängigkeit ist eine inhärente Eigenschaft der Kinasedomänen und ist auf konformationelle Änderungen des *Activation Segments* zurückzuführen, wie *Molecular Dynamic*s Simulationen und biochemische *Assays* zeigten. Außerdem ist die Temperaturabhängigkeit von CLKs spezifisch, da sich die Aktivität eines Mitgliedes der anderen SR Protein Kinase Familie (SRPK1) temperaturunabhägig zeigte. Weiterhin untersuchten wir die Rolle von CLKs als in vivo Thermometer mittels RNA Sequenzierung. Inhibierung der CLKs mit dem spezifischen Inhibitor TG003 führte zu einem nahezu kompletten Verlust von temperaturabhängigen alternativem Spleißen in HEK293 Zellen. Außerdem verringerte sich temperaturabhängige Genexpression deutlich bei Inhibierung der CLKs.

CLKs sind in der eukaryotischen Evolution durchweg konserviert, weshalb wir uns auf die Thermometer Funktion von CLK Homologen aus anderen Spezies konzentrierten. Alle getesteten Homologe zeigten dabei ein Temperaturaktivität-sprofil, welches exakt in die entsprechenden Lebenstemperaturen fällt und am oberen Ende dieser Temperaturebereiche abfällt. Außerdem schlägt der dynamische Temperaturbereich von CLK Homologen aus Reptilien eine Beteiligung bei der temperaturabhängigen Geschlechtsbestimmung vor.
Schließlich fokussierten wir uns auf ein CLK Homolog aus *Cyanidioschyzon merolae*, einer Alge die heiße Quellen besiedelt. Das Temperaturoptimum der Aktivität der LIK Kinasedomäne zeigte sich genau in der bevorzugten Lebenstemperatur von *C. merolae* mit einer maximalen Aktivität bei 48 °C und einem Aktivitätsabfall am oberen Ende des Temperaturelimits. Des Weiteren versuchten wir die Kinasedomäne zu kristallisieren und erhielten einer Struktur mit einer Auflösung von 2,5 Å. Wir identifizierten eine einzigartige Salzbrücke und konnten mittels Mutationsanalyse, in vitro Kinase *Assays* und CD Spektroskopie zeigen, dass diese Salzbrücke direkt an der Hitzestabilität und temperaturabhängiger Aktivität beteiligt ist.

Zusammengefasst bietet die vorliegende Arbeit umfassende Einblicke wie feine Änderungen der Körper- oder Umgebungstemperatur aufgenommen und in veränderte alternative Spleiß- und Genexpressionsprogramme integriert werden.

Acknowledgements

First of it all I would like to thank Prof. Dr. Florian Heyd for giving me the opportunity to work in his group, for this interesting project and especially for his encouragement, support and time.

I thank Prof. Dr. Sutapa Chakrabarti not only for doing the second review, but also for expert advice and discussions on protein biochemistry.

A special thanks goes to all collaboration partners, without whom this work would not have been possible: Prof. Dr. Petra Imhof for performing MD simulations, Dr. Christoph Weise for performing mass spectrometry and Dr. Bernd Timmermann for RNA sequencing.

All members of the Wahl lab and the Chakrabarti lab are kindly acknowledged for help and support regarding protein biochemistry experiments as well as generously providing equipment. Particularly, I would like to thank Dr. Bernhard Loll for his expertise and for many sociable evenings with an occasional afterwork beer.

The former and current members of the Heyd group deserve a huge thank you. A nice working atmosphere is mostly based on nice people. I especially thank Danny Danger, Axel, Deichwart, S. Ucker, Lachs Gretchen, GiGi and Knuckle Dackel for all the beers, discussions, table tennis, chess, football matches and legendary evenings. Furthermore, I had the luck to get the support of very skilled students, Ana, Samira and Patricia, who largely contributed to the progress of this work.

A special thanks goes to my friends Felix, Martin and Toschi. Conversations about everything but science was a welcome change from time to time. I furthermore thank the guys from Leipzig, who made me feel like coming home every single time – Paul, Adri, Carsten, Annika, Christian, Marco, Romy, Philipp, Pia and Johannes.

I cannot put into words how grateful I am to Magdalena. You were able to stand my emotional rollercoaster and supported me in any situation, no matter how difficult. It is not an exaggeration to say that this would not have been possible without you. M.

Last but not least, I thank my family - for everything!

Table of contents

List of Publications

1. Marco Preußner, Gesine Goldammer, Alexander Neumann, **Tom Haltenhof**, Pia Rautenstrauch, Michaela Müller-McNicoll, and Florian Heyd (2017). Body Temperature Cycles Control Rhythmic Alternative Splicing in Mammals. Mol Cell. 3;67(3):433-446.

   TH performed Western Blots for temperature-dependent SR protein phosphorylation and SR protein expression, overexpression and knockdown experiments with CLK1 and CLK4 and respective radioactive RT-PCRs. TH performed UV-Crosslink with SRSF2.

2. **Tom Haltenhof**, Ana Kotte, Francesca De Bortoli, Samira Schiefer, Stefan Meinke, Ann-Kathrin Emmerichs, Kristina Katrin Petermann, Bernd Timmermann, Andreas Franz, Markus C. Wahl, Petra Imhof, Marco Preußner and Florian Heyd. A conserved kinase-based body temperature sensor globally controls alternative splicing and gene expression. In review (Mol Cell).

   TH cloned and expressed all proteins together with AK. TH designed and cloned all mutants. TH established in vitro kinase assays and performed CD-spectroscopy. TH performed overexpression experiments in cell culture and did the respective radioactive, splice sensitive RT-PCRs and/or Western Blots. TH validated RNA sequencing results. TH supervised the master thesis of SS which led to figure 6 and S7, respectively. TH conceived the study together with MP and FH, analyzed the data and co-wrote the manuscript.

1. Introduction

1.1. Pre-mRNA splicing

Genetic information, stored as deoxyribonucleic acid (DNA), is transformed into biological function, which is mostly performed by proteins. During the gene expression process specific DNA sequences, called genes, are transcribed into ribonucleic acids (RNA). The resulting precursor messenger RNA (pre-mRNA) undergoes several processing steps prior to translation into a protein, amongst them co-transcriptional addition of a 7-methylguanosine cap (m7G) at the 5' end of the mRNA and polyadenylation of the 3' end, both important for mRNA stability, nuclear export and translation initiation. Furthermore, non-coding regions, called introns, are excised from the pre-mRNA and protein coding exons are joined together in a process called splicing. Intron-exon boundaries are defined through a core set of splicing signals like the 5′ splice site (ss), the branch point (BP) sequence and the 3′ ss. Splicing is accomplished by two consecutive S_N2 type transesterification reactions (Figure 1.1.).

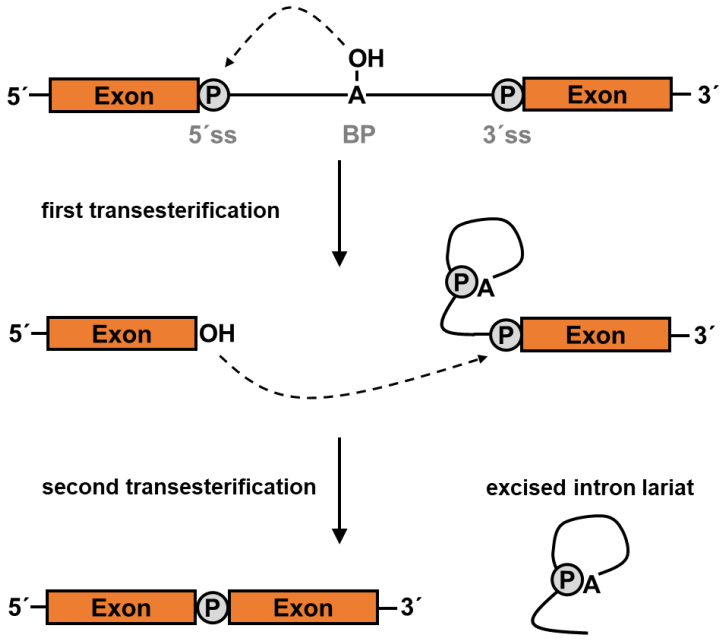

Figure 1.1.: Splicing is accomplished by two consecutive transesterification reactions. Shown are the two nucleophilic attacks (dashed arrows) that lead to the excision of the intron and joining of the two adjacent exons. Exons are depicted as orange boxes, the intron as a black line. Conserved elements important for the splicing reaction are: the 5´ and 3´ splice sites (5´ss and 3´ss) and the branch point (BP). Phosphate groups at the 5´ and 3´splice sites are illustrated as grey circles.

During the first transesterification, the 2'OH group of the branch point (BP) adenosine attacks the phosphate group at the 5' ss, generating a 2´-5´phosphodiesterbond. Subsequently, the free OH group at the 5' ss attacks the phosphodiester bond at the 3' ss resulting in the ligation of the exons and the release of the intron lariat.

In eukaryotes the splicing process is catalyzed by a large macromolecular machine, called the spliceosome. The spliceosome is made up of five small nuclear ribonucleoproteins (snRNPs) U1, U2, U5, and U4/U6 and a large set of different proteins, participating at different steps during the splicing reaction. The assembly of the spliceosome occurs in a highly dynamic and stepwise fashion (Figure 1.2.).

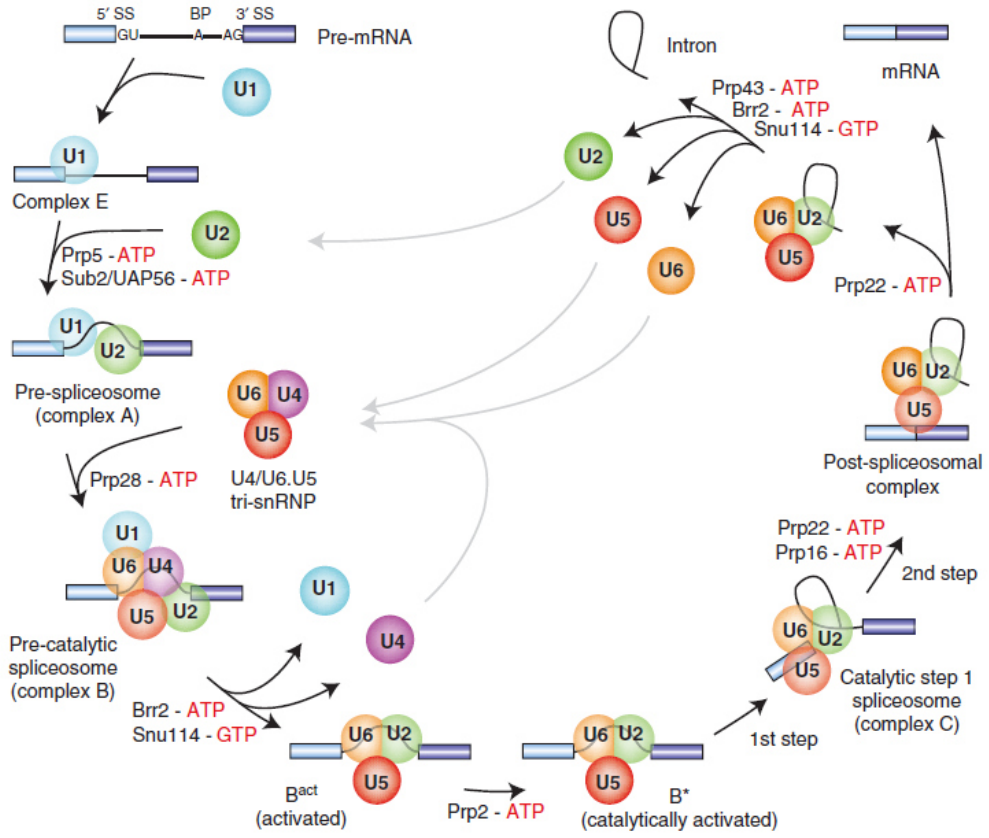

Figure 1.2.: The spliceosome is assembled in a stepwise manner. Schematic representation of the spliceosome cycle. The composition of the respective complexes E, A, B, B^{act}, B* and C are shown. Exon and intron sequences are represented by boxes and lines, respectively. The snRNPs are depicted as colored circles. Conserved ATPases/helicases and GTPases, catalyzing important conformational changes are indicated on the respective stages during the spliceosome cycle. Taken from Will and Lührmann, 2011.

The initial step of the spliceosome assembly comprises the recognition and binding of the 5´ss by the U1 snRNP, binding of the BP by the splicing factor 1 (SF1) and binding of the polypyrimidine tract and the downstream 3´ ss by U2 auxiliary factor (U2AF) in a cooperative manner, resulting in the formation of the early E complex. Thereafter the U2 snRNP replaces SF1 in an ATP-dependent manner, catalyzed by the RNA helicases Prp5 und Sub2, forming the A complex (also prespliceosome). In the next step the preassembled U4/U6·U5 tri-snRNP is recruited and forms the catalytically inactive B complex. Subsequently a series of rearrangements occurs, dependent on the activity of Brr2 and Snu114. This leads to a destabilization and release of U1 and U4 snRNPs, yielding the activated B (B^{act}) complex. Catalytic activation of the B^{act} complex is achieved by the helicase Prp2, which destabilizes the RNA core of the spliceosome, giving rise to the B* complex. The first step of the splicing reaction now takes place, resulting in the C complex. Additional conformational changes expedite the second splicing reaction, finally leading to the joining of the adjacent exons, formation of the intron lariat and release of U2, U5 and U6 snRNPs, which then can take part in the next spliceosome cycle (Nilsen et al., 2003; Wahl et al., 2009; Will and Lührmann, 2011).

1.2. Alternative pre-mRNA splicing

In many eukaryotic species, including mouse and human, the structural space of the proteome by far excels the number of protein coding genes present. It is widely accepted that this protein diversity is achieved by alternative ways of pre-mRNA splicing, resulting in multiple isoforms from one precursor. Recent findings provide evidence that ~ 65% of murine and ~ 95% of human genes undergo alternative splicing (AS) (Pan et al., 2008; Wang et al., 2008; Barbosa-Morais et al., 2012; Merkin et al., 2012). Proteins translated from alternatively spliced mRNAs differ in amino acid sequences and may exhibit different functions, like altered enzymatic activity, ligand binding, cellular localization, interaction properties or protein stability (Kelemen et al., 2013; Liu et al., 2017). Furthermore, AS can impact mRNA stability, mRNA decay or translation efficiency, thereby influencing gene expression levels and consequently protein abundance (McGlincy and Smith, 2008; Mockenhaupt and Makeyev, 2015). The major subtypes of alternative splicing are: alternative exclusion or inclusion of an exon (cassette exon), representing the most frequent mode of AS in mammals, inclusion of shortened exons by the usage of an alternative donor site at the 3´end of the exon (alternative 5´splice site) or an alternative acceptor site at the 5´end of the exon (alternative 3´splice site), mutually exclusive inclusion of exons, whereby inclusion of two or more adjacent exons is regulated such that only one exon is present in the mature mRNA and retention of an intron in the mature mRNA (intron retention) (Black, 2003; see Figure 1.3.).

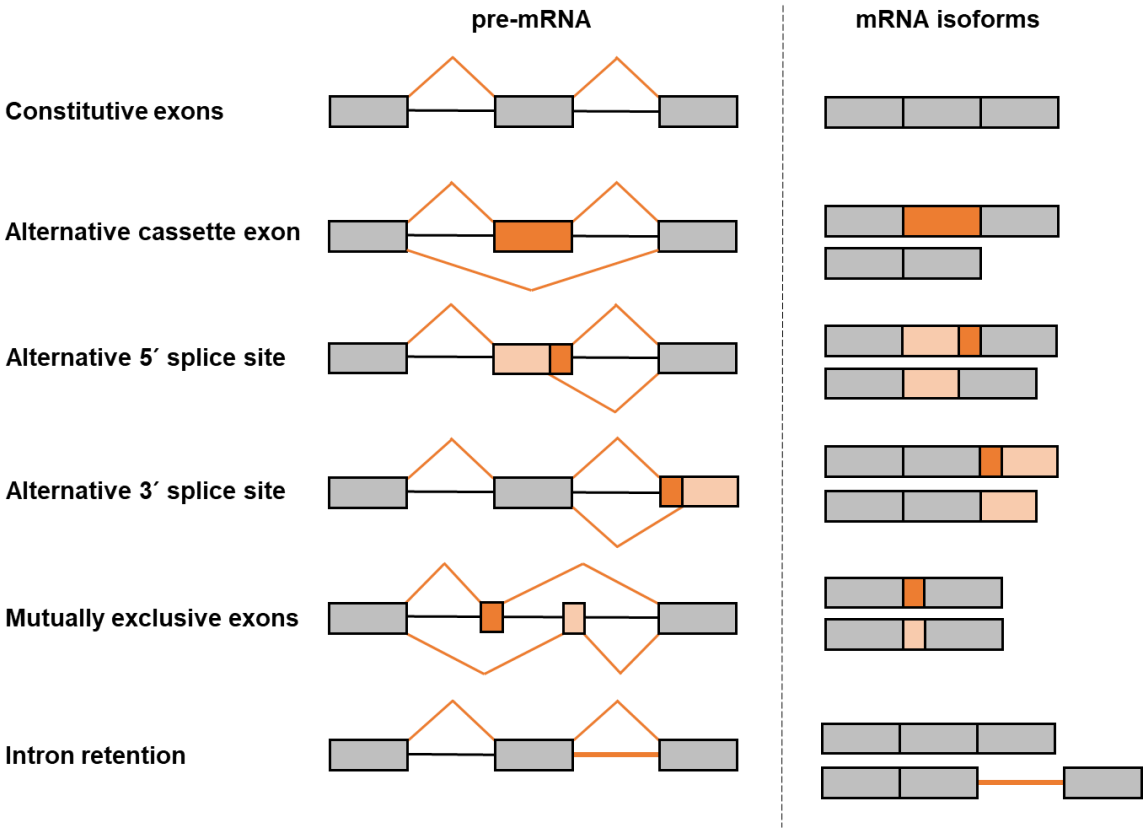

Figure 1.3.: Different modes of alternative splicing. Shown are the pre-mRNAs (left) and resulting alternatively spliced mRNA isoforms (right). Constitutive exons are illustrated as grey boxes, alternative exons or regions as orange boxes and introns as lines.

1.3. Regulation of alternative pre-mRNA splicing

Alternative splicing is the result of differential usage of competing splice sites. The splice site choice is regulated by *trans*-acting protein factors which bind *cis*-acting elements within the pre-mRNA, commonly known as splicing regulatory elements (SREs). SREs can be divided in four subgroups dependent on the position within the pre-mRNA and the type of regulation. Elements promoting splice site usage are intronic splicing enhancers (ISE) or exonic splicing enhancers (ESE). Accordingly, repressive elements are intronic splicing silencers (ISS) and exonic splicing silencers (ESS). However, it has also been proposed that the presence of SREs is necessary for recognition of constitutively spliced exons (Han et al., 2011). Two major classes of *trans*-acting factors have been identified: heterogeneous nuclear ribonucleoproteins (hnRNPs) and the serine/arginine- rich (SR proteins) splicing factors (Busch and Hertel, 2012). Generally, SR proteins are thought to activate splice site usage by binding to ESEs, which promotes the recruitment of spliceosomal core components or auxiliary factors to the respective splice sites (Long and Caceres, 2009). In contrast hnRNPs are believed to repress splice site usage by a variety of mechanisms (Figure 1.4.) (Fu and Ares, 2014). For example, some hnRNPs seem to antagonize SR protein function, by preventing them from binding to regulatory elements (Mayeda and Krainer, 1992; Zhu et al., 2001). Furthermore, it has been shown that hnRNP I (PTB) prevents onward spliceosome assembly, after initial recognition of splice sites (Izquierdo et al., 2005; Sharma et al., 2008).

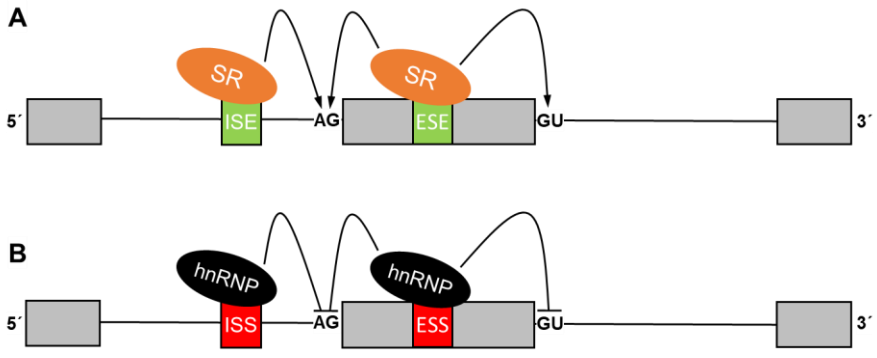

Figure 1.4.: AS is regulated by splicing factors. (A) SR proteins bind to cis-regulatory elements within the exon (ESE) or the intron (ISE), promoting the usage of a splice site. (B) HnRNPs repress the usage of a splice site by binding to exonic (ESS) or intronic (ISS) sequence elements.

However, each alternative splicing event is controlled by a network of classical splicing factors and a variety of other RNA-binding proteins (RBPs) (Taliaferro et al., 2016), which can act in either a cooperative or a competitive manner. Additionally, splicing factors can cross-regulate each other, are expressed in a cell- or tissue-dependent manner and their activity can be modulated by posttranslational modifications (Fu and Ares, 2014). Position of SREs relative to the splice sites as well as sequence context further influence regulatory potential of the bound splicing factor. Lastly, RNA secondary structures (McManus and Graveley, 2011; Taliaferro et al., 2016) and transcription elongation speed affect accessibility of SREs (de la Mata and Kornblihtt, 2006; Kornblihtt, 2015; Naftelberg et al., 2015).

AS is regulated in numerous cellular processes and in a cell-type- , tissue- and developmental stage-specific manner (Wang et al., 2008; Paronetto et al., 2016; Neumann et al., 2019). For instance, alterations of splicing programs have implications in the transition of neuronal progenitor cells to fully differentiated neurons (Quesnel-Vallières et al., 2015; Zhang et al., 2016), hepatocyte differentiation (Sen et al., 2013) and heart development (Salomonis et al., 2009). Furthermore, differential splicing patterns occur in nearly every tissue (Castle et al., 2008). Therefore, it is of no wonder that misregulation of AS contributes to a plethora of diseases (Tazi et al., 2009).

1.4. Serine-arginine (SR)-rich proteins

1.4.1. Structural features of SR proteins

SR proteins are a family of highly conserved and structurally related splicing factors. SR proteins occur in plants, metazoans and some lower but not all eukaryotes (Twyffles, Gueydan and Kruys, 2011). To date the main criterion to define the family of `classical´ SR proteins is solely based on sequence similarities giving rise to analogues structural elements. Accordingly, SR proteins share a modular structure of at least one N-terminal RNA recognition motif (RRM) and an arginine/serine-rich (RS) domain with more than 50 amino acids (>40% RS content) (Manley and Krainer 2010). With respect to this definition 12 `classical´ SR proteins are present in human (see Figure 1.5.).

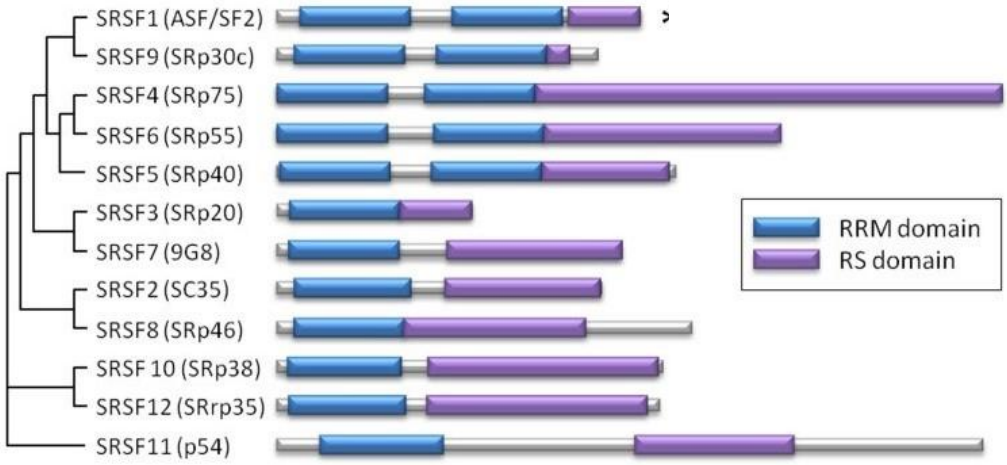

Figure 1.5.: Representation of the human SR protein family. Shown is the classification of human SR proteins after Manley and Krainer (2011). Alternate names are denoted in the parentheses. Modified from Blanco and Bernabéu 2012.

RRM domains dictate the binding of SR proteins to their target RNAs (Liu et al., 1998; Liu et al., 2000). Thereby the number of RRMs within SR proteins, their spacing and combination with other domains determines substrate specificity (Clery et al. 2008). RS domains are considered to be largely unstructured (Haynes and Iakoucheva, 2006) and are required for essentially all functions of SR proteins as they serve as protein interaction modulators promoting protein-protein interactions of homotypic nature or with SR-related proteins (e.g. SR protein kinases or components of the spliceosome) (Graveley, 2000; Shepard and Hertel, 2009). Furthermore, the RS domain serves as a nuclear localization signal as it interacts with transportin-SR, a nuclear import receptor specific for SR proteins (Kataoka et al., 1999; Lai et al., 2001). Interestingly, it has been reported, that RS domains

are also capable of directly contacting the pre-mRNA on the BP (Shen et al., 2004 and Shen and Green, 2004).

1.4.2. Posttranslational modifications of SR proteins

Several posttranslational modifications have been reported to occur in the SR protein family. Methylation of arginine residues between two RRMs of SRSF1 for instance has been shown to influence sub-cellular localization (Sinha et al., 2010). Also, lysine acetylation in SR proteins has been detected, yet a function remains to be investigated (Choudhary et al., 2009). However, the by far most important modification of the SR protein family is phosphorylation within the RS domains. SR protein phosphorylation is catalyzed by two classes of kinases, SRPKs and CLKs (Koizumi et al., 1999; Yeakley et al., 1999) which act in a symbiotic manner to control sub-cellular and sub-nuclear localization of the SR proteins (Aubol et al., 2016; Aubol et al., 2018). Phosphorylation of SR proteins within the cytoplasm by SRPKs facilitates nuclear import. Once in the nucleus, SR proteins accumulate in complex structures called nuclear speckles (Hall et al., 2006). Subsequent CLK phosphorylation activity is necessary to release SR proteins from the speckles, upon which they can take part in the splicing reaction. Moreover, phosphorylation of SR proteins is essential to mediate the recruitment and assembly of spliceosomal components (Mermoud et al., 1994; Cao et al., 1997; Pandit et al., 2008). For the splicing catalysis per se, the RS domain needs to be partially dephosphorylated (Misteli et al, 1997; Cao et al., 1997; Shi et al., 2006; Shi and Manley, 2007). It is thought that this dephosphorylation modulates protein-protein interactions within the spliceosome which is important for the first step of the splicing reaction to proceed (Xiao and Manley, 1998, Shin et al., 2004).

1.4.3. Role of SR proteins in pre-mRNA splicing

SR proteins fulfill essential functions in both constitutive and alternative splicing. General functions in splicing activation comprise the recruitment and stabilization of spliceosomal components and the pre-mRNA transcript. More precisely, SR proteins promote U1 snRNP binding to the 5´ss via bridging with the U1-70K RNA binding domain, U2 snRNP binding to the 3´ss via interaction with U2AF and incorporation of the U4/U6·U5 tri-snRNP into the prespliceosom (Kohtz et al., 1994; Jamison et al., 1995; Roscigno and Garcia-Blanco, 1995; Graveley, 2000; Cho et al., 2011; Zhou and Fu, 2013). Furthermore, SR proteins can prevent binding of U2AF to a splice site when bound to intronic sequences (Hertel and Maniatis, 1999) (see also Figure 1.6. for a graphical summary).

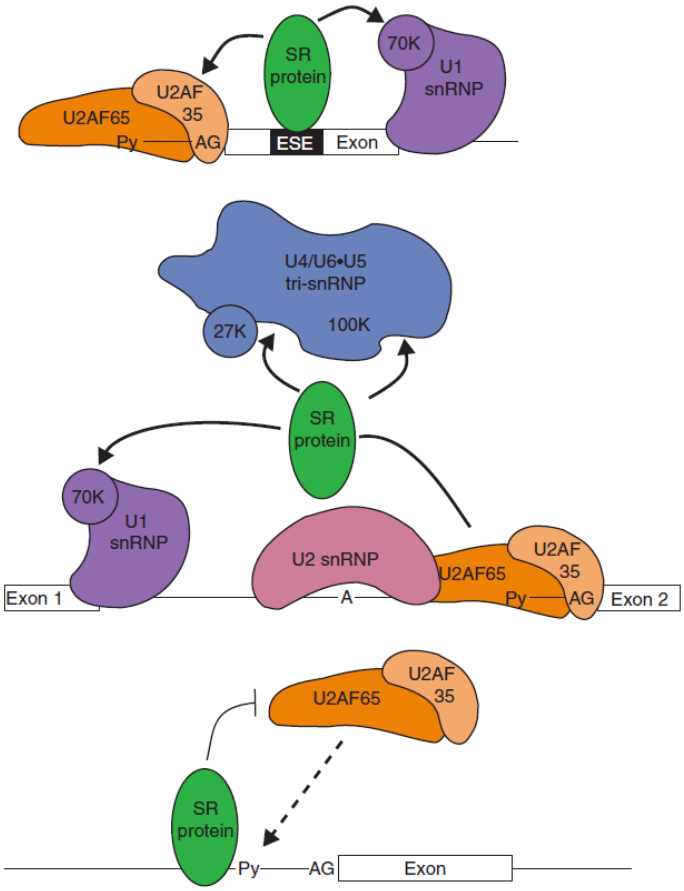

Figure 1.6.: General functions of SR proteins during spliceosome assembly. Top: ESE bound SR proteins recruit U1-70K and U2AF^{35} to the adjacent splice sites (exon definition). Middle: SR proteins bridge the spliceosomal components bound at the splice sites and recruits the U4/U6·U5 tri-snRNP. Bottom: Intronic bound SR protein prevents binding of U2AF to the 3´splice site. From Shepard and Hertel, 2009.

The best understood function of SR proteins is their role in splice site selection via binding to ESEs or ISEs (Liu et al., 1998; Liu et al., 2000; Zhou and Fu, 2013). SR proteins show a binding preference for purine-rich exonic sequences (Pandit et al., 2013), and it is generally thought that SR protein binding to ESEs promotes adjacent splice site usage consequently leading to exon inclusion (Ibrahim et al., 2005, Bradley et al., 2015). In contrast, evidence is provided for exon skipping stimulation via SR protein binding to ISEs (Erkelenz et al., 2013). Interestingly, it was shown that exon skipping can also be stimulated if an SR protein binds to ESEs in constitutive exons which flank an alternative exon (Han et al., 2011). SR proteins can further interact with the C-terminal domain of RNA polymerase II (Pol II) (de la Mata and Kornblihtt, 2006) or the histone H3 tail (Loomis et al., 2009; Luco et al., 2010), thereby facilitating co-transcriptional splice site selection (Das et al., 2006; Sapra et al., 2009).

However, overall splicing regulation through SR proteins is a well-orchestrated process of high complexity that is often controlled by combinatorial mechanisms rather than a single event. In fact, the SR protein regulated splicing outcome is position- and context-dependent (Shen and Mattox, 2012, Fu and Ares, 2014). Furthermore SR proteins can influence each other in a synergistic or competitive manner (Liu et al., 2000; Zhou and Fu, 2013), can antagonize effects of other splicing factors or be antagonized by those (Fu and Ares, 2014).

1.4.4. Role of SR proteins in other mRNA processing events

Besides their `canonical´ role in splicing regulation, SR proteins have been implicated in a variety of postsplicing events. It is known that several SR proteins can shuttle between the nucleus and the cytoplasm dependent on the phosphorylation state of the respective RS domains. This suggests a possible role of SR proteins in mRNA export and cytoplasmatic events. Indeed SRSF3 and SRSF7, two shuttling SR proteins (see Jeong, 2017), can serve as an adaptor for the nuclear export factor 1 (NXF1), connecting completed splicing with NXF1 mediated mRNA export (Tintaru et al., 2007; Müller-McNicoll et al., 2016). Interestingly, SR proteins have been reported to be involved in several other cellular functions, which was exemplarily shown for SRSF1. For instance, SRSF1 was described to directly - and independently of splicing regulatory activity - influence mRNA stability of the *PKCI-r* mRNA (Lemaire et al., 2002). SRSF1 is furthermore implicated in translation initiation regulation of bound mRNAs. Within this mechanism, SRSF1 mediates the interaction with mTOR kinase and PP2A phosphatase, resulting in a stimulation of mTOR and a repression of PP2A activity. mTOR and PP2A are key regulators of 4E-BP, a competitive inhibitor of cap-dependent translation. SRSF1 dependent activity modulation results in hyperphosphorylated 4E-BP, finally enhancing cap recognition and translational initiation (Michlewski et al., 2008). The list of SRSF1 functions can even be extended to contributions in NMD (Zhang and Krainer, 2004), protein sumoylation (Pelisch et al., 2010) and genome stability (Li and Manley, 2005). An overview of SRSF1 functions is graphically summarized in Figure 1.7..

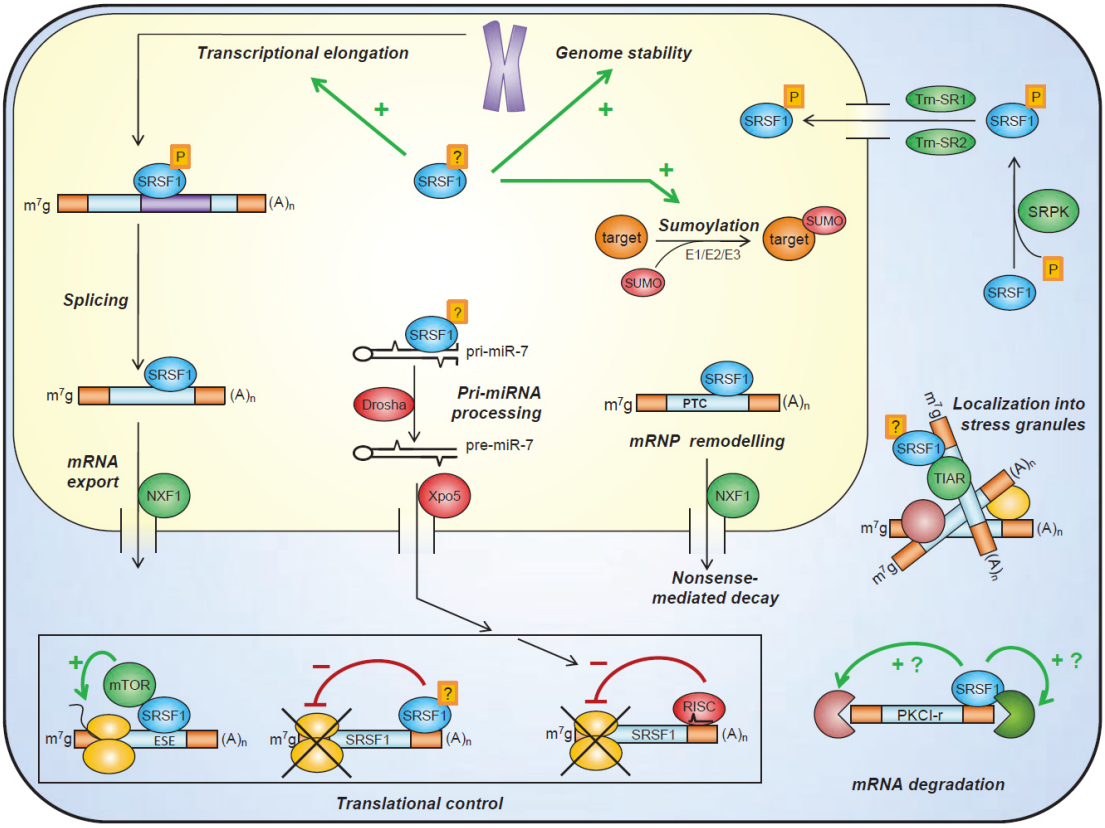

Figure 1.7.: Roles of SRSF1 in various mRNA processing steps. ESE, exonic splicing enhancer; NXF1, nuclear export factor 1; P, phosphate group; RISC, RNA-induced silencing complex; Xpo5, exportin 5. Question marks indicate unknown mechanisms. Taken from Gueydan and Kruys, 2011.

The importance and versatility of SR proteins in mRNA metabolism, establishes this class of proteins as key regulators of fundamental cellular processes. This is further highlighted by the fact, that SR protein dysregulation as well as mutations in these proteins are associated with a vast number of diseases (Fredericks et al., 2015). For example, either depletion or overexpression of SRSF1 is implicated in cancer progression (Anczukow et al., 2012). SRSF3 and SRSF6 have been reported to be upregulated in lung cancer, cervical cancer, breast cancer and skin cancer (Jia et al., 2010; Jensen et al., 2014; Cohen-Eliav et al., 2013; Fredericks et al., 2015). Furthermore, mutations within SRSF2 negatively influenced survival in patients with primary myelofibrosis (Lasho et al., 2012).

1.5. SR protein kinases

Phosphorylation of serines within RS domains is a critical step to control localization, activity and interaction properties of SR proteins. Several kinases or kinase activities have been reported to phosphorylate SR proteins in vitro, such as protein kinases A and C (PKA and PKC) (Colwill et al. 1996), dual-specificity tyrosine phosphorylation-regulated kinases (DYRKs) (de Graaf et al., 2004), AKT (also PKB) (Blaustein et al., 2005), topoisomerase I (Rossi et al., 1996) and cdc2p34 (Okamoto et al., 1998). However, as aforementioned only two families of kinases are considered to be specific SR protein kinases, which are serine/arginine-rich protein-specific kinase (SRPKs) and Cdc2-like kinases (CLKs) (Gui et al. 1994; Kuroyanagi et al., 1998; Colwill et al., 1996; Duncan et al., 1998 etc.). With respect to their functions SRPKs and CLKs are also termed splicing kinases. Several structural and catalytic features make these kinases unique enzymes, which will be discussed in the following.

1.5.1. Serine/arginine-rich protein-specific kinases (SRPKs)

SRPKs are highly conserved throughout eukaryotic evolution (Giannakouros et al., 2011). In mammals the SRPK family comprises three members, SRPK1, SRPK2 and SRPK3. While SRPK1 is ubiquitously expressed, SRPK2 and SRPK3 expression is restricted to certain tissues in mammals (Zhou and Fu, 2013), suggesting non redundant functions. SRPKs exclusively phosphorylate their substrates on serine residues preferentially flanked by arginines. Unlike most kinases SRPKs phosphorylate their substrates in a processive manner, which means that once the substrate is bound a multi-site phosphorylation takes place without releasing the substrate prior to completion (Aubol et al., 2003). Interestingly, it has been reported that SRPK1 activity is regiospecific, phosphorylating about 10–12 serines in the N-terminal portion of the SRSF1 RS domain, called RS1 (Velazquez-Dones et al., 2005; Ma et al., 2008). SRPKs are mainly located in the cytoplasm, but a fraction appears to be nuclear, where they fulfill different functions. SRPK activity in the cytoplasm facilitates nuclear import of SR proteins by enhancing the affinity from the SR protein to the respective nuclear receptor (Yun et al., 2003; Aubol et al., 2018). In contrast, nuclear SRPK activity promotes the release of CLKs from tightly bound hyperphosphorylated SR proteins (Aubol et al., 2016; Aubol et al., 2018). SRPK subcellular localization appears to be regulated in a cell-cycle dependent manner, as SRPK1 preferentially translocates to the nucleus at the end of the G2 phase (Ding et al., 2006) and seems to play a role in chromatin reorganization during G2/M transition (Nikolakaki et al., 1997; Takano et al., 2004; Loomis et al., 2009).

SRPKs adopt a typical kinase fold with an N-terminal lobe mostly composed of β-strands and the typical αC α-helix and a large C-terminal lobe predominantly α-helical. A non-conserved insert of approximately 250 amino acids divides the kinase core in two structural entities and is important for subcellular localization, as deletion shifted SRPK appearance exclusively to the nucleus (Ding et al., 2006). Furthermore, SRPKs harbor N- and C-terminal extensions and a MAP kinase (MAPK) insert within the kinase domain (Ghosh and Adams, 2011). The MAPK insert and the loop between the αF and αG α -helices constitute a distinct docking groove in close proximity to the active site of the kinase (Ngo et al., 2005; Ngo et al., 2008). The docking groove is bound by a specific docking motif in SRSF1, which is located between RRM2 and the RS domain. This interaction is based on electrostatic interactions mediated by alternate arginine residues within SRSF1 and acidic residues from the kinase. Interestingly, deletion of the SRSF1 docking motif did not result in a loss of phosphorylation activity by SRPK1, but significantly increased the content of phosphorylated serines within the RS domain (Ngo et al., 2005), suggesting that this interaction is indispensable for regiospecificity of SRPK1. The `fixation´ of the docking motif from SRSF1 allows the RS1 segment to slide through the active site during catalysis, giving rise to the processive and directional (C-to-N direction) phosphorylation (Ngo et al. 2008). An active and dynamic cross-talk between SRPK1 and SRSF1 during this multi-site phosphorylation ensures proper extension and finally termination of the reaction (Aubol and Adams, 2011) (see Figure 1.8. for a graphical summary of the multi-site phosphorylation mechanism).

Another interesting feature of SRPKs is that they are constitutively active. This rare feature among kinases is likely based on the properties of the SRPK1 activation segment which adopts an active conformation in the crystal structure without posttranslational modifications (Ngo et al., 2007).

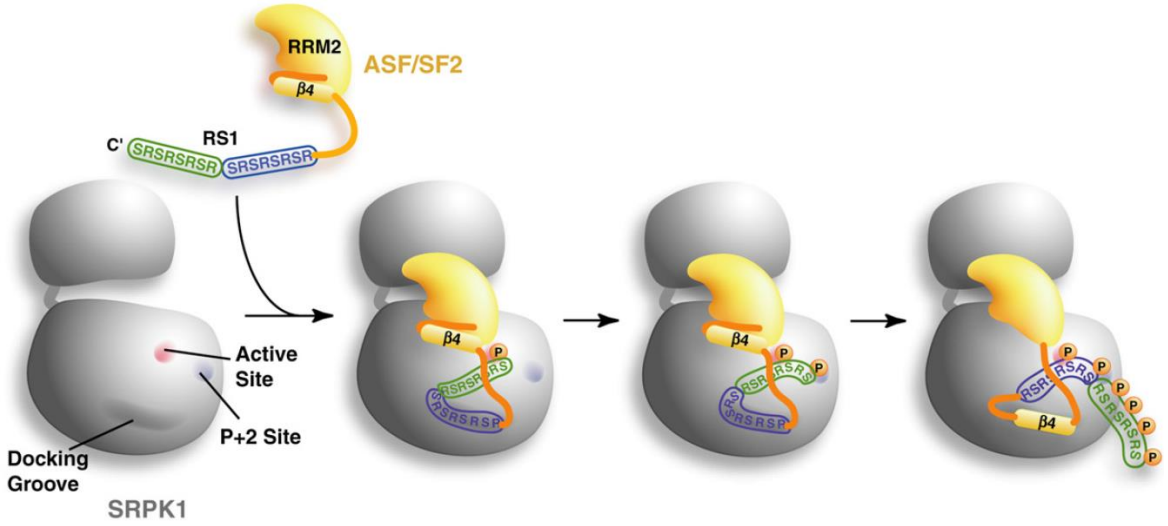

Figure 1.8.: Scheme of the multi-site phosphorylation mechanism of SRPK1. Binding of SRSF1 to the SRPK1 docking groove induces structural changes leading to binding of RRM2 of SRSF1. This induces the processive phosphorylation to start in a directional manner through a sliding mechanism. If phosphorylation is completed the beta-4 motif in RRM2 binds to the docking groove of SRPK1, ultimately leading to the release of the SR protein from SRPK1. Taken from (Ngo et al., 2008).

Besides the role of SRPKs in regulating the sub-cellular distribution of SR proteins, other contributions during the splicing reaction are known. For example, human SRPK1 was found to be associated with the U1-snRNP, suggesting a role in 5´splice site selection (Kamachi et al., 2002). Additionally, SRPK2 appears to be required for U4/U6·U5 tri-snRNP formation by phosphorylating PRP28 (Mathew et al., 2008).

1.5.2. Cdc2-like kinases (CLKs)

CLKs represent the second family of specific SR protein kinases, exclusively found in the nucleus (Aubol et al., 2016) and generally implicated in the regulation of constitutive and alternative splicing. CLKs seem to play a major role in the recovery after heat- and osmotic-shock (Ninomiya et al., 2011) and are furthermore implicated in HIV-1 gene expression and influenza virus replication (Karlas et al., 2010; Wong et al., 2011).

CLKs occur in a variety of organisms and are highly conserved throughout eukaryotic evolution ranging from plants to humans (Yun et al., 1994). The human and the mouse CLK families comprise four members, simply termed CLK1-4. CLKs share a conserved signature motif “EHLAMMERILG”. The LAMMER motif is thought to be necessary for specific substrate recognition which has been exemplarily shown for the fission yeast homolog Lkh1 (Kang et al., 2010). In contrast to SRPKs, CLKs are dual-specificity kinases, generally harboring a tyrosine and a serine/threonine kinase activity. However, substrates are exclusively phosphorylated on serine/threonine residues, whereupon CLK activity is preferentially targeted towards serine residues (Nayler et al., 1997, Bullock et al., 2009). CLK activity is less restrictive with respect to amino acids flanking serines, as both serine-arginine and serine-proline dipeptides are recognized and phosphorylated (Velazquez-Dones et al., 2005). It has been shown that CLK1 lacks a regiospecificity for SRSF1 like SRPK1 and is capable of phosphorylating SR repeats present in RS1 as well as SP/SR repeats in the RS2 segment of SRSF1 (Aubol et al., 2013). CLK1 is also able to complement RS domain phosphorylation of SRSF1 if the RS1 segment is pre-phosphorylated by SRPK1 (Velazquez-Dones et al., 2005), which is necessary to facilitate SR protein release from nuclear speckles and subsequently for splicing regulation (Colwill et al., 1996, Aubol et al., 2018).

CLKs also show a typical kinase fold, but comprise elements exclusively found in this family of kinases. For instance, CLKs harbor a MAPK-like insertion in the C-terminal lobe. In contrast to the SRPK1 MAPK insertion, the insertion in CLKs does not constitute a clear docking site, but rather forms a shallow groove which is based on the presence of a unique α-helix followed by a two-strand β-sheet (Bullock et al., 2009), suggesting that the substrate recognition and binding mechanism is different from SRPKs. CLKs are also constitutively active kinases, as the activation segment adopts an active conformation without posttranslational modifications as seen in SRPKs (Bullock et al., 2009). Besides the LAMMER motif and the MAPK-like insert, CLKs comprise further specific structural features like an extended β-hairpin (βhp/βhp´) located at the interface of the N-terminal and C-terminal lobe and a unique a-helix (αH) at the bottom of the C-terminal lobe (see Figure 1.9.). A function of these regions so far remains unknown. Deletion of these elements,

however resulted in a complete loss of CLK activity (unpublished data, Heyd lab), suggesting a role in substrate binding or catalysis.

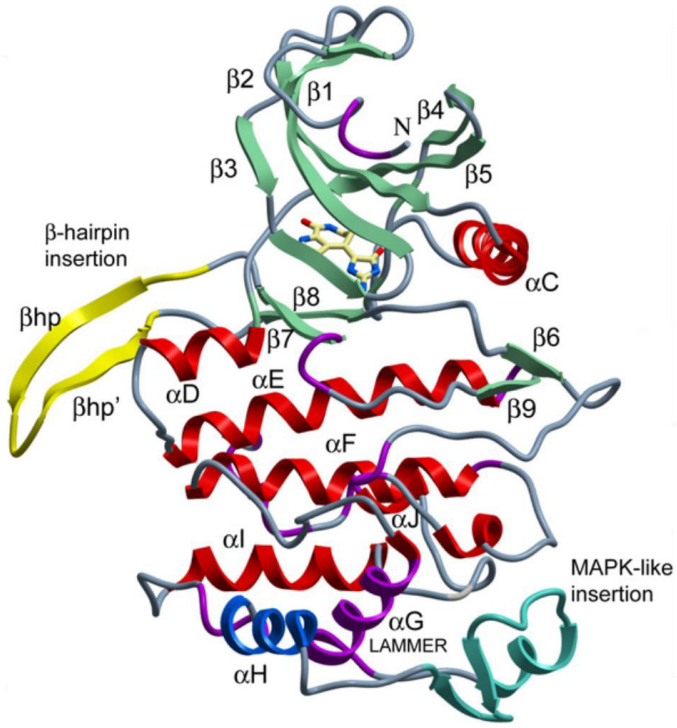

Figure 1.9.: Structure of the human CLK1 kinase domain. Shown are classical kinase elements like the N-terminal lobe (green) and the C-terminal lobe (red). Unique elements found only in CLKs are the β-hairpin (yellow), the MAPK-like insertion (turquoise), the αH-helix (blue) and the LAMMER signature motif located within the αG-helix (violet). Taken from Bullock et al., 2009.

Additionally, all CLK family members possess relatively long N-terminal regions (150-300 amino acids) containing multiple RS repeats and therefore classified as RS domains (Colwill et al., 1996). While the kinase domains of CLKs show high sequence similarities, the N-termini differ in sequence content and length, suggesting specific functions. Due to the presence of disorder-promoting amino acids (Aubol et al., 2014), the N-termini are considered to be largely unstructured, which might also explain the lack of a full length CLK structure so far. Interestingly, N-termini of CLKs resemble RS domains of their target SR proteins and are important for recognition of those and other RS domain-containing proteins (Colwill et al., 1996). For instance, it has been shown that the N-terminus of CLK1 promotes high affinity binding to SRSF1 via interaction with the RS domain. This is on the one hand necessary to generate the hyperphosphorylated state of SRSF1 and on the other hand to induce cooperative binding to RNA (Aubol et al., 2014). Furthermore, the N-terminus mediates oligomerization of CLK1, thereby contributing to substrate specificity (Keshwani et al., 2015). Several classical nuclear localization sequences have been identified within

the CLK1 N-terminus, but interestingly deletion did not affect subcellular localization. Instead, it could be shown that CLK1 and SRSF1 form a high-affinity complex via interaction of the RS domain and the N-terminus in the cytoplasm. Subsequent binding to transportin SR2 then facilitates nuclear import of the whole complex (George et al., 2019).

1.6. Aim of this thesis

Temperature is an omnipresent external factor of significant importance for essentially all biological processes. Extreme changes in external temperature can be noxious or even life threatening, thus organisms evolved exquisite thermo-sensory systems. However, the core body temperature of homoeothermic organisms is kept constant around a set point, but still time of the day dependent body temperature oscillations occur, for instance in mammals in a range of ~ 1 to 4 °C (Buhr et al., 2010; Refinetti and Menaker, 1992; Saini et al., 2012). Strikingly, these subtle body temperature oscillations are sufficient and necessary to control time of the day dependent alternative splicing and are controlled through temperature-dependent phosphorylation of SR proteins. Among the specific SR protein kinases, CLKs represent a promising candidate for regulating temperature-dependent SR protein phosphorylation as they are considered to be stress-related kinases, which play an important role in the recovery after a heat-shock. Based on this assumption the major questions of the present thesis are formulated as follows:

1. Are CLKs capable of controlling temperature-dependent SR protein phosphorylation and alternative splicing?

2. What is the underlying mechanism of temperature-dependent CLK activity?

3. What are possible implications of temperature- and CLK controlled alternative splicing?

To answer the above mentioned questions, a combination of classical biochemical, cell biology, structural biology, molecular dynamics simulation and global transcriptome sequencing approaches were used.

2. Results

2.1. Body temperature cycles control rhythmic alternative splicing in mammals

This subchapter and subchapter 2.2. refer to: Marco Preußner, Gesine Goldammer, Alexander Neumann, Tom Haltenhof, Pia Rautenstrauch, Michaela Müller-McNicoll and Florian Heyd (2017). Body Temperature Cycles Control Rhythmic Alternative Splicing in Mammals. Mol Cell. 3;67(3):433-446.

Since my contribution to this paper is confined to experiments dealing with SR protein kinases, the main focus of the study will only be outlined in the following by the abstract of the publication (see also Figure 2.1.1. for a graphical abstract).

The core body temperature of all mammals oscillates with the time of the day. However, direct molecular consequences of small, physiological changes in body temperature remain largely elusive. Here we show that body temperature cycles drive rhythmic SR protein phosphorylation to control an alternative splicing (AS) program. A temperature change of 1°C is sufficient to induce a concerted splicing switch in a large group of functionally related genes, rendering this splicing-based thermometer much more sensitive than previously described temperature-sensing mechanisms. AS of two exons in the 5` UTR of the *TATA-box binding protein (Tbp)* highlights the general impact of this mechanism, as it results in rhythmic TBP protein levels with implications for global gene expression in vivo. Together our data establish body temperature-driven AS as a core clock-independent oscillator in mammalian peripheral clocks.

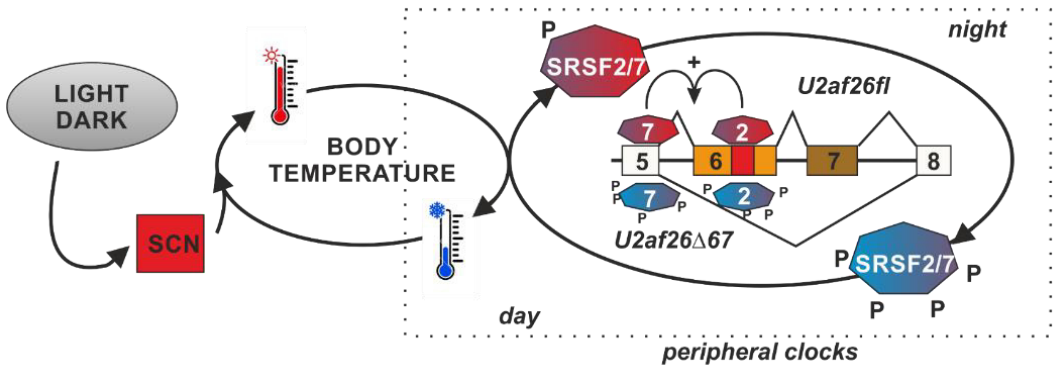

Figure 2.1.1.: Model showing rhythmic alternative splicing regulation through body temperature cycles.

2.2. CLKs contribute to temperature-dependent SR protein phosphorylation and alternative splicing

Having shown that body temperature cycles regulate rhythmic and time of the day dependent AS we aimed to identify upstream regulators of this process. Knock down and overexpression experiments identified SR proteins, well known splicing factors, as regulators of temperature-dependent AS. Interestingly, we observed that the phosphorylation state of SR proteins appeared to be temperature-dependent (hyperphosphorylated at lower temperatures and hypophosphorylated at higher temperatures) whereas protein expression levels and binding abilities of SR proteins were not affected by temperature. The phosphorylation level of SR proteins determines their activity (Xiao and Manley, 1998; Yeakley et al., 1999; Kadri et al., 2015) and is controlled by two classes of specific SR protein kinases, SRPKs (SR protein kinases, SRPK1-3) and CLKs (CLK1-4) (Dominguez et al., 2016; Ghosh and Adams, 2011). CLKs play an important role in the recovery after a heat-shock (Ninomiya et al., 2011). Hence, we reasoned that these kinases may contribute to temperature-dependent phosphorylation of SR proteins and subsequently to AS. To test this hypothesis we first used the CLK1/4 inhibitor TG003 in mouse 3T3 cells. The resulting hypo-phosphorylation of SR proteins recapitulates the situation at higher temperatures and should therefore promote inclusion of exons 6 and 7 of the model gene *U2af26*. Indeed, we found these exons to be more included upon CLK1/4 inhibition (Figure 2.2.1. A, B) and consistent with that, knockdown of either CLK1 or CLK4 had the same effect (Figure 2.2.1. C, D). Additionally, overexpression of CLK4 led to increased phosphorylation of SR proteins (Figure 2.2.1. E), promoting skipping of exons 6 and 7 (Figure 2.2.1. F). Finally, overexpression of CLK4 under heat shock conditions counterbalanced the heat shock response on *U2af26* (Figure 2.2.1. G and H), altogether suggesting a prominent role of CLK1 and CLK4 in controlling cold-induced SR protein phosphorylation and consequently AS in a temperature-dependent manner. Of note, inhibiting serine/threonine protein phosphatase activity (PP1, PP2A and PP2B) with the specific inhibitor ocadaic acid (OA) resulted in repression of exon inclusion of *U2af26*, essentially recapitulating the splicing pattern at higher temperatures (Figure 2.2.1. A), therefore suggesting a role of these phosphatases in heat-induced dephosphorylation of SR proteins.

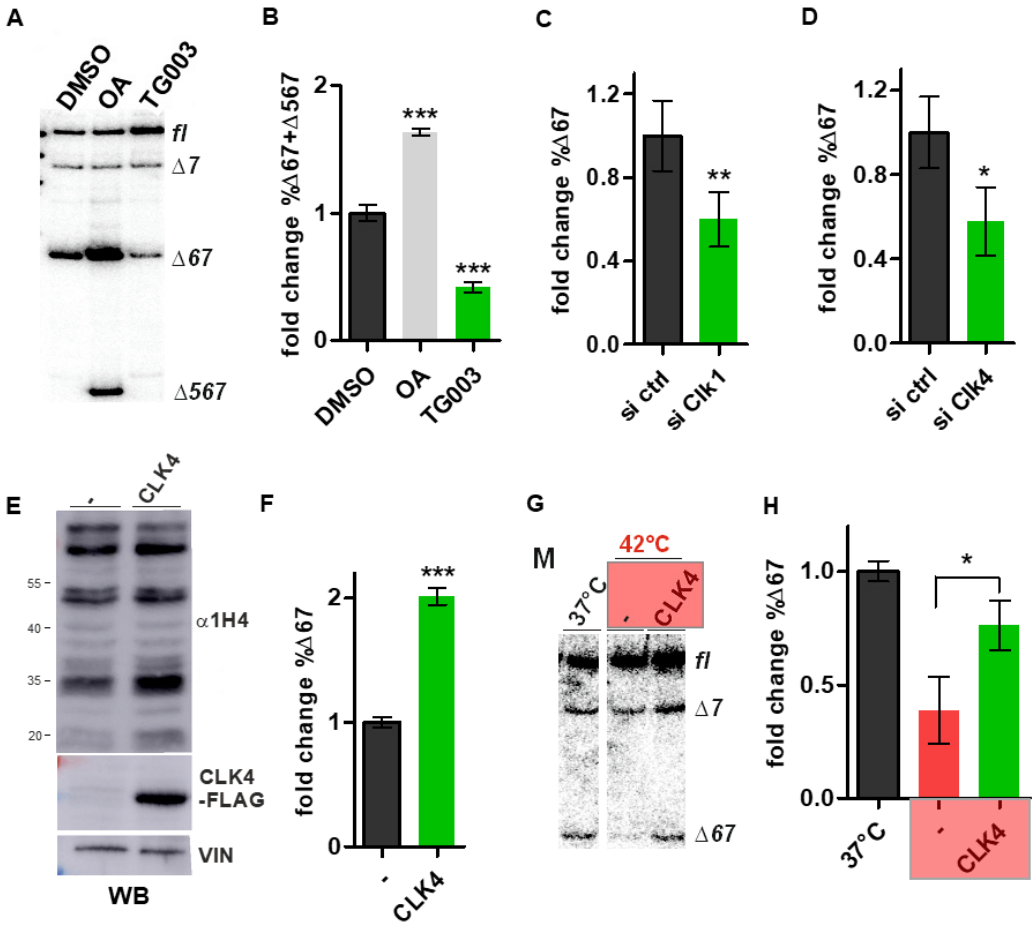

Figure 2.2.1.: CLK1/4 contribute to temperature-dependent SR protein phosphorylation and AS. (A) Representative gel of a radioactive splice-sensitive RT-PCR for *U2af26* skipping of exons 7 (Δ7), 6 and 7 (Δ67) and 5, 6 and 7 (Δ567). 3T3 cells were treated with either OA (1 µM), TG003 (50 µM) or DMSO as a solvent control. (B). Combined skipping of exons 6, 7 and 5-7 were quantified relative to DMSO. (C, D) Quantification of *U2af26* exons 6 and 7 skipping upon *Clk1* or *Clk4* knockdown relative to control siRNA. (E) Western blot confirming CLK4-Flag overexpression and subsequent increase of SR protein phosphorylation (α-1H4 antibody). Vinculin served as a loading control. (F) Quantification of *U2af26* exons 6 and 7 skipping after CLK4 overexpression relative to transfection control. (G) Representative gel of *U2af26* exons 6 and 7 skipping upon heat shock and heat shock rescue with CLK4 overexpression relative to 37°C. (H) *U2af26* exons 6 and 7 skipping were quantified relative to the 37°C control. Data of quantifications represent mean ± SD of at least three independent experiments. Student'st test-derived p values: * < 0.05; ** < 0.01; *** < 0.001.

2.3. CLK activity is highly responsive to physiological temperature changes and heat-inactivation is reversible

This subchapter as well as all following subchapters in the results part refer to: Tom Haltenhof, Ana Kotte, Francesca De Bortoli, Samira Schiefer, Stefan Meinke, Ann-Kathrin Emmerichs, Kristina Katrin Petermann, Bernd Timmermann, Andreas Franz, Markus C. Wahl, Petra Imhof, Marco Preußner and Florian Heyd. A conserved kinase-based body temperature sensor globally controls alternative splicing and gene expression.

Based on the findings of the first study we further investigated the role of CLKs as potential temperature sensors. Therefore we first expressed and purified mouse GST-tagged CLK1 and 4 from bacteria (Figure 2.3.1. A). We then used the purified CLK proteins in in vitro kinase assays and recorded auto- and SR-repeat (mimicking RS domains of SR proteins) phosphorylation. In a temperature gradient from 33 °C – 40 °C, we found the activity of both CLKs to be strongly temperature-dependent with higher activity at lower temperature, matching the phosphorylation state of SR proteins in vivo (Preussner et al., 2017) (Figure 2.3.1. B). CLKs consist of an unstructured N-terminus and C-terminal kinase domain (Ghosh and Adams, 2011). To identify the temperature-sensitive region within the proteins, we purified the kinase domains alone and repeated the in vitro kinase assay. We again observed a strong temperature-dependent auto- and SR-peptide phosphorylation (Figure 2.3.1. C), confirming that the temperature dependence is an inherent feature of the CLK kinase domain. Of note, the temperature activity profiles of the full length proteins are slightly shifted, suggesting a contribution of the unstructured N-termini in setting the exact temperature range. Next, we wished to address specificity of this temperature dependence. To this end we purified a member of another family of SR protein kinases, namely SRPK1 and compared temperature activity profiles to CLKs in a range between 16 °C and 56 °C. As before, the activity of CLKs was strongly reduced between 32 °C and 36 °C already starting to decrease at 24 °C for CLK1 (Figure 2.3.1. D). In contrast, SRPK1 activity was constant between 16 °C and 52 °C with a loss of activity at 56 °C, confirming that temperature sensitivity in the physiological temperature range is specific for CLKs.
In addition we could show that heat inactivation of CLK1/4 activity is reversible, as activity could be quickly restored when shifting the kinases back from 38 °C to 34 °C (Figure 2.3.1. E). Furthermore we could not detect substantial changes of secondary structure elements in CD spectra at 25, 34 and 38 °C (Figure 2.3.1. F), suggesting that heat inactivation is not based on global unfolding of the protein, but rather on small conformational changes within the kinase domains.

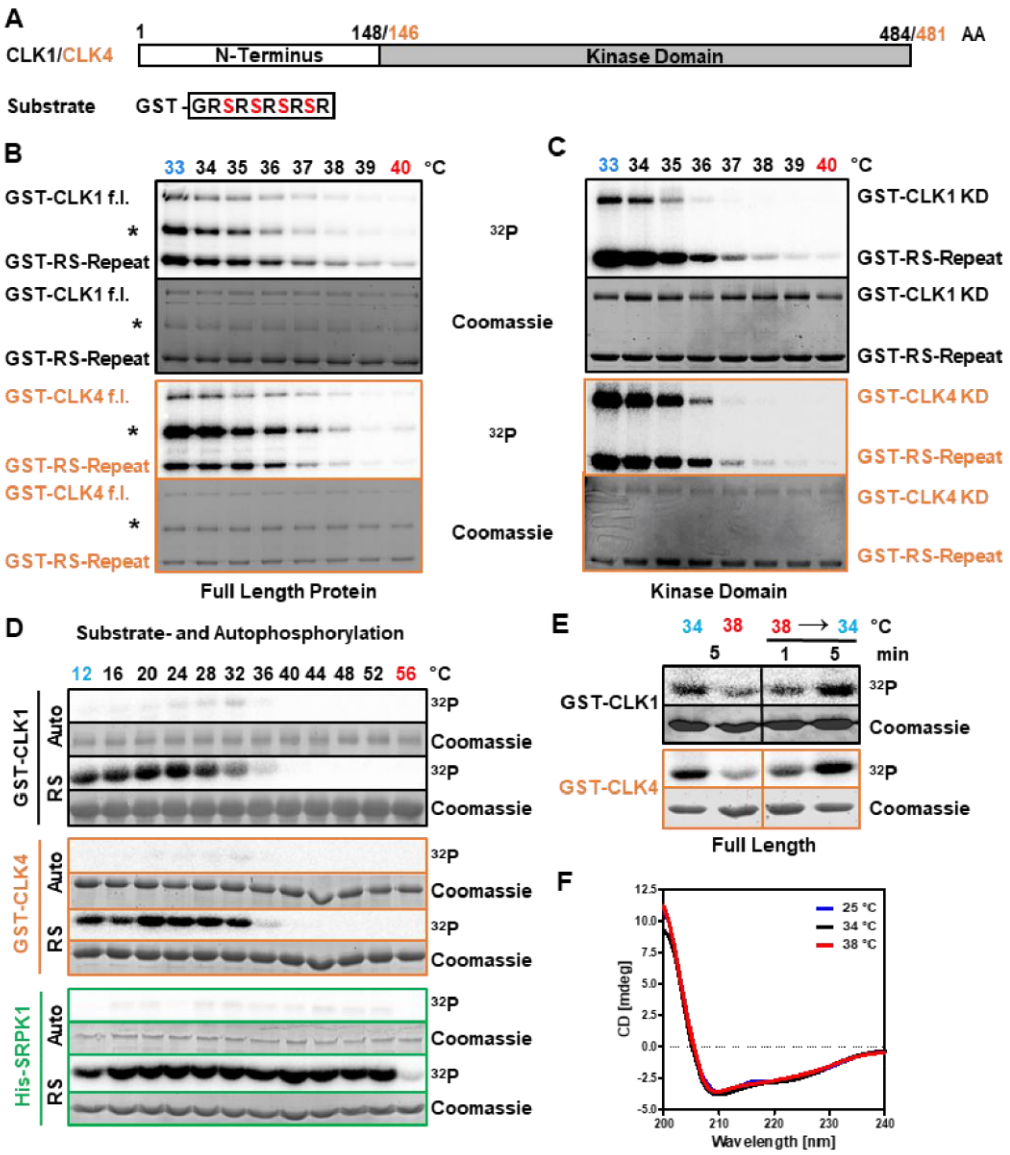

Figure 2.3.1.: CLK1/4 activity is highly responsive to physiological temperature changes. (A) Schematics of CLK1/4 kinases and an arginine/serine (RS) peptide substrate. (B, C) In vitro kinase assays with full length kinases (B) and kinase domains (C) in a physiological temperature range (CLK1 (top, black) and CLK4 (bottom, orange)). (D) Temperature-dependent kinase activity of CLK1 (black), CLK4 (orange) and SRPK1 (green) was investigated in a temperature range from 12 °C to 56 °C. Assays were performed as in A. (E) Heat- inactivation of CLK1/4 is reversible. Substrate phosphorylation was investigated after incubation at 38 °C for 20 min followed by a shift back of the reactions to 34°C for the indicated times. (F) CD spectroscopy of the CLK1 kinase domain at 25 °C (blue) 34 °C (black) and 38 °C (red). Samples were pre-incubated at the indicated temperatures for 5 min. Data represent the mean of three recorded spectra.

2.4. CLKs globally control temperature-dependent alternative splicing and gene expression

Having shown that CLK activity reacts extremely sensitive to subtle temperature changes within a physiological relevant range in vitro, we investigated the thermometer-like function in vivo with respect to SR protein phosphorylation and AS. To this end we first performed a Western Blot with the phospho-SR specific antibody 1H4. It is known that a heat shock induces hypo-phosphorylation of SR proteins (Shin et al., 2004). Accordingly, we subjected HEK293 cells to a heat shock (42 °C, 2h) followed by a shift back to 35 °C. In the dimethyl sulfoxide (DMSO) control a rapid re-phosphorylation of several SR proteins could be observed, whereas the presence of the CLK1/4 inhibitor TG003 almost completely blocked re-phosphorylation (Figure 2.4.1. A, B), confirming that CLKs are the main kinases controlling temperature-dependent SR protein phosphorylation in vivo.

Next, we performed RNA-seq to analyze AS in dependence of temperature and CLK activity. For this HEK293 cells were kept at 35 °C or 39 °C respectively for 6 hours in the presence or absence of TG003. We found around 1750 cassette exons which reacted in a temperature-dependent manner in the DMSO control samples (Figure 2.4.1. C). Notably, TG003 treatment resulted in an almost complete loss of temperature response in AS (Figure 2.4.1. C). In fact, the 35 °C TG003 sample essentially matched the splicing pattern of the 39 °C DMSO sample, strongly supporting the hypothesis that cold-induced CLK activity is causal for the observed temperature-dependent AS. To obtain a quantitative measure for this observation, we focused on cold-included exons, which represent around 80% of the temperature-sensitive exons in our setting. This analysis revealed a strongly reduced median percent spliced in (PSI) change in TG003-treated cells (DMSO: 30% (39°C) to 63% (35°C), TG003: 15% (39°C) to 33% (35°C)) (Figure 2.4.1. D). We additionally chose four targets which were temperature- and TG003-responsive and could validate the RNA-seq results via splicing-sensitive RT-PCR for all of them (Figure 2.4.1. E).

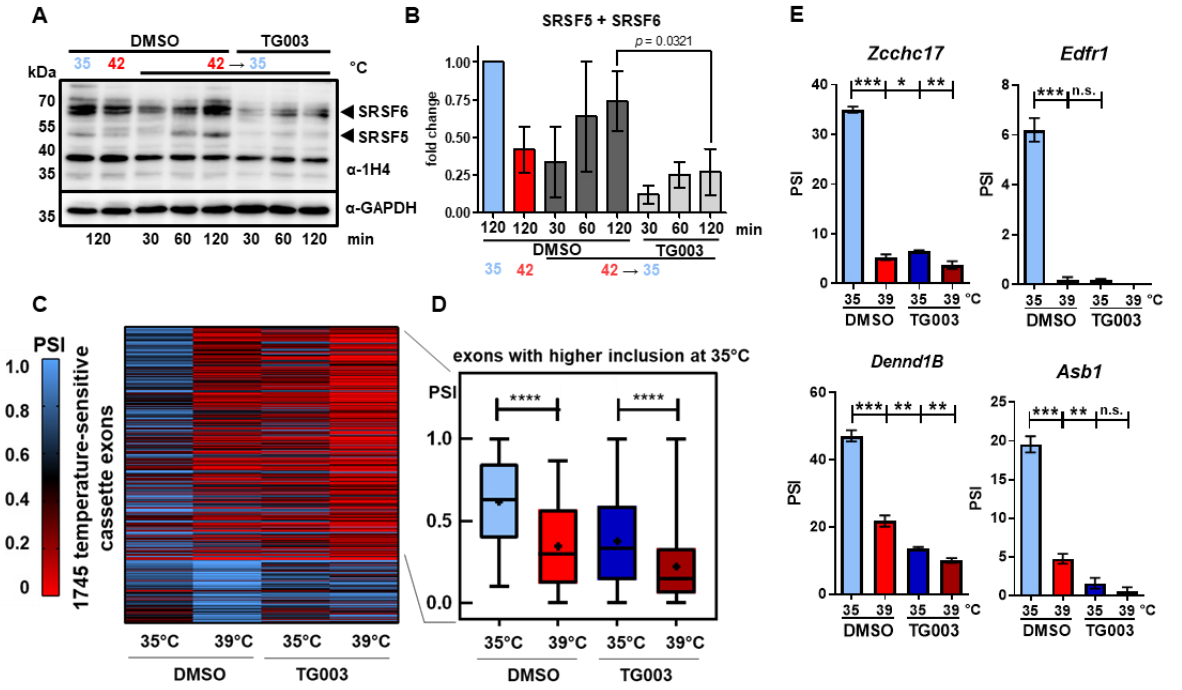

Figure 2.4.1.: CLK1/4 act as molecular thermometer that connects physiological temperature changes with SR protein phosphorylation and AS. (A) HEK293 cells were incubated at 35 °C overnight, then placed at 42 °C, treated with TG003 or DMSO for 2 hours and shifted back to 35 °C A representative Western Blot using the phospho-SR-specific antibody 1H4 is shown. GAPDH served as a loading control. (B) Quantification of Western Blots as in (A) relative to the 35 °C DMSO sample. (C, D) HEK293 cells were pre-entrained at 39 °C for 12 hours. After addition of DMSO or TG003 cells were shifted to 35 °C (or maintained at 39 °C). RNA was extracted after 6 hours and analyzed by RNA-Seq. In (C) a heatmap of percent spliced in (PSI) values of all (1745) skipped exon events that are temperature-dependent in control (DMSO) is shown (n=3). (D) Box-Whisker-Plots of all cold-included exons. Note that the median PSI of the 35 °C TG-003 almost perfectly matches median PSI of the 39 °C DMSO sample. Statistical significance was determined by 1-way ANOVA (Tukey's multiple comparisons test, **p<0.01, ****p<1x10^{-15}). (E) Quantification of radioactive splice-sensitive RT-PCRs for *Zcchc17*, *Edfr1*, *Dennd1B* and *Asb1* temperature-dependent AS. Data represent the mean ± SD of three independent experiments. Statistical significance was determined by unpaired t-test. Derived p values: * < 0.05; ** < 0.01; *** < 0.001. Bioinformatic analysis was done by M. Preussner.

Besides the regulation of AS, SR proteins are involved in the regulation of further pre-mRNA processing events (Long and Caceres, 2009). Hence, we analyzed our RNA-seq data with respect to the expression of whole transcripts. Around 1000 transcripts showed temperature-dependent expression in the DMSO control samples. Strikingly, more than 50% of these genes lost temperature response upon TG003 treatment (Figure 2.4.2. A), suggesting that CLK driven SR protein phosphorylation in a temperature-dependent manner substantially impacts on gene expression. As an interesting example we found the cold-induced RNA-binding protein (*Cirbp*) to be responsive to TG003 treatment as the cold-induced increase in expression at 35 °C was completely abolished upon use of the inhibitor (Figure 2.4.2. B).

Interestingly, our splicing analysis revealed an alternative 3'-end in the *Cirbp* mRNA. Instead of the canonical last exon 7a an alternative exon 7b (which is coupled to exon 8 inclusion) is used. Exon 7b inclusion is strongly promoted by higher temperature in the DMSO control but temperature sensitivity is abolished in the TG003 samples (Figure 2.4.2. C, D). Moreover, we observed evolutionary conserved elements including the 3' splice site of exon 7b in all vertebrates downstream of the canonical polyadenylation site (Figure 2.4.2. C, bottom). Warm-induced inclusion of exon 7b was also observable in primary mouse hepatocytes (Figure 2.4.2. D), suggesting an evolutionary conservation of the AS event. In addition, we found that young mice exposed to a lower ambient temperature, which results in a decreased body temperature (Preussner et al., 2017), showed reduced exon 7b inclusion in liver, which anti-correlated with increased total *Cirbp* expression (Figure 2.4.2. D). We further used the CRISPR/Cas9 technique and generated cell lines lacking exons 7b to 8 in HEK293 cells (Figure 2.4.2. E), resulting in increased *Cirbp* levels (Figure 2.4.2. F) and a decrease in temperature response. However, some residual temperature dependence could be observed, suggesting that further elements contribute to temperature-dependent expression of *Cirbp*.

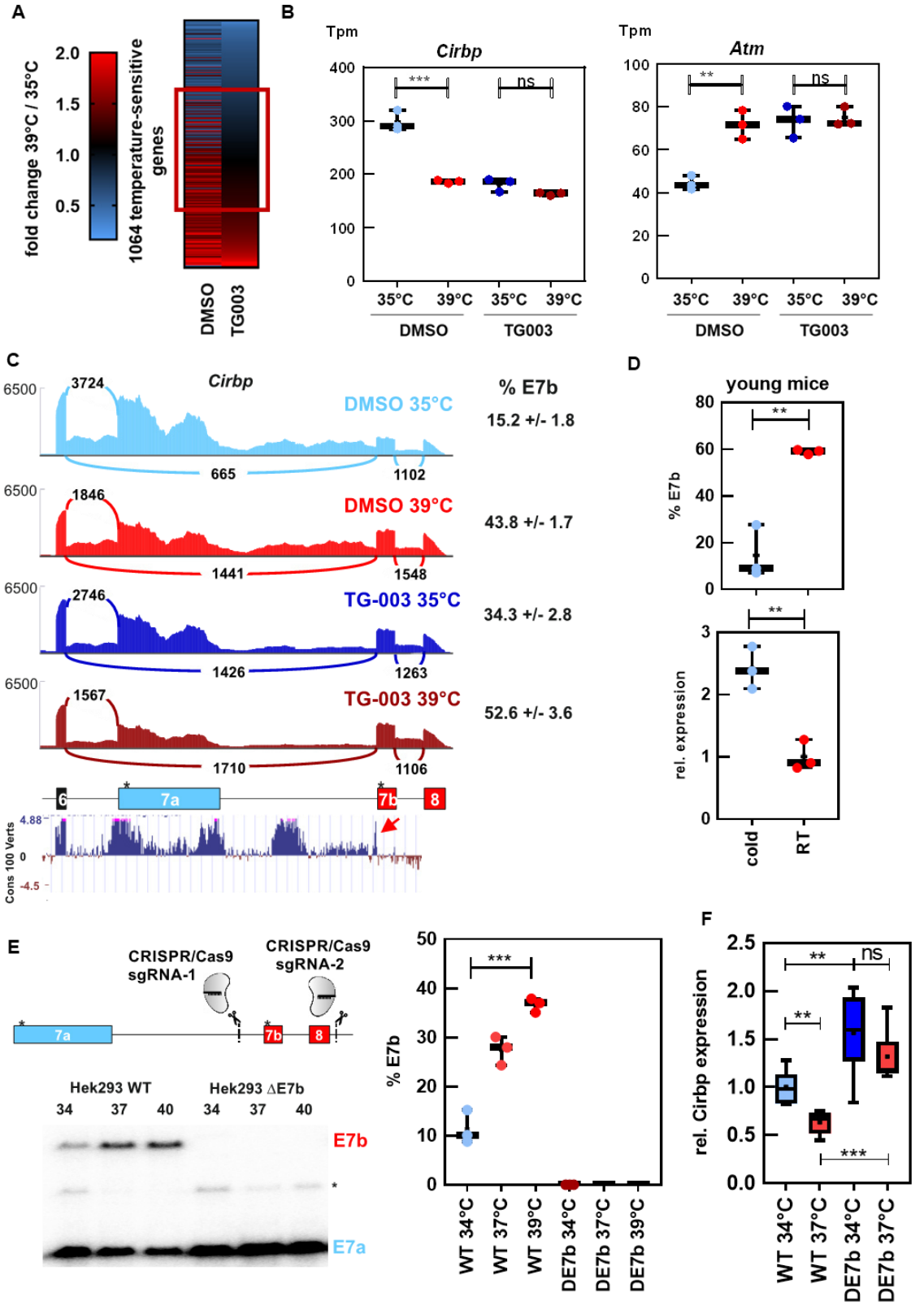

Figure legend on the next page

Figure 2.4.2.: CLK activity controls body temperature-dependent gene expression. (A) Heatmap of 1064 genes with >1.3-fold changed gene expression in DMSO. Genes with a fold-change <1.3 in TG003 (n=507) are indicated by a red box. (B) Examples with abolished temperature-dependent gene expression, amongst them *Cirbp*. Plotted are the transcripts per million (tpm) values. Statistical significance was determined by unpaired t-test. (C) Temperature-dependent AS of the *Cirbp* 3'-end. Top: Exon/Intron structure of the pre-mRNA. Exons are depicted by boxes, introns by lines, the asterisks indicate stop codons. Below, a Sashimi blots shows the read distribution in the region for the different conditions (y-axis set to 6500 reads per base). The lines indicate junction reads. Percentage of the E7b isoform was calculated in the triplicate samples, mean and standard deviation are depicted on the right. At the bottom Basewise comparison among 100 vertebrates by PhyloP is shown. The red arrowhead marks the conserved 3' splice site of exon 7b. (D) *Cirbp* splicing and gene expression in the liver of young mice (12-13 days) kept at room temperature (RT) or at 18°C for 2 hours. Splicing was analyzed by splicing-sensitive RT-PCR with a forward primer in exon 6 and two reverse primers in exons 7a and 7b, gene expression was analyzed by qRT-PCR and is shown normalized to *Hprt* and RT. Statistical significance was determined by unpaired t-tests, **p<0.01. (E) Depletion of exon 7b using CRISPR/Cas9 in Hek293 cells (top: position of guide RNAs), radioactive RT-PCR investigating *Cirbp* AS at the indicated temperatures is shown (bottom) and quantified (right, n=3, mean +/-SD). Statistical significance was determined by unpaired t-tests, ***p<0.001. (F) Increased *Cirbp* expression and reduced temperature dependence in cells lacking the temperature dependent exon 7b. *Cirbp* expression was investigated after 12 hours at the indicated temperatures by qPCR (relative to *Gapdh*, n>5, statistical significance was determined by unpaired t-tests, **p<0.01). Experiments for this figure were performed by M. Preussner, A.-K. Emmerichs, K. Petermann, and S. Meinke.

2.5. CLK temperature dependence is based on subtle conformational changes within the activation segment

The previous experiments revealed that CLKs act as thermometer in vitro and in vivo. Our investigations focused now on how the temperature sensitivity of CLKs is achieved in molecular detail. We therefore performed molecular dynamics (MD) simulations with the published structures of human CLK1 and SRPK1 kinase domains at 20 °C and 40 °C (done by Prof. Dr. Petra Imhof, see publication II for details). The MD simulations revealed no significant, global conformational changes of the kinase domains. Interestingly, the activation segment of CLK1 showed higher flexibility at 40 °C with a movement towards the binding groove. The respective region of SRPK1 however showed rather more flexibility at 20 °C. For experimental evidence of the contribution of the activation segments, we generated swap mutants and performed in vitro kinase assays (Figure 2.5.1. A). Introduction of the SRPK1 activation segment into CLK1, led to a complete loss of temperature sensitivity in the contemplated temperature range (Figure 2.5.1. B, left). SRPK1 in contrast gained temperature sensitivity by introduction of the CLK1 activation segment (Figure 2.5.1. B, right). We further wished to determine the involved amino acids within the activation segments. Thus, we performed an alanine scan of the CLK1 activation segment and found two neighboring amino acids, R342A and H343A, which shifted the inactivation temperature towards warmer temperatures (Figure 2.5.1. C). Consistent with

this finding, these two residues are found in close proximity to one another as well as to the ATP within the active center of CLK1 in our MD simulations exclusively at 40 °C. Differently, H343 is far away from the active center at 20 °C (Figure 2.5.1. D). By aligning the activation segments of CLK1 and SRPK1, we noticed that the histidine at position 343 in CLK1 is replaced by a glutamine in the temperature-insensitive SRPK1. Consequently, we introduced the glutamine in the CLK1 activation segment, resulting in a complete loss of temperature sensitivity in the physiological relevant temperature range (Figure 2.5.1. E).

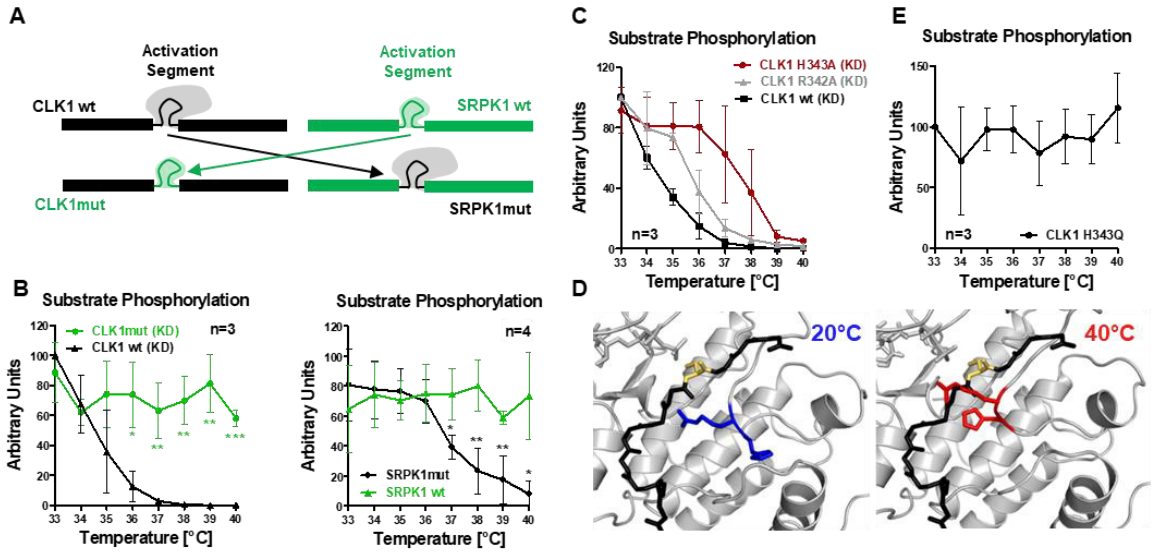

Figure 2.5.1.: Mechanistic and structural basis for temperature-controlled CLK1/4 activity. (A, B) Generation of activation segment switch hybrids (A) transfers loss and gain of temperature sensitivity (B). Quantification of CLK1 kinase domain (KD) wt, R342A and H343A activities. R342A and H343A represent the mutants with the strongest effect on the temperature profile based on an alanine scan in the activation segment. (D) Histidine 343 is required for temperature sensitivity. Kinase assay with the CLK1 H343Q mutant as in B (n=3, mean +/- SD). (E) Zoom into CLK1 kinase domain binding groove at 20 °C (left) and 40 °C (right) as modelled by MD simulations, the substrate (modelled from PDB:1JBP) is shown in black. Critical residues R343 and H344, as well as the ATP are highlighted. At high temperature R343 and H344 adopt a conformation that interferes with substrate binding. The serine, which becomes phosphorylated, is shown in yellow.

2.6. CLK temperature dependence is evolutionarily conserved

Since CLKs are conserved throughout eukaryotic evolution (Yun et al., 1994), we next asked whether CLK homologs from other species also exhibit a thermo-sensory function. To test this we cloned and purified CLK homologs from three poikilotherms (*A. mississippiensis* (American alligator; CLK4), *T. scripta elegans* (Red-eared slider turtle; CLK1) and *D. melanogaster* (darkener of apricot kinase; DOA)), species which adapt to the ambient temperature and thus experience stronger variations in body temperature. In vitro kinase assays revealed that the activity temperature profiles of all three kinases exactly fell into the preferred living temperature ranges with a drop of activity at the upper limit (Fig 2.6.1. A – C). Of note, temperature activity profiles of alligator, turtle and fly CLKs are markedly different from the mouse homologs (see publication II for details). Interestingly, in diverse reptiles sex determination is controlled by the temperature at which eggs are incubated (Capel, 2017). However, a temperature sensor remains elusive. Since temperature activity profiles of alligator and turtle CLK homologs also covered respective male (MPT) and female (FPT) producing temperatures of these species, we performed in vitro kinase assays for the exact FPTs and MPTs. Remarkably, alligator CLK4 and turtle CLK1 activities are reduced to around 20% at the higher temperature (for alligator 33 °C = MPT, for turtle 31.5 °C = FPT) (Figure 2.6.1. D – G). This `switch´-like behavior of the examined reptile CLKs suggests a potential role in temperature-dependent sex determination (TSD). To gain further evidence for this assumption we continued with cell culture experiments in two turtle cell lines (Red eared slider turtle and Common box turtle). In recent studies it has been shown that temperature-dependent AS, more precisely intron retention (IR) events in Jumonji histone deacetylases (e.g. *Jarid2*), are associated with TSD (Deveson et al., 2017; Ge et al., 2018). Therefore, we subjected both cell lines to the respective MPTs (26 °C) and FPTs (31.5 °C) and performed RT-qPCR for IR of intron 15 of *Jarid2*. We could confirm temperature-dependent IR with a higher inclusion level at MPT, consistent with results from literature. In contrast treatment with TG003, which also inhibits turtle CLKs in vitro (data not shown), significantly reduced IR level at MPT but had no effect at FPT (Figure 2.6.1. H).

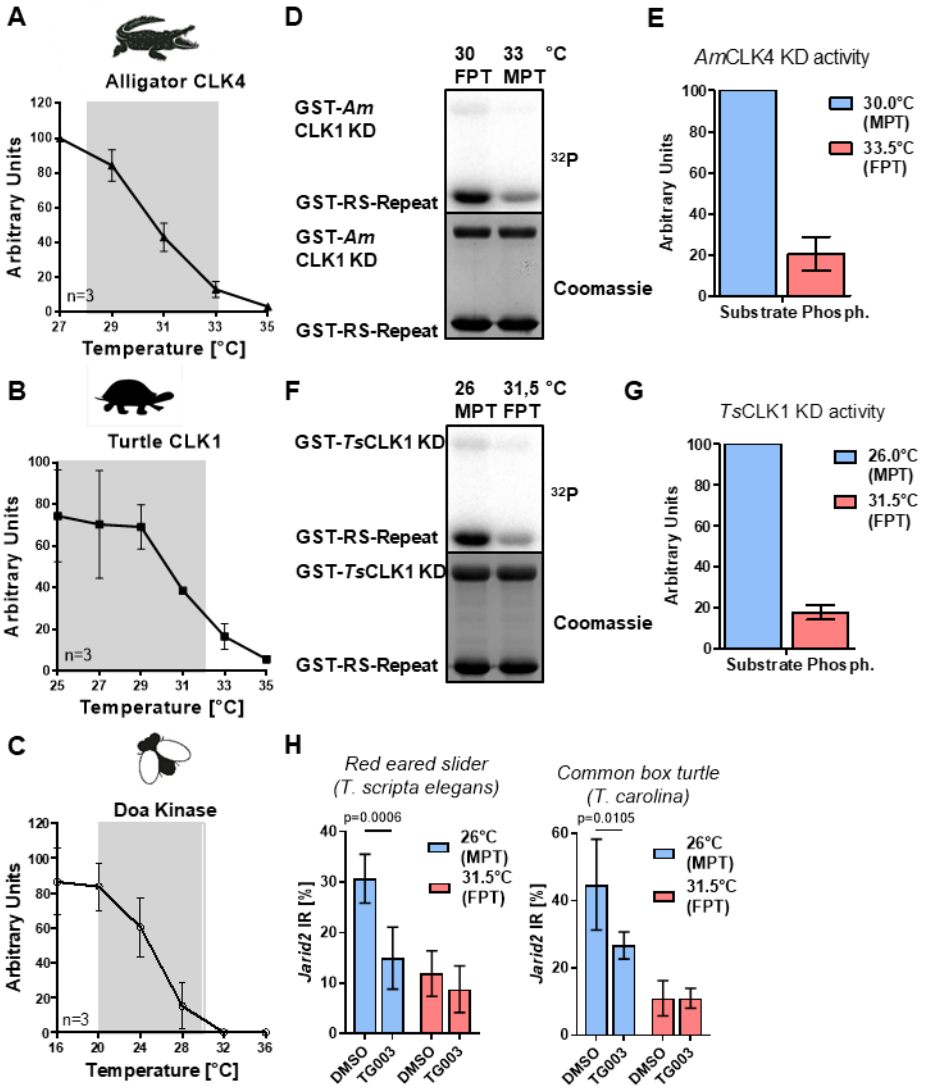

Figure 2.6.1.: Temperature-dependent activity of CLK homologs is evolutionarily adapted. (A-C) In vitro kinase assays of alligator (A), turtle (B) and fly (C) CLK homologs. Preferred living temperatures of the respective species are grey boxed (D, E) In vitro kinase assay of the alligator CLK4 at female producing temperature (FPT, 30 °C) or male producing temperature (MPT, 33 °C). (E, n=3, mean +/- SD). (F, G) In vitro kinase assay of the turtle CLK1 kinase domain (identical in *T. scripta* and *T. carolina*) at MPT (26 °C) and FPT (31.5 °C), quantifications of substrate phosphorylation in (G, n=3, mean +/- SD). (H) Quantification of an intron retention (*Jarid2* Intron 15) event involved in TSD in two independent turtle cell lines (*T. carolina* and *T. scripta*, cell lines established from heart and spleen tissue, respectively) at MPT or FPT with or without the CLK inhibitor TG003, using RT-qPCR. Data represent mean +/- SD of three independent experiments.

3. Discussion

Temperature represents one of the most important external factors in life. Due to the fact that temperature is omnipresent, but mostly not in a fixed spatial or temporal fashion, the ability of organisms to sense potentially harmful temperatures is indispensable. Therefore, diverse organisms, including humans, have evolved exquisite thermo-sensory systems (Tan and Katsanis, 2009). Numerous studies dealt with the consequences of cold or heat exposure (reviewed in Foulkes and Wood, 2007 and in Yarmolenko et al., 2011) or the receptors sensing these temperatures (e.g. Gong et al., 2019; Bautista et al., 2007; Caterina et al. 1997 and reviewed in Wetsel, 2011). However, most research so far concentrated on rather extreme and noxious temperature conditions. In contrast, less attention was paid to consequences of subtle temperature changes e.g. as small as circadian body temperature oscillations in mammals. Hence, this thesis aimed to shed light on molecular mechanisms of temperature perception in a physiological range with respect to alternative splicing, gene expression and a thermometer sensing these small temperature changes.

3.1. Body temperature cycles control rhythmic alternative splicing in mammals

Homoeothermic organisms maintain their core body temperature (CBT) in a narrow, tightly controlled range. Most mammals exhibit a temperature around a set point of 37 °C, but still circadian (~24-hour) temperature oscillations occur within a range of ~ 1 - 4°C (Buhr et al., 2010; Refinetti and Menaker, 1992; Saini et al., 2012). It has been suggested that oscillating expression of a substantial fraction of circadian genes depends on CBT changes (Brown et al., 2002; Buhr et al., 2010; Saini et al., 2012), but so far no data is available if and how these subtle temperature changes influence AS.

In the first publication we showed that a time of the day dependent AS switch of *U2af26*, as already shown in 2014 in our lab (see Preussner et al., 2014), is regulated by such CBT cycles (Preussner et al., 2017). We demonstrated for the first time that these small temperature fluctuations are not only sufficient, but necessary to generate rhythmic AS of *U2af26* and, besides that, additionally for a large group of functionally related genes in a concerted manner. This rhythmic AS program is independent from classical circadian mechanisms, as a continuous temperature input is necessary to maintain rhythmicity (Preußner and Heyd, 2018). We further identified SR proteins as regulators of temperature-dependent AS.

SR proteins are well known splicing factors which are involved in all (pre-) mRNA processing events, e.g. transcription, splicing, nuclear export, translation and mRNA stability (Long

and Caceres, 2009; Maslon et al., 2014; Muller-McNicoll et al., 2016; Zhong et al., 2009, Karni et al. 2007). SR protein activity is controlled by their phosphorylation state which in turn regulates their sub-cellular or sub-nuclear localization (Yeakley et al., 1999) or their interaction abilities (Manley, 1998) finally resulting in an altered AS output. Indeed we found the phosphorylation state of several SR proteins (SRSF2 and SRSF7) to be temperature-dependent while expression and binding abilities were not affected by temperature.

SR protein phosphorylation is a highly dynamic process, which needs to be tightly controlled as dysfunction of SR proteins were reported to be associated with diseases (Fredericks et al., 2015; Hartmann et al., 2001). A network of kinases and phosphatases regulates SR protein phosphorylation. Exemplarily, it has been shown that heat shock leads to dephosphorylation of SRSF10, which requires the activity of the phosphatase PP2A (Shi and Manley, 2007). Inhibiting PP2A activity with the inhibitor ocadaic acid (OA) resulted in repression of exon inclusion of *U2af26* in our settings, basically recapitulating the situation at higher temperatures. However, OA also inhibits the phosphatase PP1 and it remains to be clarified which of these phosphatase or their concerted action contribute to the observed splicing output. Phosphorylation of SR proteins is regulated by two classes of kinases, SRPKs and CLKs (Koizumi et al., 1999; Yeakley et al., 1999). Since CLKs have been shown to rephosphorylate several SR proteins after heat shock (Ninomiya et al., 2011), we considered it likely that these kinases play a role in cold-induced hyper-phosphorylation of SR proteins. Indeed, inhibition, knock down and overexpression of CLK1/4 proved a contribution in temperature-responsive SR protein phosphorylation and AS. Altogether this suggested PP1/PP2A and CLK1/4 as potential thermos-sensors controlling rhythmic AS via dynamic SR protein phosphorylation.

However, it stands to reason that upstream regulators of SR protein phosphorylation must be controlled in a temperature-dependent manner as well. Expression, posttranslational modifications, altered interaction networks or temperature-dependent activity of the kinases or phosphatases could account for the temperature-dependent SR protein phosphorylation state and AS, but remain to be investigated.

Considering the role of SR proteins in several posttranscriptional mRNA processes, it becomes likely that temperature-dependent control of SR protein phosphorylation also impacts gene expression in the body temperature range. As an interesting example we showed that *Tbp*, a core transcription factor (Kornberg, 2007), is alternatively spliced in the 5´UTR in a temperature-dependent manner, leading to oscillating protein expression and ultimately oscillating expression of its target genes. Taken together the above described mechanism defines a thermo-sensory system which translates the input body temperature into altered AS and gene expression programs.

3.2. CLK1/4 act as thermometer in vitro and in vivo

So far we showed that rhythmic AS is controlled by oscillating body temperature cycles (Goldammer et al., 2018; Preussner et al., 2017). We further identified CLK1 and CLK4 as potential regulators of cold-induced SR protein phosphorylation. As the splicing response was observable already 30 min after temperature change, we reasoned that a direct thermo-sensing ability of CLKs rather than expression or changed interaction networks might explain temperature-dependent SR protein phosphorylation and AS. Based on this assumption we showed that CLK1 and CLK4 activity reacts extremely sensitive to subtle temperature changes in a physiological relevant temperature range in vitro. Phosphorylation of a short RS-repeat (mimicking RS domains of SR proteins) and autophosphorylation were significantly increased at lower temperatures matching the observed phosphorylation state of SR proteins in vivo (Preussner et al., 2017). Additionally, inhibition of CLK1/4 in HEK293 cells almost completely blocked rephosphorylation of SR proteins after heat shock, confirming that CLKs are the main kinases of temperature-dependent phosphorylation of many if not all SR proteins, which is also consistent with literature data (Ninomiya et al., 2011).

CLKs consist of an intrinsically disordered N-terminus and a C-terminal catalytically active kinase domain. Our kinase assays reveal that temperature responsiveness is independent of the N-terminus and therefore an inherent feature of the respective kinase domains. Though the N-terminus slightly shifts the temperature activity profile and seems to be important for setting the exact temperature range. It is known that the N-terminus of CLKs promotes binding to SR proteins by contacting their respective RS domains, but it is also able to interact with the kinase domain itself (Keshwani et al., 2015), providing a possible explanation for the slightly shifted temperature activity profile of the full length proteins.

We further demonstrated that heat-inactivation of CLKs is reversible and secondary structure elements remain intact at higher temperatures, suggesting that slight conformational changes rather than global denaturation account for the observed temperature profile (see also discussion part 3.3.). Moreover, we showed that this temperature dependence is not a feature of all SR protein kinases as SRPK1 activity appeared to be stable over the contemplated temperature range. Interestingly, it has been shown that SRPK1 and CLK1 operate in a symbiotic manner. While CLK1 mobilizes SR proteins from nuclear speckles by phosphorylating Ser-Arg and Ser-Pro dipeptides within a certain segment of the RS domain of SRSF1 (RS2) (Velazquez-Dones et al., 2005), nuclear SRPK1 facilitates the release of CLK from the tightly bound phospho-SR protein (pSR) (Aubol et al., 2014; Aubol et al., 2016). This finally results in liberated pSR which than can actively take part in the splicing reaction. Consequently, heat-inactivation of CLKs should inhibit mobilization of SR proteins from nuclear speckles. At the same time, cytoplasmatic

phosphorylation of SR proteins by temperature-independent SRPK1 and subsequent import and localization in speckles should therefore lead to increased nuclear speckle size. Indeed, it has been shown that splicing factors including SR proteins accumulate in enlarged speckles under heat-shock conditions (Spector and Lamond, 2011), supporting this hypothesis. For physiological temperature changes, however, it remains to be proven.

Finally, we provide corroborative evidence that CLKs act as thermometer also in living cells, globally regulating both AS and gene expression. This suggests possible implications for a variety of biological processes. For instance, it has been reported that CLK1 appearance is regulated in a cell cycle dependent manner (Dominguez et al. 2016), providing a possible link of body temperature and cell cycle progression. CLK activity is also likely to impact gene expression under pathological conditions such as hypothermia, septic shock or fever. Furthermore, our findings from poikilotherms suggest a role of the respective CLK homologs in temperature dependent sex determination in reptiles (further discussed in 3.4.). Additionally, we offer an explanation for altered gene expression programs due to (circadian) body temperature oscillations, by elucidation of an CLK- and temperature-dependent AS event in the Cold-inducible RNA-binding protein (*Cirbp*) controlling its expression. CIRBP encodes for a RNA-binding protein, which is imputed in regulation of stability, export and translation of its target RNAs (Yang and Carrier 2001; Morf et al., 2012). Furthermore, CIRBP has been described to be required for high amplitude circadian gene expression (Morf et al., 2012) and is itself expressed in a temperature-dependent manner in mouse peripheral tissues and brain (Nishiyama et al., 1997; Sundgren-Andersson et al., 1998; Kornmann et al., 2007). First hints of how CIRBP expression is controlled in a temperature-dependent manner were presented from Gotic and colleagues (Gotic et al., 2016), showing that not de novo transcription but rather splicing efficiency accounts for the observed Cirbp expression pattern. Our findings now add another mechanisms for temperature control of Cirbp expression, thus directly connecting temperature-dependent CLK activity and posttranscriptionally controlled (circadian) gene expression. However, we cannot rule out the possibility that a cooperative mechanism of both the splicing efficiency (Gotic et al., 2016, Horii et al., 2019) and our observed AS event are required to regulate *Cirbp* expression, because we observed some residual temperature dependence upon deletion of the temperature-responsive Exon 7b by CRISPR/Cas9.

Interestingly, it has been reported that only about 30% of all diurnally expressed mRNAs are dependent on de novo transcription (Koike et al., 2012; Menet et al., 2012), suggesting that the remaining 70% are likely controlled via posttranscriptional mechanisms. Considering the fact that a substantial fraction of circadian genes are controlled by body temperature (Kornmann et al., 2007), our findings of temperature-controlled AS and gene expression by CLKs might deliver an explanation for this phenomenon.

To the best of our knowledge CLKs represent the most sensitive thermo-sensors described so far. Indeed, other temperature-sensing receptors have been identified, but can clearly be differentiated from CLKs. For instance, TRPM8, a member of the transient receptor potential (TRP) ion channel family, senses cool temperatures with an activation threshold of < 28 °C (Bautista et al. 2007 and reviewed in Wetsel, 2011). GluK2, a member of the ionotropic glutamate receptor family, shows an even lower activation threshold of < 20 °C (Gong et al. 2019). Additionally, heat-sensing receptors have been reported, e.g. TRPV1, being activated at temperatures above 43 °C (Caterina et al., 1997). All above-mentioned receptors share the properties that they reside in sensory neurons and sense rather extreme and potentially noxious temperatures, thereby inducing protection mechanisms. In contrast, CLKs are broadly expressed in diverse tissues and are able to respond to slight endogenous temperature changes. Our combined results therefore define CLKs as a novel class of temperature-sensors, ultimately adapting AS and gene expression to changes in body temperature as well as innocuous ambient temperatures.

3.3. Mechanistic insights of CLK1 temperature sensitivity

To gain further insights into molecular details of CLK temperature dependence, we performed MD simulations and showed that no global structural changes of the kinase domains occur, supporting the assumption that rather small conformational rearrangements must account for the temperature sensitivity. Indeed, we only found slightly increased flexibility of the CLK1 activation segment at 40 °C, showing a movement towards the substrate binding site of CLK1. The SRPK1 activation segment in contrast showed rather reduced flexibility at 40 °C, altogether suggesting a role of this region in generating temperature sensitivity. The activation segment represents a regulatory element of kinases, which is typically 20 - 35 residue long and forms a crucial part of the substrate binding site (Nolen et al., 2004). In many kinases the activation segment needs to be phosphorylated for generating a conformation competent for activity. However, in the published human CLK1 structure the activation segment adopts a typical conformation of active kinases without being phosphorylated (Bullock et al., 2009). This indicates that a temperature-dependent conformational switch of the activation segment could indeed account for the observed activity change of CLKs in dependence of temperature. Consequently, we generated activation segment swap mutants, resulting in a loss of temperature dependence for CLK1 and a gain of temperature dependence for SRPK1, providing evidence for a thermo-sensory function of this region in CLKs. We further demonstrated that two amino acids within the activation segment of CLK1, R343 and H344 are critical for generation of temperature dependence of CLKs, as their mutation to alanine shifted the inactivation

temperature towards the heat. Strikingly, mutation of the histidine to glutamine (present in SRPK1 at this position) in CLK1, abolished temperature sensitivity altogether.

Activation segments can further be subdivided in secondary structure elements. One of those represents the so called P+1 loop, located at the C-terminal portion of the activation segment, which is crucial for the interaction with the substrate (Nolen et al., 2004). R343 and H344 are exactly located within the P+1 loop and underwent the most significant conformational change in our MD simulations. At 40 °C particularly the arginine is pushed into the binding cleft, suggesting that an altered formation of the binding pocket at higher temperatures might prevent binding of the substrate. If so, the substrate K_m must be temperature-dependent as well. So far we failed to prove this assumption e.g. by isothermal titration calorimetry (ITC) due to constraints of protein stability and required amounts. To overcome these issues the surface plasmon resonance technique would serve as an alternative. Although we could confirm the MD simulation data with biochemical assays, a direct observation of the temperature-dependent structural rearrangements is indispensable to clarify the underlying mechanism in molecular detail. A recently developed method could be used for this aim. Temperature-jump solution X-ray scattering (T-jump SAXS/WAXS) allows to study protein motions in dependence of temperature and would therefore be suitable in this context (Thompson et al., 2019). Classical NMR experiments could be conducted as well.

Finally, our observations are in accordance with a current model of temperature-dependent behavior of enzymes. The so called Equilibrium Model (EQM) signifies that a not denatured, but inactive intermediate is in rapid equilibrium with the active form. The inactive form at the same time can be clearly differentiated from denaturation, because it operates over shorter timescales and structural changes are almost imperceptible (Daniel and Danson, 2010; Daniel and Danson, 2013).

It can be concluded that small structural rearrangements within the activation segment of CLKs cause temperature dependence. The two critical amino acids are conserved in all tested CLK homologs (data not shown), suggesting an evolutionary function of CLKs as thermo-sensors. Furthermore, our findings create a base for the rational design of kinases with distinct temperature activity profiles.

3.4. A role for CLKs in temperature-dependent sex determination (TSD) of reptiles?

In many reptiles the sex of the offspring is determined by external clues such as temperature. For instance, in the turtle species *Trachemys scripta* incubation of eggs at 26 °C exclusively leads to male offspring, whereas incubation at 31.5 °C results in females only. Our data from reptilian CLKs suggested a role in TSD as the activity of an alligator and a turtle CLK homolog essentially behaved like an on-off switch at the respective male producing (MPT) or female producing temperatures (FPT).

TSD is known for more than 50 years (Charnier M., 1966) and ever since considerable advances have been made to uncover underlying mechanisms. A recent study identified the lysine-specific demethylase 6B (*Kdm6b*) as a regulator of TSD (Ge et al., 2018). *Kdm6b* expression is high at male producing temperature (MPT) but low at female producing temperature (FPT) in *Trachemys scripta*. Among the genes regulated by *Kdm6b* is doublesex- and mab-3-related transcription factor 1 (*Dmrt1*), which is a key regulator of the male pathway (Ge et al., 2017). *Kdm6b* acts on *Dmrt1* expression by removing repressive methylations of lysine 27 on histone 3 (H3K27me3) within the *Dmrt1* promotor region, allowing *Dmrt1* to be highly expressed at MPT. These striking findings added another piece to the puzzle of TSD, but a thermo-sensor regulating *Kdm6b* expression in a temperature-dependent manner still remains largely elusive. However, another study reported alternative intron retention (IR) events occurring in a temperature-dependent manner in Jumonji chromatin modifiers in dragon, alligator and turtle, amongst them *Kdm6b* and *Jarid2* (Jumonji and AT-rich interaction domain containing 2) (Deveson et al., 2017). In both cases highest intron retention levels were observed when expression peaked in a temperature- and developmental stage-dependent manner. Our cell culture experiments in two turtle cell lines revealed that the IR event in *Jarid2* is dependent on the cold-induced activity of the turtle CLK1 homolog (TsCLK1), as inhibition of TsCLK1 at MPT reduced IR to the level at FPT, whereas no effect was observable at FPT, suggesting an involvement of CLKs in regulating this TSD associated event. However, we only see very low and temperature-independent IR of *Kdm6b* in our setting. It is possible that temperature-dependent IR of *Kdm6b* (or the IR event per se) exclusively occurs during the sex fate decision in the developing gonads, whereas *Jarid2* IR may be functional systemically also in fully differentiated cells. It also remains unclear to date what these IR events in *Kdm6b* and *Jarid2* entail. The high abundance of the IR containing isoforms (see Deveson et al., 2017) excludes degradation via NMD. The presence of premature stop codons in the respective introns suggests either translation of truncated protein isoforms with potentially altered functions, or a detention of the IR containing isoforms in the nucleus preventing them from being translated. Yet, the ladder possibility is unlikely, because less protein would contradict

the findings from Ge and colleagues (Ge et al., 2018). Considering that Jarid2 is a part of the polycomb repressive complex 2 (PRC2), facilitating efficient binding to its target loci (Kaneko et al., 2014; Sanulli et al., 2015), it appears to be likely, that a truncated protein isoform exhibits altered functions in this process. PRC2 possesses an intrinsic methyltransferase activity and can, amongst others, mono-, di- and tri-methylate lysine 27 in histone 3 (H3K27) (Laugesen, Højfeldt and Helin 2019), finally silencing the respective locus. Thus, PRC2 would counteract Kdm6b demethylase activity on the *Dmrt1* locus at turtle MPT. Therefore, it seems plausible that the Jarid2 IR isoform may change binding properties of the PRC2 complex. However, since it is not clear if Jarid2 is able to facilitate PRC2 binding to the Dmrt1 promotor region this remains speculation.
Interestingly, temperature- and developmental stage-dependent *Cirbp* expression has been implicated in TSD of a turtle species (Schroeder et al., 2016). According to that it has been speculated that *Cirpb* contributes to the regulation of Kdm6b and Jarid2 IR events (Georges and Holleley, 2018). As we have shown that CLKs control AS and with this gene expression of *Cirbp* in a temperature-dependent manner in a mammalian system, a similar mechanism in reptiles seems to be possible. This assumption is further supported by the fact that the 3´splice site and intronic regions downstream of the canonical exon 7a, likely responsible for the temperature-dependent AS of exon 7b in mammalian, are highly conserved amongst vertebrates, including reptiles. To fully understand the underlying mechanism the CLK controlled AS event in *Cirbp* in reptiles, the connection of *Cirbp* and the IR events and the role of these IR events within TSD remain to be investigated.

Altogether we suggest a contribution of CLKs within the TSD process, albeit molecular mechanisms are unclear so far. However, we do not claim that we have discovered the one enigmatic thermometer here since a fundamental process like sex determination is most likely a synergy of several pathways. Nevertheless, a stabilizing or initializing function of temperature-controlled CLK activity regulating downstream AS events and gene expression appears to be plausible.

Appendix: Structural insights of temperature adaption of a CLK homolog from *Cyanidioschyzon merolae*

Contributions to this project:

TH cloned and expressed all proteins. TH designed and cloned all mutants. TH helped AK with large scale purifications. TH performed kinase assays, CD-spectroscopy and generated samples for mass spectrometry. TH conceived the study together with FDB and analyzed the data.

Material and Methods

Cloning

Open reading frame (ORF) encoding for CLK1 kinase domain was amplified from a murine cDNA sample or for *C.merolae* Lammer-like kinase from *C. merolae* genomic DNA and cloned into the pGEX-6P-1 vector using the restriction sites *Eco*RI at the 5'-end and *Xho*I at the 3'-end. All point mutations and element exchanges were introduced via 2-step PCR. The pGEX-6P-1 vector guides the production of N-terminally glutathione S-transferase (GST)-tagged, PreScission-cleavable fusion proteins. Constructs were confirmed by sequencing.

Protein expression and purification and crystallographic procedures

Data presented here is based on time-consuming optimization of protein purification and crystallographic procedures. Furthermore the crystal structure of LlK is so far not publicly deposited anywhere, which is why purification procedures are only briefly outlined here and buffer compositions and crystallographic procedures are omitted.

All proteins were produced in *Escherichia coli* BL21 pLys cells in LB-medium for 4 hours at 18 °C after induction at an OD_{600} of ~ 0.6 with 0.4 mM IPTG. The following steps were performed at 4 °C. Cells were resuspended in solubilization buffer and lysed by sonication. Cell debris was separated from the soluble fraction by centrifugation for 45 min at 55,900 x g in an Avanti J-26 XP centrifuge (Beckman Coulter). Target proteins were captured on glutathione agarose (Macherey-Nagel) and washed with solubilization buffer. The GST-tag was cleaved with 1:50 PreScission on the column overnight. The flow-through was collected followed by concentration and size exclusion chromatography (SEC) in solubilization buffer using a Superdex 200 column (GE Healthcare).

Kinase assay

Reaction mixtures contained the respective kinase, GST-RS substrate, kinase buffer (70 mM Tris-HCl (pH 7.6), 10 mM $MgCl_2$, 5 mM DTT) and ~2mM [γ-^{32}P]ATP (~0.025 Ci mmol^{-1}) in a final volume of 15 µl. Proteins were affinity purified with glutathione, but not eluted. Bead slurry with bound kinases and substrate were mixed 1:1 and washed 5 times with lysis buffer. After the final wash, samples were split into 9 fractions, supernatant was discarded and 14 µl 1X kinase buffer was added to each fraction. Reaction mixtures were pre-incubated without [γ-^{32}P]ATP for 20 min at indicated temperatures, then 1µl [γ-^{32}P]ATP (2mM final concentration) was added followed by another 5 min incubation step. Reactions were stopped by adding 6X SDS-loading dye, samples were heated to 95°C for 5 min and analyzed on a 12% SDS PAGE. Gels were stained with Coomassie and imaged. Afterwards, they were transferred onto filter papers and dried for 1 hour in a gel drier. The dried gels were exposed to phosphoscreens overnight. Detection was carried out with a Phosphoimager and ImageQuant TL software.

Generation of mass spectrometry samples

For analyzing the phosphorylation state of the short RS-repeat peptide, first a kinase assay was carried out (see above), followed by cleavage of the RS-repeat from the GST-tag. Briefly, 1 µM of the respective kinase and 10 µM of the purified GST-RS-repeat were incubated in a reaction volume of 90 µl in 1x kinase buffer at 32, 40 and 48 °C for 20 min without ATP. Subsequently, ATP was added to a final concentration of 200 µM followed by a 10 min incubation step. Assay was stopped by addition of EDTA (final 20 mM). Samples were incubated with glutathione agarose for 1h at 4 °C, and washed three times with a suitable buffer for mass spectrometry (25mM NH_4HCO_3, pH 7.9). The RS-repeat was removed from GST with a 1:50 dilution PreScission overnight. Supernatant was separated from glutathione agarose by centrifugation and sent for mass spectrometry analysis.

CD spectroscopy based thermal melting analyses

All tested kinases were measured in kinase reaction buffer (see kinase assay). CD measurements were performed with a JASCO 1.30 spectropolarimeter. Thermal melting was measured at 220 nm, with temperature ramping from 25 °C to 90 °C in 1 °C/min steps.

Results

In this study we aimed to investigate temperature-dependent kinase activity of a CLK homolog from *Cyanidioschyzon merolae* (LAMMER-like dual specificity kinase (LIK)), an acidophilic, unicellular red algae growing in hot springs, tolerating temperatures up to 56 °C. To this end we cloned and purified the kinase domain from LIK and performed in vitro kinase assays ranging from 12 - 56 °C. Strikingly, we observed a maximum activity at around 48 °C, exactly fitting the living temperature of *C. merolae* (Figure A1 A and B). In accordance with the data from mouse CLKs, the activity of LIK kinase domain dropped at the upper limit of the preferred living temperature between 48 °C and 52 °C. CD spectroscopy revealed a melting temperature of ~ 55 °C (data not shown), thus excluding global unfolding as reason of the activity decrease.

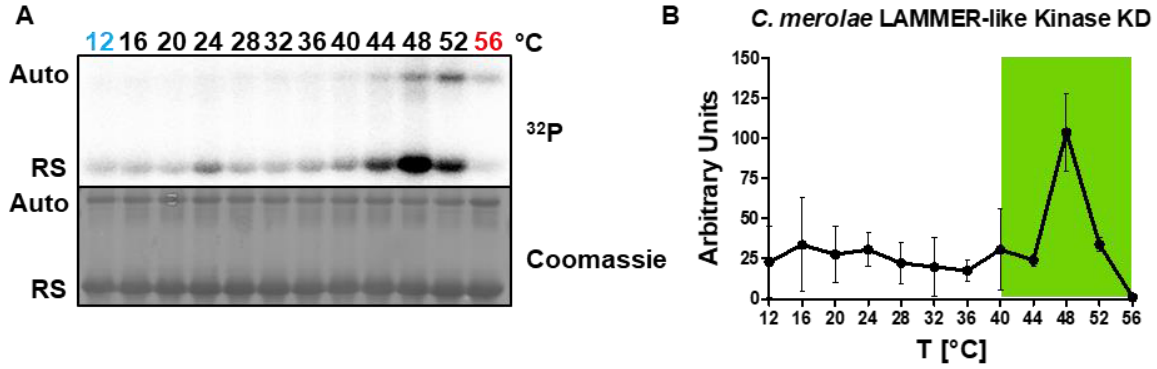

Figure A1: *C. merolae* LAMMER-like kinase KD activity is adapted to high temperatures. (A) In vitro kinase assay of *C. merolae* LAMMER like kinase (LIK) kinase domain in a temperature range from 12 to 56°C. GST-RS-repeat served as a substrate (RS). (B) Quantification of in vitro kinase assay (n=3, mean +/- SD). Preferred living temperature of *C. merolae* is green boxed.

In order to gain insights into temperature-dependent activity and heat-stability of LIK we crystallized the kinase domain (residues 448 - 816) and obtained a structure at a resolution of 2.5 Å (done by F. De Bortoli, A. Kotte and B. Loll) (Figure A2).

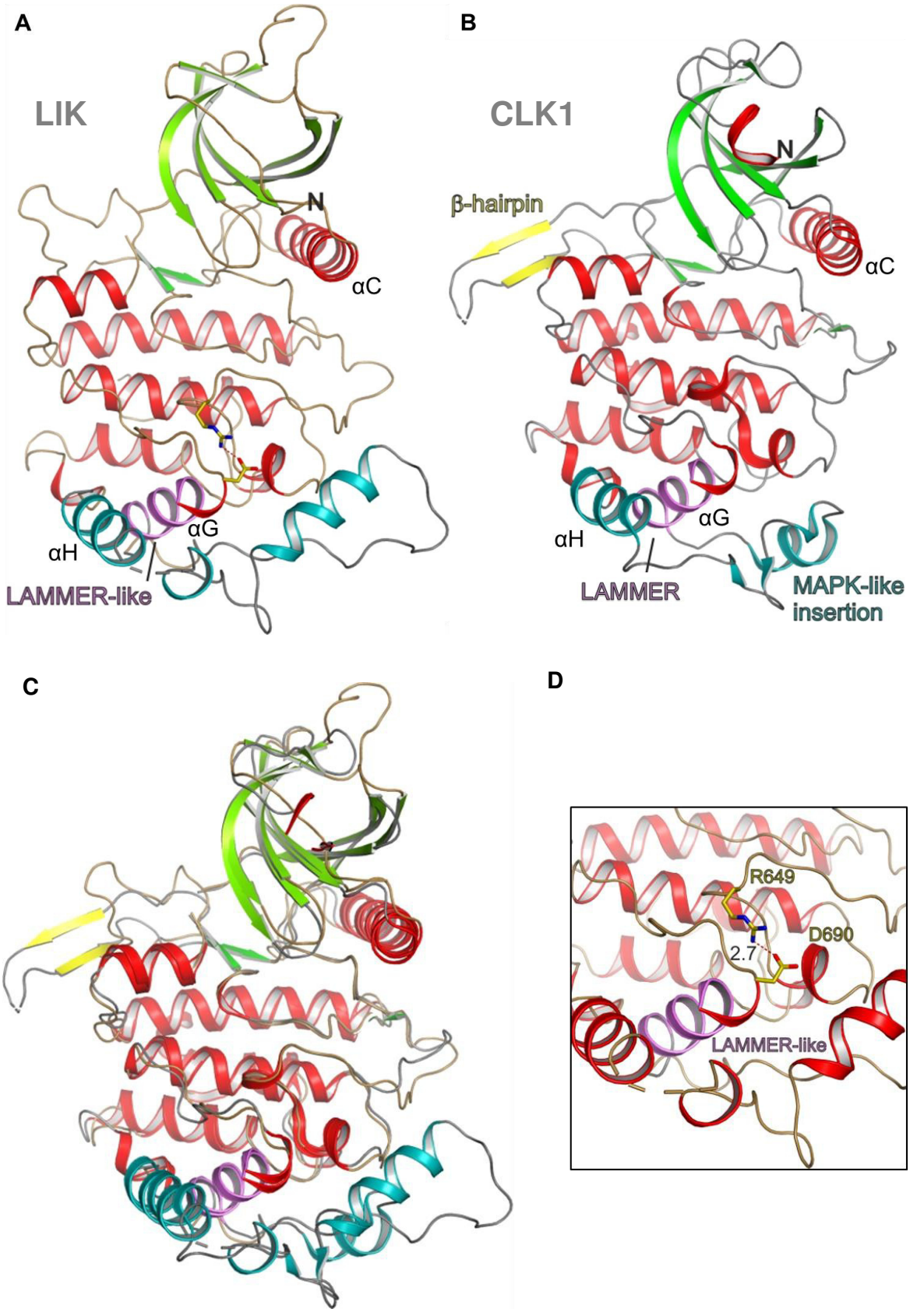

Figure legend on the next page

Figure A2: Crystal structure of *C. merolae* LIK kinase domain. (A) Overall structure of the LIK kinase domain. The CLK family signature motif (EHLAMMERILG) is located within the αG α-helix shown in magenta. As the sequence present in LIK is EHLQLMQKLLQ, the motif is termed LAMMER-like. (B) Overall structure of the human CLK1 kinase domain (PDB code 1Z57). Structural insertions specific for CLKs are highlighted in different colors. (C) Superimposition of LIK and CLK kinase domains. Note that the β-hairpin (yellow) is not present in the Llk structure. Furthermore, the MAPK-like insert in CLK1 is replaced by an extended loop and a large α-helix in LIK (turquoise). (D) Zoom into the LIK kinase core. Arginine 649 within the P+1 loop of the activation segment forms a salt bridge with aspartate 690. In hCLK1 the aspartate is replaced by a serine (S383).

The structure of the LIK kinase domain displays a classical kinase fold. The N-terminal lobe is rich in β-sheets and comprises the αC helix (Figure A2 A). The C-terminal lobe is mainly composed of α-helices, forming the kinase core. Overall LIK exhibits a conformation typical for active kinases with a well ordered activation segment. As in the human CLK1 kinase domain structure (Figure A2 B), LIK harbors an additional α-helix (αH) at the bottom of the C-terminal lobe, which is exclusively found in CLKs (Bullock et al., 2009). However, the MAPK-like insert, found in CLK1, looks markedly different in LIK. Instead of a small α-helix followed by a two-strand β-sheet, the insertion in LIK comprises an extended loop region followed by a large α-helix. Additionally, the unique CLK β-hairpin insert located between the N-terminal and C-terminal lobe is replaced by a short loop region. With respect to heat-stability of LIK we noticed that the arginine 649 within the P+1 loop of the activation segment forms a salt bridge with aspartate 690 located on the top of the αG helix (Figure A2 D). In contrast to LIK, the aspartate is replaced by a serine in CLK1 (S383), preventing the formation of a salt bridge. Hence, we reasoned that the salt bridge might lock the activation segment in a conformation competent for activity also at higher temperatures.

To test this hypothesis we replaced the serine with an aspartate in hCLK1 to generate the salt bridge and broke the salt bridge in LIK by introducing the serine. We then performed kinase assays at 32 °C (high activity of CLK1, moderate activity of LIK), 40 °C (no activity of CLK1, moderate activity of LIK) and 48 °C (maximum activity of LIK) (Figure A3 A and B).

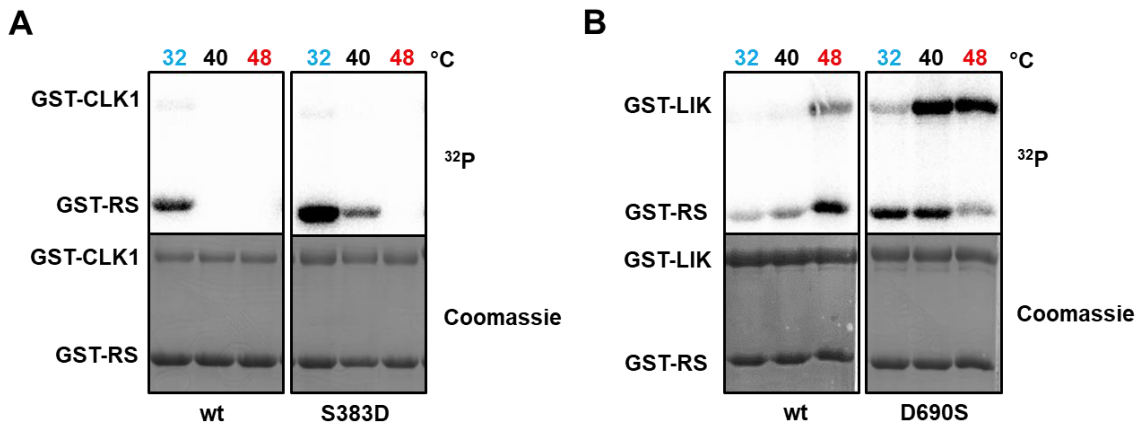

Figure A3: Salt bridge switch mutants exhibit temperature-dependent activity characteristics of the respective homologs. (A) In vitro kinase assays of GST-tagged wild type CLK1 (wt) or CLK1 S383D performed at 32 °C, 40 °C and 48 °C. A GST-RS-repeat served as a substrate. Coomassie stained SDS-PAGE shows equal loading of the proteins and the substrate. (B) In vitro kinase assay as in A with GST-tagged wild type LIK (wt) or LIK D690S.

As expected wild type CLK1 was active at 32 °C, but neither at 40 °C nor at 48 °C activity was observable (Figure A3 A, left), consistent with the previous results from this study. In contrast, formation of the salt bridge in CLK1 led to detectable activity at 40 °C, however reduced in comparison to 32 °C (Figure A3 A, right). CD spectroscopy revealed a slightly increased melting temperature of mCLK1 S383D of ~ 43 °C (CLK1 wt ~ 40 °C, data not shown), which also explains that no activity is observable at 48 °C. In contrast, LIK showed moderate activity at 32 °C and 40 °C and an increased activity at 48 °C (Figure A3 B, left). Breakage of the salt bridge significantly reduced activity at 48 °C compared to 32 °C and 40 °C (Figure A3 B, right). The melting temperature of LIK D690S was determined with ~ 44 °C (LIK wt ~ 55 °C, data not shown), suggesting that stability is reduced. Interestingly, autophosphorylation of LIK D690S appeared to be strongly increased relative to substrate phosphorylation and was even detectable at 48 °C. We further performed MALDI-TOF mass spectrometry with the substrate peptide and could recapitulate the results from the in vitro kinase assays, as wt CLK1 phosphorylated the substrate only at 32 °C, whereas CLK1 S383D showed substantial substrate phosphorylation also at 40 °C (Figure A4 A and B). Accordingly, we detected substrate phosphorylation by wt LIK at 32, 40 and 48 °C, but only at 32 °C and 40 °C for LIK D690S (Figure A5 A and B). However, we observed that CLK1 phosphorylated 3 serines within the peptide. Neither temperature nor presence or absence of the salt bridge influenced this multi-site phosphorylation behavior. In contrast, LIK phosphorylated only one serine within the substrate independent of temperature and the presence or absence of the salt bridge.

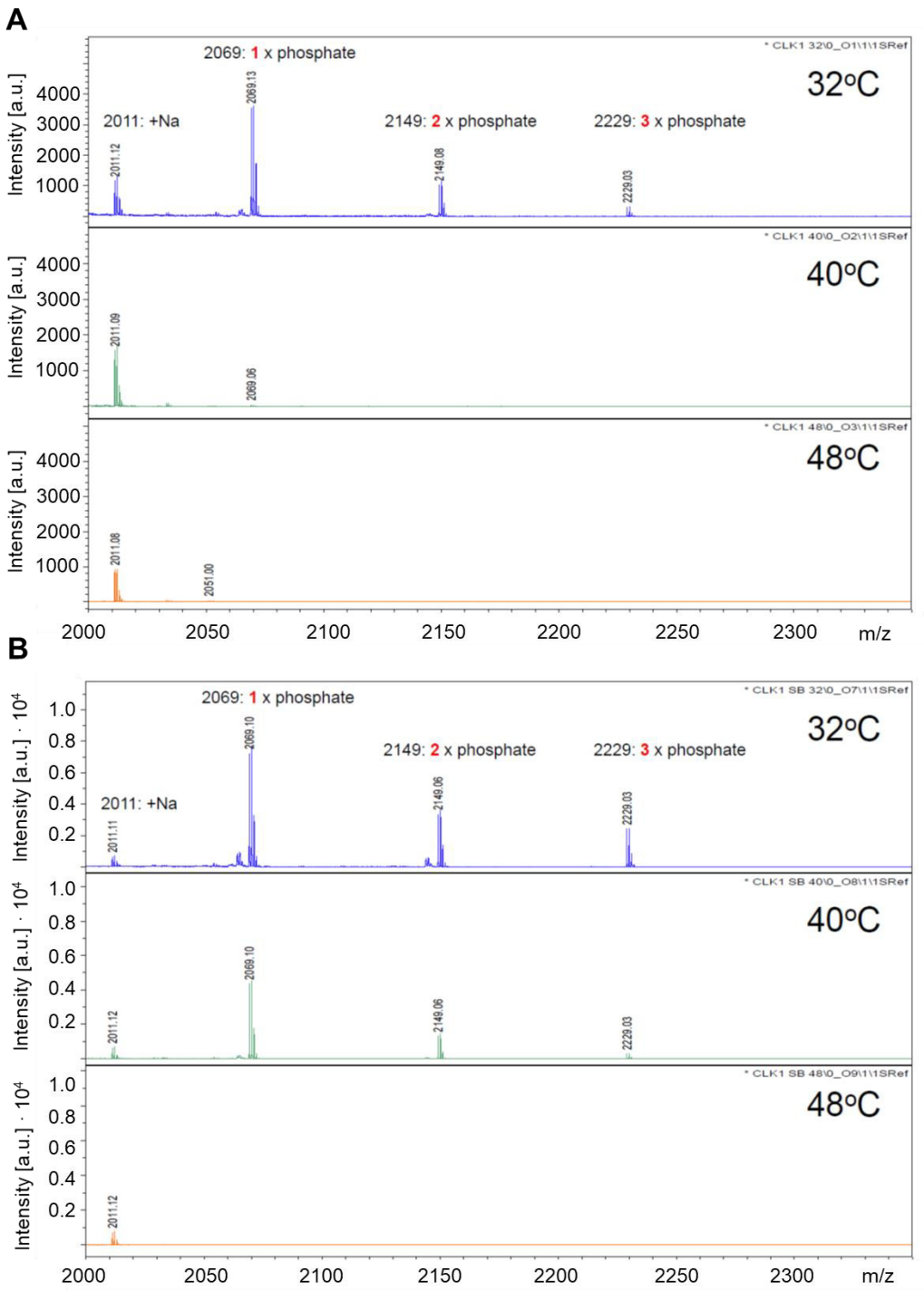

Figure A4: MALDI-TOF mass spectrometry of a RS-repeat substrate peptide after phosphorylation by CLK1. (A) Spectra of the peptide GPLGSPEFGRSRSRSRSR taken after in vitro kinase assays performed with wild type CLK1 at 32 °C, 40 °C and 48 °C for 10 min. Phosphorylated species are marked at the respective m/z ratios. (B) Spectra as in A. Kinase assays were performed with CLK1 S383D. Note the presence of phosphorylation also at 40 °C.

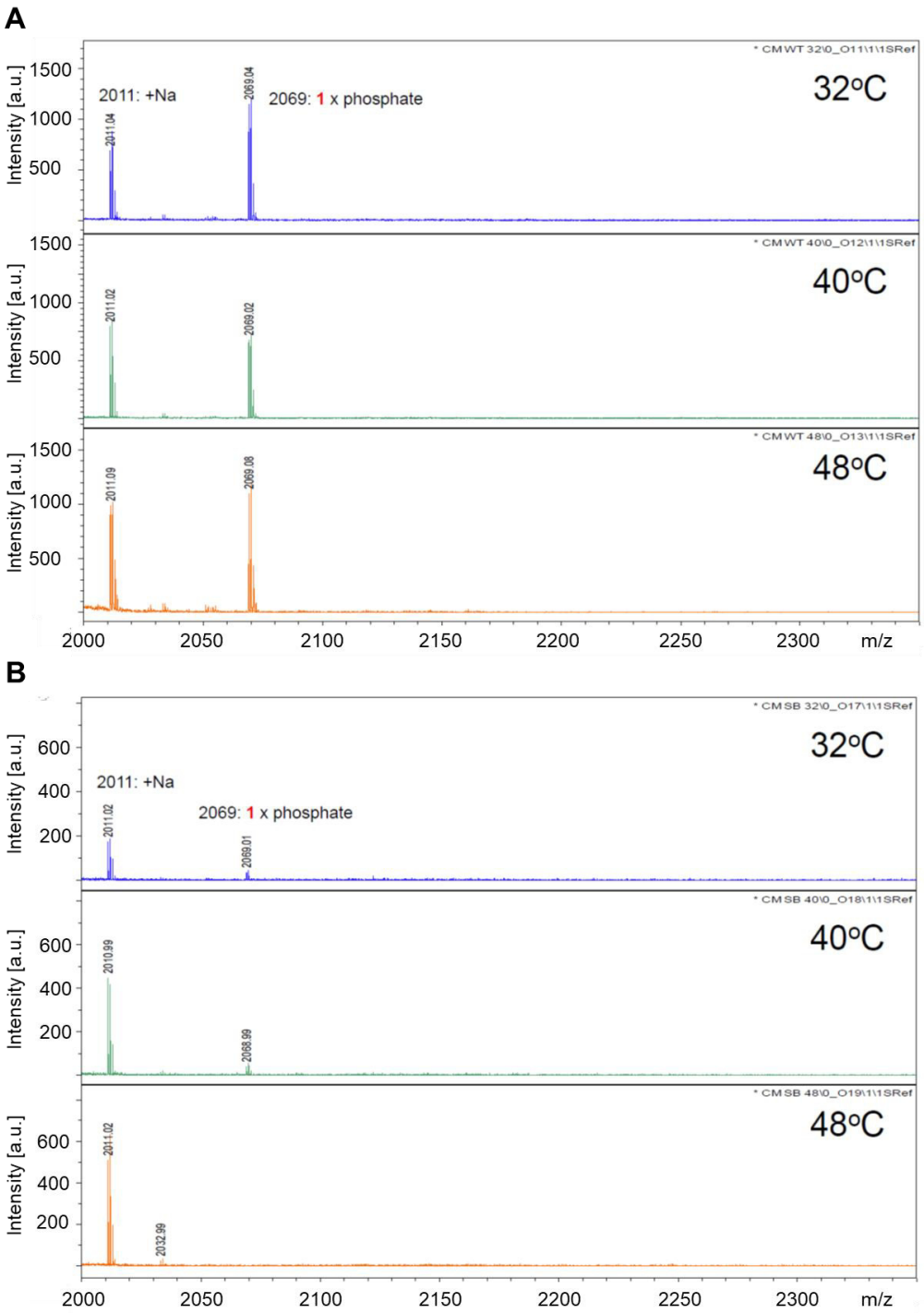

Figure A5: MALDI-TOF mass spectrometry of a RS-repeat substrate peptide after phosphorylation by LIK. (A) Spectra of the peptide GPLGSPEFGRSRSRSRSR taken after in vitro kinase assays performed with wild type LIK at 32 °C, 40 °C and 48 °C for 10 min. Phosphorylated species are marked at the respective m/z ratios. (B) Spectra as in A. Kinase assays were performed with LIK D690S.

Discussion

Cyanidioshyzon merolae is member of *Cyanidialis*, an order of red algae which branched off quite early in eukaryotic evolution approximately 1.3 billion years ago (Yoon et al., 2004). It is a unicellular algae with a very simple architecture and is therefore used as a model organism to study different aspects of eukaryotic evolution. Furthermore, *C. merolae* inhabits sulfuric hot springs (pH 1.5, ~ 45 °C), which may resembles ancient earth environments. The ability to tolerate relatively high temperatures makes *C. merolae* also interesting for structural biologists as heat-stable proteins are unique among eukaryotes.

Within this part of the thesis we demonstrate that a CLK homolog from *C. merolae* (LIK) exhibits a temperature activity optimum exactly in the preferred living range of the organism with a maximum activity at 48 °C. Furthermore, the activity significantly dropped already at 52 °C, the upper limit of the preferred living temperature of *C. merolae*. Using CD spectroscopy we determined a melting temperature of ~ 55 °C, suggesting that conformational changes may account for the loss in activity rather than global unfolding (as shown for CLK1). To gain insights into structural features contributing to heat-stability and temperature-dependent activity, we intended to obtain a crystal structure of LIK. Consequently, the kinase domain of LIK was expressed, purified and its crystal structure determined to 2.5 Å resolution. The structure adopts a canonical kinase fold, as present in all kinases within all kingdoms of life. Notable differences to other kinase subfamilies are observed in secondary structure elements. The activation segment of LIK adopts a structured conformation without any posttranslational modifications. Together with the overall closed conformation of the kinase domain, typical for active kinases, this suggests that LIK is a constitutively active kinase like CLK1 and SRPK1 which do not need posttranslational modifications or interactivation partners for catalysis (Bullock et al., 2009; Ngo et al., 2005; Ngo et al., 2008). The LIK kinase domain harbors an additional α-helix (αH) at the bottom of the C-terminal lobe, which is exclusively found in CLKs (Bullock et al., 2009). Interestingly, the CLK specific β-hairpin insert located between the N-terminal and C-terminal lobe is replaced by a shortened loop segment. Furthermore, LIK comprises an unusual extended loop followed by a large α-helix at the bottom of the C-terminal lobe, instead of the MAPK-like insert found in CLKs. Taken together LIK shows a somewhat exceptional composition of elements. Indeed, typical insertions of CLKs are present, yet others are missing, suggesting that unique CLK elements like the β-hairpin or the MAPK-like insert evolved later during eukaryotic evolution.

We furthermore identified a salt bridge formed between arginine 649 within the activation segment and aspartate 690 located on top of the αG α-helix within the C-terminal lobe of LIK. The arginine within the activation segment is conserved in both kinases, but the salt bridge is not formed in CLK1 as the neighboring aspartate is replaced

by a serine. As shown in publication II of this thesis, the arginine in CLK1 undergoes a conformational change at warmer temperatures such that it moves towards the active site and likely blocks substrate access. Presence of the salt bridge in LIK may prevent this conformational switch also at a temperature of 48 °C. It is conceivable that after exceedance of a certain threshold temperature enough energy is provided to break the salt bridge, possibly resulting in the aforementioned conformational change of the arginine and consequently reduced activity.

Also, we found that deletion of the salt bridge in LIK resulted in a decreased melting temperature, suggesting that it stabilizes the whole enzyme at higher temperatures. However, the temperature-dependent activity increase up to 48 °C remains to be investigated. In accordance with the Q10 rule of biological reactions it appears likely that the enzymatic reaction rate increases with increasing temperature in this particular temperature range. To test this, reaction rates at the respective temperatures could be determined.

Interestingly, we observed much stronger autophosphorylation of the LIK D690S variant compared to the wild type. It has been reported that kinases are able to dimerize via their activation segments, leading to autophosphorylation of non-consensus sites (Pike et al., 2008). Increased flexibility of the activation segment due to the breakage of the salt-bridge may promotes dimer or oligomer formation or loosens substrate requirements, thus accepting LIK itself as a substrate. Yet, we cannot exclude the possibility that the autophosphorylation is intra-molecular.

We furthermore observed that LIK phosphorylated only one serine residue within the substrate, whereas CLK1 was capable of phosphorylating three serine residues under identical conditions. CLKs belong to the class of processive kinases which means that they are able to phosphorylate at multiple sites without releasing the substrate prior to completion (Velazquez-Dones et al., 2005 Aubol et al., 2013). Mass spectrometry data do not provide information on the phosphorylation mechanism per se, still they allow to conclude that LIK phosphorylates this substrate in a distributive manner, which would be a clear distinction from CLKs. To confirm these assumptions, first substrate preferences of LIK need to be addressed. This could for instance be achieved with peptide arrays. Secondly, a start trap assay (Aubol et al., 2003) could be used to assess the exact phosphorylation mechanism.

LIK appears to have unique structural and functional properties, though showing an astonishing homology of ~ 40 % compared to the mouse CLK1 kinase domain. Commonly, CLKs are known as splicing kinases, exhibiting specialized functions within the splicing regulation process. However, *C. merolae* possesses only 26 intron containing genes, of which only one harbors more than one intron (Matsuzaki et al., 2014), precluding the necessity of a complex splicing regulatory network. Together with the lack of CLK specific

structural insertions, this suggests that LIK may represent a prototypic and less specialized precursor of splicing-related kinases of higher eukaryotes. The fact that the kinome of *C. merolae* comprises only 62 kinases (Wheeler et al., 2008) further supports this hypothesis.

References

Alvarez, M., Estivill, X. and de la Luna, S. (2003). DYRK1A accumulates in splicing speckles through a novel targeting signal and induces speckle disassembly. J. Cell Sci. *116*, 3099–3107.

Anczukow, O., Rosenberg, A.Z., Akerman, M., Das, S., Zhan, L., Karni, R., Muthuswamy, S.K., and Krainer, A.R. (2012). The splicing factor SRSF1 regulates apoptosis and proliferation to promote mammary epithelial cell transformation. Nat. Struct. Mol. Biol. *19*, 220–228.

Aubol, B.E., Plocinik, R.M., Hagopian, J.C., Ma, C.T., McGlone, M.L., Bandyopadhyay, R., Fu, X.D., and Adams, J.A. (2013). Partitioning RS domain phosphorylation in an SR protein through the CLK and SRPK protein kinases. J. Mol. Biol. *425*, 2894-2909.

Aubol, B. E., and Adams, J. A. (2011). Applying the brakes to multisite SR protein phosphorylation: substrate-induced effects on the splicing kinase SRPK1. Biochemistry *50*, 6888–6900.

Aubol, B. E., Chakrabarti, S., Ngo, J., Shaffer, J., Nolen, B., Fu, X. D., Ghosh, G., and Adams, J. A. (2003). Processive phosphorylation of alternative splicing factor/splicing factor 2. Proc. Natl. Acad. Sci. *100,* 12601–12606.

Aubol, B. E., Keshwani, M. M., Fattet, L., & Adams, J. A. (2018). Mobilization of a splicing factor through a nuclear kinase-kinase complex. Biochem. J. *475*, 677–690.

Aubol, B. E., Wu, G., Keshwani, M. M., Movassat, M., Fattet, L., Hertel, K. J., Fu, X.D. and Adams, J. A. (2016). Release of SR Proteins from CLK1 by SRPK1: A Symbiotic Kinase System for Phosphorylation Control of Pre-mRNA Splicing. Mol. Cell *63*, 218–228.

Aubol, B.E., Plocinik, R.M., Keshwani, M.M., McGlone, M.L., Hagopian, J.C., Ghosh, G., Fu, X.D., and Adams, J.A. (2014). N-terminus of the protein kinase CLK1 induces SR protein hyperphosphorylation. Biochem J. *462*, 143-152.

Aubol, B.E., Wu, G., Keshwani, M.M., Movassat, M., Fattet, L., Hertel, K.J., Fu, X.D., and Adams, J.A. (2016). Release of SR Proteins from CLK1 by SRPK1: A Symbiotic Kinase System for Phosphorylation Control of Pre-mRNA Splicing. Mol. Cell *6*, 218-228.

Barbosa-Morais, N.L., Irimia, M., Pan, Q., Xiong, H.Y., Gueroussov, S., Lee, L.J., Slobodeniuc, V., Kutter, C., Watt, S., Çolak, R., et al. (2012). The Evolutionary Landscape of Alternative Splicing in Vertebrate Species. Science *21*, 1587–1594.

Bautista, D.M., Siemens, J., Glazer, J.M., Tsuruda, P.R., Basbaum, A.I., Stucky, C.L., Jordt, S.E., and Julius, D. (2007). The menthol receptor TRPM8 is the principal detector of environmental cold. Nature *448*, 204-208.

Black, D.L. (2003). Mechanisms of alternative pre-messenger RNA splicing. Annu. Rev. Biochem. *72*, 291-336.

Blanco, F. J., and Bernabéu, C. (2012). The Splicing Factor SRSF1 as a Marker for Endothelial Senescence. Front. Physiol. *3*, 54.

Blaustein, M., Pelisch, F., Tanos, T., Munoz, M.J., Wengier, D., Quadrana, L., Sanford, J.R., Muschietti, J.P., Kornblihtt, A.R., Caceres, J.F., Coso, O.A., and Srebrow, A. (2005). Concerted regulation of nuclear and cytoplasmic activities of SR proteins by AKT. Nat. Struct. Mol. Biol. *12*, 1037–1044.

Bradley, T., Cook, M. E., and Blanchette, M. (2015). SR proteins control a complex network of RNA-processing events. RNA *21*, 75–92.

Brown, S.A., Zumbrunn, G., Fleury-Olela, F., Preitner, N., and Schibler, U. (2002). Rhythms of mammalian body temperature can sustain peripheral circadian clocks. Curr. Biol. *12*, 1574–1583.

Bubulya P.A., Prasanth K. V., Deerinck T.J., Gerlich D., Beaudouin J., Ellisman M.H., Ellenberg J., and Spector D.L. (2004). Hypophosphorylated SR splicing factors transiently localize around active nucleolar organizing regions in telophase daughter nuclei. J. Cell Biol. *167*, 51–63.

Buhr, E.D., Yoo, S.H., and Takahashi, J.S. (2010). Temperature as a universal resetting cue for mammalian circadian oscillators. Science *330*, 379-385.

Busch, A., and Hertel, K.J. (2012). Evolution of SR protein and hnRNP splicing regulatory factors. Wiley Interdiscip. Rev. RNA *3*, 1-12.

Cao, W., Jamison, S.F., and Garcia-Blanco, M.A. (1997). Both phosphorylation and dephosphorylation of ASF/SF2 are required for pre-mRNA splicing in vitro. RNA *3*, 1456-1467.

Capel, B. (2017). Vertebrate sex determination: evolutionary plasticity of a fundamental switch. Nat. Rev. Genet. *18*, 675-689.

Castle, J. C., Zhang, C., Shah, J. K., Kulkarni, A. V., Kalsotra, A., Cooper, T. A., and Johnson, J. M. (2008). Expression of 24,426 human alternative splicing events and predicted cis regulation in 48 tissues and cell lines. Nat. Genet. *40*, 12.

Caterina, M.J., Schumacher, M.A., Tominaga, M., Rosen, T.A., Levine, J.D., Julius, D. (1997). The capsaicin receptor: A heat-activated ion channel in the pain pathway. Nature *389*, 816–824

Charnier, M. (1966). Action of temperature on the sex ratio in the Agama agama (Agamidae, Lacertilia) embryo. (in French) C. R. Seances Soc. Biol. Fil. *160*, 620–622.

Cho, S., Hoang, A., Sinha, R., Zhong, X.Y., Fu, X.D., Krainer, A.R., and Ghosh, G. (2011). Interaction between the RNA binding domains of Ser-Arg splicing factor 1 and U1-70K snRNP protein determines early spliceosome assembly. Proc. Natl. Acad. Sci. *108*, 8233-8238.

Choudhary, C., Kumar, C., Gnad, F., Nielsen, M.L., Rehman, M., Walther, T.C., Olsen, J.V., and Mann M. (2009). Lysine acetylation targets protein complexes and co-regulates major cellular functions. Science *325*, 834–840.

Clery, A., Blatter, M., and Allain, F.H. (2008). RNA recognition motifs: boring? Not quite. Curr. Opin. Struct. Biol. *18*, 290–298.

Cohen-Eliav, M., Golan-Gerstl, R., Siegfried, Z., Andersen, C.L., Thorsen, K., Ørntoft, T.F., Mu, D., and Karni, R. (2013). The splicing factor SRSF6 is amplified and is an oncoprotein in lung and colon cancers. J. Pathol. *229*, 630-639.

Colwill, K., Pawson, T., Andrews, B., Prasad, J., Manley, J. L., Bell, J. C., & Duncan, P. I. (1996). The Clk/Sty protein kinase phosphorylates SR splicing factors and regulates their intranuclear distribution. EMBO J. *15*, 265–275.

Czerwinski, M., Natarajan, A., Barske, L., Looger, L.L., and Capel, B. (2016). A timecourse analysis of systemic and gonadal effects of temperature on sexual development of the red-eared slider turtle *Trachemys scripta elegans*. Dev. Biol. *420*, 166-177.

Daniel, R.M., and Danson, M.J. (2010). A new understanding of how temperature affects the catalytic activity of enzymes. Trends Biochem. Sci. *35*, 584-591

Daniel, R.M., and Danson, M.J. (2013). Temperature and the catalytic activity of enzymes: a fresh understanding. FEBS Lett. *587*, 2738-2743.

Das, R., Dufu, K., Romney, B., Feldt, M., Elenko, M., and Reed, R. (2006). Functional coupling of RNAP II transcription to spliceosome assembly. Genes Dev. *20*, 1100–1109.

de Graaf, K., Hekerman, P., Spelten, O., Herrmann, A., Packman, L.C., Büssow, K. Müller-Newen, G. and Becker, W. (2004). Characterization of cyclin L2, a novel cyclin with an arginine/serine-rich domain: phosphorylation by DYRK1A and colocalization with splicing factors. J. Biol. Chem. *279*, 4612–4624.

de la Mata, M., and Kornblihtt, A.R. (2006) RNA polymerase II C-terminal domain mediates regulation of alternative splicing by SRp20. Nat. Struct. Mol. Biol. *13*, 973–980.

Deveson, I.W., Holleley, C.E., Blackburn, J., Marshall Graves, J.A., Mattick, J.S., Waters, P.D., and Georges, A. (2017). Differential intron retention in *Jumonji* chromatin modifier genes is implicated in reptile temperature-dependent sex determination. Sci. Adv. *13*, e1700731.

Ding, J.H., Zhong, X.Y, Hagopian, J.C., Cruz, M.M., Ghosh, G., Feramisco, J., Adams, J.A. and Fu, X.D. (2006). Regulated cellular partitioning of SR protein-specific kinases in mammalian cells. Mol. Biol. Cell. *17*, 876–885.

Dominguez, D., Tsai, Y.H., Weatheritt, R., Wang, Y., Blencowe, B.J., and Wang, Z. (2016). An extensive program of periodic alternative splicing linked to cell cycle progression. eLife *5*, e10288.

Duncan, P.I., Stojdl, D.F., Marius, R.M., Scheit, K.H. and Bell, J.C. (1998). The Clk2 and Clk3 dual-specificity protein kinases regulate the intranuclear distribution of SR proteins and influence pre-mRNA splicing. Exp. Cell Res. *241*, 300–308.

Eperon, I. C., Makarova, O. V., Mayeda, A., Munroe, S. H., Caceres, J. F., Hayward, D. G. and Krainer, A. R. (2000) Selection of alternative 5´ splice sites: role of U1 snRNP and models for the antagonistic effects of SF2/ASF and hnRNP A1 Mol. Cell. Biol. *20*, 8303–8318

Erkelenz, S., Mueller, W.F., Evans, M.S., Busch, A., Schoneweis, K., Hertel, K.J., and Schaal, H. (2013). Position-dependent splicing activation and repression by SR and hnRNP proteins rely on common mechanisms. RNA. *19*, 96–102.

Eswaran, J., Bernad, A., Ligos, J.M., Guinea, B., Debreczeni, J.E., Sobott, F., Parker, S.A., Najmanovich, R., Turk, B.E., and Knapp, S. (2008). Structure of the human protein kinase MPSK1 reveals an atypical activation loop architecture. Structure *16*, 115-124.

Foulkes, T., and Wood, J.N. (2007). Mechanisms of cold pain. Channels *1*, 154–160.

Fredericks, A. M., Cygan, K. J., Brown, B. A. and Fairbrother, W. G. (2015). RNA-Binding Proteins: Splicing Factors and Disease. Biomolecules. *5*, 893–909.

Fu, X.D., and Ares, M., Jr. (2014). Context-dependent control of alternative splicing by RNA-binding proteins. Nat. Rev. Genet. *15*, 689–701.

Ge, C., Ye, J., Weber, C., Sun, W., Zhang, H., Zhou, Y., Cai, C., Qian, G., and Capel, B. (2018). The histone demethylase KDM6B regulates temperature-dependent sex determination in a turtle species. Science *360*, 645-648.

Ge, C., Ye, J., Zhang, H., Zhang, Y., Sun, W., Sang, Y., Capel, B., and Qian, G. (2017). Dmrt1 induces the male pathway in a turtle species with temperature-dependent sex determination. Development *144*, 2222-2233.

George, A., Aubol, B.E., Fattet, L., and Adams, J.A. (2019). Disordered protein interactions for an ordered cellular transition: Cdc2-like kinase 1 is transported to the nucleus via its Ser-Arg protein substrate. J. Biol. Chem. *294*, 9631-9641.

Georges, A., and Holleley, C.E. (2018). How does temperature determine sex? Science *360*, 601-602.

Ghosh, G., and Adams, J. A. (2011). Phosphorylation mechanism and structure of serine-arginine protein kinases. FEBS J. *278*, 587–597.

Giannakouros, T., Nikolakaki, E., Mylonis, I., and Georgatsou, E. (2011) Serine-arginine protein kinases: a small protein kinase family with a large cellular presence. FEBS J. *278*, 570–586.

Gong, J., Liu, J., Ronan, E.A., He, F., Cai, W., Fatima, M., Zhang, W., Lee, H., Li, Z., Kim, G.H., Pipe, K.P., Duan, B., Liu, J. and Xu, X.Z.S. (2019). A Cold-Sensing Receptor Encoded by a Glutamate Receptor Gene. Cell *178*, 1375-1386.

Graveley, B.R. (2000). Sorting out the complexity of SR protein functions. RNA *6*, 1197-1211.

Gui, J.F., Lane, W.S., and Fu, X.D. (1994). A serine kinase regulates intracellular localization of splicing factors in the cell cycle. Nature *369*, 678–682.

Hall, L.L., Smith, K.P., Byron, M., and Lawrence, J.B. (2006). Molecular anatomy of a speckle. Anat. Rec. A Discov. Mol. Cell. Evol. Biol. *288*, 664-675

Han, J., Ding, J.H., Byeon, C.W., Kim, J.H., Hertel, K.J., Jeong, S., and Fu, X.D. (2011). SR proteins induce alternative exon skipping through their activities on the flanking constitutive exons. Mol. Cell. Biol. *31*, 793–802.

Hartmann, A.M., Rujescu, D., Giannakouros, T., Nikolakaki, E., Goedert, M., Mandelkow, E.-M., Gao, Q.S., Andreadis, A., and Stamm, S. (2001). Regulation of alternative splicing of human tau exon 10 by phosphorylation of splicing factors. Mol. Cell. Neurosci. *18*, 80–90.

Haynes, C., & Iakoucheva, L. M. (2006). Serine/arginine-rich splicing factors belong to a class of intrinsically disordered proteins. Nucleic Acids Res. *34*, 305–312.

Hertel, K.J., and Maniatis, T. (1999). Serine-arginine (SR)-rich splicing factors have an exon-independent function in pre-mRNA splicing. Proc. Natl. Acad. Sci. *96*, 2651-2655.

Horii, Y., Shiina, T., Uehara, S., Nomura, K., Shimaoka, H., Horii, K., and Shimizu, Y. (2019). Hypothermia induces changes in the alternative splicing pattern of cold-inducible RNA-binding protein transcripts in a non-hibernator, the mouse. Biomed. Res. *40*, 153-161.

Ibrahim, E. C., Schaal, T. D., Hertel, K. J., Reed, R., and Maniatis, T. (2005). Serine/arginine-rich protein-dependent suppression of exon skipping by exonic splicing enhancers. Proc. Natl. Acad. Sci. *102*, 5002–5007.

Izquierdo, J.M., Majós, N., Bonnal, S., Martínez, C., Castelo, R., Guigó, R., Bilbao, D., and Valcárcel, J. (2005). Regulation of Fas alternative splicing by antagonistic effects of TIA-1 and PTB on exon definition. Mol. Cell *19*, 475–484.

Jamison S.F., Pasman Z., Wang J., Will C., Lührmann R., Manley J.L., and Garcia-Blanco M.A. (1995) U1 snRNP-ASF/SF2 interaction and 5′ splice site recognition: Characterization of required elements. Nucleic Acids Res. *23*, 3260–3267.

Jensen, M.A., Wilkinson, J.E., and Krainer, A.R. (2014). Splicing factor SRSF6 promotes hyperplasia of sensitized skin. Nat. Struct. Mol. Biol. *21*, 189-97.

Jeong S. (2017). SR Proteins: Binders, Regulators, and Connectors of RNA. Mol. Cells *40*, 1–9.

Jia, R., Li, C., McCoy, J.P., Deng, C.X., and Zheng, Z.M. (2010). SRp20 is a proto-oncogene critical for cell proliferation and tumor induction and maintenance. Int. J. Biol. Sci. *6*, 806-26.

Kadri, F., Pacifici, M., Wilk, A., Parker-Struckhoff, A., Del Valle, L., Hauser, K.F., Knapp, P.E., Parsons, C., Jeansonne, D., Lassak, A., and Peruzzi, F. (2015). HIV-1-Tat protein inhibits SC35-mediated tau exon 10 inclusion through upregulation of DYRK1A kinase. J. Biol. Chem. *290*, 30931–30946.

Kamachi, M., Le, T.M., Kim, S.J., Geiger, M.E., Anderson, P. and Utz, P.J. (2002). Human autoimmune sera as molecular probes for the identification of an autoantigen kinase signaling pathway. J. Exp. Med. *196*, 1213–1225.

Kaneko, S., Bonasio, R., Saldaña-Meyer, R., Yoshida, T., Son, J., Nishino, K., Umezawa, A., and Reinberg, D. (2014). Interactions between JARID2 and noncoding RNAs regulate PRC2 recruitment to chromatin. Mol. Cell *53*, 290–300.

Kang, W. H., Park, Y. H., and Park, H. M. (2010). The LAMMER kinase homolog, Lkh1, regulates Tup transcriptional repressors through phosphorylation in *Schizosaccharomyces pombe*. J. Biol. Chem. *285*, 13797–13806.

Karlas, A., Machuy, N., Shin, Y., Pleissner, K.P., Artarini, A., Heuer, D., Becker, D., Khalil, H., Ogilvie, L.A., Hess, S., Mäurer, A.P., Müller, E., Wolff, T., Rudel, T., and Meyer, T.F. (2010). Genome-wide RNAi screen identifies human host factors crucial for influenza virus replication. Nature *463*, 818–822.

Karni, R., de Stanchina, E., Lowe S.W., Sinha, R., Mu, D., Krainer, A.R. (2007). The gene encoding the splicing factor SF2/ASF is a proto-oncogene. Nat. Struct. Mol. Biol. *14*, 185-193.

Kataoka, N., Bachorik, J. L., and Dreyfuss, G. (1999). Transportin-SR, a nuclear import receptor for SR proteins. J. Cell Biol. *145*, 1145–1152.

Kelemen, O., Convertini, P., Zhang, Z., Wen, Y., Shen, M., Falaleeva, M., and Stamm, S. (2013). Function of alternative splicing. Gene *514*, 1–30.

Keshwani, M.M., Hailey, K. L., Aubol, B. E., Fattet, L., McGlone, M. L., Jennings, P. A., & Adams, J. A. (2015). Nuclear protein kinase CLK1 uses a non-traditional docking mechanism to select physiological substrates. Biochem. J. *472*, 3.

Kohtz, J.D., Jamison, S.F., Will, C.L., Zuo, P., Lührmann, R., Garcia-Blanco, M.A., and Manley, J.L. (1994). *Protein–protein interactions and 5'-splice-site recognition in mammalian mRNA precursors*. Nature *368*, 119–124.

Koike, N., Yoo, S.H., Huang, H.C., Kumar, V., Lee, C., Kim, T.K., and Takahashi, J.S. (2012). Transcriptional architecture and chromatin landscape of the core circadian clock in mammals. Science *338*, 349–354.

Koizumi, J., Okamoto Y., Onogi H., Mayeda, A., Krainer, A. R. and Hagiwara, M. (1999). The subcellular localization of SF2/ASF is regulated by direct interaction with SR protein kinases (SRPKs). J. Biol. Chem. *274*, 11125-11131.

Kornberg, R.D. (2007). The molecular basis of eukaryotic transcription. Proc. Natl. Acad. Sci. *104*, 12955–12961.

Kornblihtt, A. R. (2015). Transcriptional control of alternative splicing along time: Ideas change, experiments remain. RNA. *21*, 670–672.

Kornmann, B., Schaad, O., Bujard, H., Takahashi, J.S., and Schibler, U. (2007). System-driven and oscillator-dependent circadian transcription in mice with a conditionally active liver clock. PLoS Biol. *5*, e34.

Kuroyanagi, N., Onogi H., Wakabayashi T., and Hagiwara, M. (1998). Novel SR-protein-specific kinase, SRPK2, disassembles nuclear speckles. Biochem. Biophys. Res. Commun. *242*, 357–364.

Lai, M.C., Lin, R.I., and Tarn, W.Y. (2001) Transportin-SR2 mediates nuclear import of phosphorylated SR proteins. Proc. Natl. Acad. Sci. *98*, 10154-10159.

Lasho, T.L., Jimma, T., Finke, C.M., Patnaik, M., Hanson, C.A., Ketterling, R.P., Pardanani, A., and Tefferi, A. (2012). SRSF2 mutations in primary myelofibrosis: significant clustering with IDH mutations and independent association with inferior overall and leukemia-free survival. Blood *120*, 4168-71.

Laugesen, A., Højfeldt, J.W., and Helin, K. (2019). Molecular Mechanisms Directing PRC2 Recruitment and H3K27 Methylation. Mol. Cell *74*, 8-18.

Lemaire, R., Prasad, J., Kashima, T., Gustafson, J., Manley, J. L., and Lafyatis, R. (2002). Stability of a PKCI-1-related mRNA is controlled by the splicing factor ASF/SF2: a novel function for SR proteins. Genes Dev., *16*, 594–607.

Li, X. and Manley, J.L. (2005). Inactivation of the SR protein splicing factor ASF/SF2 results in genomic instability. Cell 122, 365–378.

Liu, H.X., Chew, S.L., Cartegni, L., Zhang, M.Q., and Krainer, A.R. (2000) Exonic splicing enhancer motif recognized by human SC35 under splicing conditions. Mol. Cell. Biol. *20*, 1063-1071.

Liu, H.X., Zhang, M., and Krainer, A.R. (1998). Identification of functional exonic splicing enhancer motifs recognized by individual SR proteins. Genes Dev. *12*, 1998-2012.

Liu, Y., Gonzàlez-Porta, M., Santos, S., Brazma, A., Marioni, J.C., Aebersold, R., Venkitaraman, A.R., and Wickramasinghe, V.O. (2017). Impact of Alternative Splicing on the Human Proteome. Cell Rep. *20*, 1229–1241.

Long, J.C., and Caceres, J.F. (2009). The SR protein family of splicing factors: master regulators of gene expression. Biochem. J. *417*, 15-27.

Loomis, R.J., Naoe, Y., Parker, J.B., Savic, V., Bozovsky, M.R., Macfarlan, T., Manley, J.L. and Chakravarti, D. (2009). Chromatin binding of SRp20 and ASF/SF2 and dissociation from mitotic chromosomes is modulated by histone H3 serine 10 phosphorylation. Mol .Cell *33*, 450–461.

Luco R.F., Pan Q., Tominaga K., Blencowe B.J., Pereira-Smith O.M., and Misteli T. (2010) Regulation of alternative splicing by histone modifications. Science *327*, 996–1000.

Lujan, D.A., Ochoa, J.L., and Hartley, R.S. (2018). Cold-inducible RNA binding protein in cancer and inflammation. Wiley Interdiscip. Rev. RNA *9*, 2.

Ma, C.T., Velazquez-Dones, A., Hagopian, J.C., Ghosh, G., Fu, X.D., and Adams, J.A. (2008). Ordered multi-site phosphorylation of the splicing factor ASF/SF2 by SRPK1. J. Mol. Biol. *376*, 55–68.

Manley, J.L. and Krainer, A.R. (2010). A rational nomenclature for serine/arginine-rich protein splicing factors (SRproteins). Genes Dev. *24*, 1073–1074.

Maslon, M.M., Heras, S.R., Bellora, N., Eyras, E., and Caceres, J.F. (2014). The translational landscape of the splicing factor SRSF1 and its role in mitosis. eLife, e02028.

Mathew, R., Hartmuth, K., Mohlmann, S., Urlaub, H., Ficner, R. and Lührmann, R. (2008). Phosphorylation of human PRP28 by SRPK2 is required for integration of the U4/U6-U5 tri-snRNP into the spliceosome. Nat. Struct. Mol. Biol. *15*, 435–443.

Matsuzaki, M., Misumi, O., Shin-i, T. et al. (2004). Genome sequence of the ultrasmall unicellular red alga Cyanidioschyzon merolae 10D. Nature *428*, 653–657

Mayeda, A., and Krainer, A.R. (1992). Regulation of alternative pre-mRNA splicing by hnRNP A1 and splicing factor SF2. Cell *68*, 365–375.

McGlincy, N.J., and Smith, C.W.J. (2008). Alternative splicing resulting in nonsense-mediated mRNA decay: what is the meaning of nonsense? Trends Biochem. Sci. *33*, 385–393.

McManus, C.J., and Graveley, B.R. (2011). RNA structure and the mechanisms of alternative splicing. Curr. Opin. Genet. Dev. *21*, 373–379.

Menet, J.S., Rodriguez, J., Abruzzi, K.C., and Rosbash, M. (2012). Nascentseq reveals novel features of mouse circadian transcriptional regulation. eLife *1*, e00011.

Merkin, J., Russell, C., Chen, P., and Burge, C.B. (2012). Evolutionary Dynamics of Gene and Isoform Regulation in Mammalian Tissues. Science *338*, 1593–1599.

Mermoud, J.E., Cohen, P.T., and Lamond, A.I. (1994). Regulation of mammalian spliceosome assembly by a protein phosphorylation mechanism. EMBO J. *13*, 5679-5688.

Michlewski, G., Sanford, J.R., and Caceres, J.F. (2008). The splicing factor SF2/ASF regulates translation initiation by enhancing phosphorylation of 4E-BP1. Mol. Cell *30*, 179–189.

Misteli, T., Caceres, J.F., and Spector, D.L. (1997). The dynamics of a pre-mRNA splicing factor in living cells. Nature *387*, 523–527.

Mockenhaupt, S., and Makeyev, E.V. (2015). Non-coding functions of alternative pre-mRNA splicing in development. Semin. Cell .Dev. Biol. *47-48*, 32–39.

Morf, J., Rey, G., Schneider, K., Stratmann, M., Fujita, J., Naef, F., and Schibler, U. (2012). Cold-inducible RNA-binding protein modulates circadian gene expression posttranscriptionally. Science *338*, 379–383.

Muller-McNicoll, M., Botti, V., de Jesus Domingues, A.M., Brandl, H., Schwich, O.D., Steiner, M.C., Curk, T., Poser, I., Zarnack, K., and Neugebauer, K.M. (2016). SR proteins are NXF1 adaptors that link alternative RNA processing to mRNA export. Genes Dev. *30*, 553-566.

Naftelberg, S., Schor, I.E., Ast, G., and Kornblihtt, A.R. (2015). Regulation of Alternative Splicing Through Coupling with Transcription and Chromatin Structure. Annu. Rev. Biochem. *84*, 165–198.

Nakagawa, O., Arnold, M., Nakagawa, M., Hamada, H., Shelton, J.M., Kusano, H., Harris, T.M., Childs, G., Campbell, K.P., Richardson, J.A., Nishino, I., and Olson, E.N. (2005). Centronuclear myopathy in mice lacking a novel muscle-specific protein kinase transcriptionally regulated by MEF2. Genes Dev. *19*, 2066-77.

Nayler, O., Stamm, S. and Ullrich, A. (1997). Characterization and comparison of four serine- and arginine-rich (SR) protein kinases. Biochem. J. *326*, 693–700.

Neumann, A., Schindler, M., Olofsson, D., Wilhelmi, I., Schürmann, A., and Heyd, F. (2019). Genome-wide identification of alternative splicing events that regulate protein transport across the secretory pathway. J. Cell Sci. *132*, 8.

Ngo, J.C., Chakrabarti, S., Ding, J.H., Velazquez-Dones, A., Nolen, B., Aubol, B.E., Adams, J.A., Fu, X.D., and Ghosh, G. (2005). Interplay between SRPK and Clk/Sty kinases in phosphorylation of the splicing factor ASF/SF2 is regulated by a docking motif in ASF/SF2. Mol. Cell *20*, 77–89.

Ngo, J.C., Giang, K., Chakrabarti, S., Ma, C.T., Huynh, N., Hagopian, J.C., Dorrestein, P.C., Fu, X.D., Adams, J.A., and Ghosh, G. (2008). A sliding docking interaction is essential for sequential and processive phosphorylation of an SR protein by SRPK1. Mol. Cell *29*, 563-576

Ngo, J.C., Gullingsrud, J., Giang, K., Yeh, M.J., Fu, X.D., Adams, J.A., McCammon, J.A., and Ghosh, G. (2007). SR protein kinase 1 is resilient to inactivation. Structure. *15*, 123–133.

Nikolakaki, E., Meier, J., Simos, G., Georgatos, S.D. and Giannakouros, T. (1997). Mitotic phosphorylation of the lamin B receptor by a serine/arginine kinase and p34(cdc2). J. Biol. Chem. *272*, 6208–6213.

Nilsen T.W. (2003). The spliceosome: The most complex macromolecular machine in the cell? Bioessays. *25*, 1147–1149.

Ninomiya, K., Kataoka, N., and Hagiwara, M. (2011). Stress-responsive maturation of Clk1/4 pre-mRNAs promotes phosphorylation of SR splicing factor. J. Cell Biol. *195*, 27-40.

Nishida, A., Kataoka, N., Takeshima, Y., Yagi, M., Awano, H., Ota, M., Itoh, K., Hagiwara, M., Matsuo, M. (2011). Chemical treatment enhances skipping of a mutated exon in the dystrophin gene. Nat. Commun. *2*, 308.

Nishiyama, H., Itoh, K., Kaneko, Y., Kishishita, M., Yoshida, O., and Fujita, J. (1997). A glycine-rich RNA-binding protein mediating cold-inducible suppression of mammalian cell growth. J. Cell Biol. *137*, 899–908.

Nolen, B., Taylor, S., and Ghosh, G. (2004). Regulation of protein kinases; controlling activity through activation segment conformation. Mol Cell. *5*, 661-75.

Okamoto, Y., Onogi, H., Honda, R., Yasuda, H., Wakabayashi, T., Nimura, Y., and Hagiwara, M. (1998). Cdc2 kinase-mediated phosphorylation of splicing factor SF2/ASF. Biochem. Biophys. Res. Commun. *249*, 872-878.

Pan, Q., Shai, O., Lee, L.J., Frey, B.J., and Blencowe, B.J. (2008). Deep surveying of alternative splicing complexity in the human transcriptome by high-throughput sequencing. Nat. Genet. *40*, 1413-1415.

Pandit, S., Wang, D., and Fu, X.D. (2008). Functional integration of transcriptional and RNA processing machineries. Curr. Opin. Cell Biol. *20*, 260-265.

Pandit, S., Zhou, Y., Shiue, L., Coutinho-Mansfield, G., Li, H., Qiu, J., Huang, J,, Yeo, G.W., Ares, M. Jr., and Fu, X.D. (2013). Genome-wide analysis reveals SR protein cooperation and competition in regulated splicing. Mol Cell. *50*, 223-235.

Park, S. Y., Piao, Y., Thomas, C., Fuller, G. N., and de Groot, J. F. (2016). Cdc2-like kinase 2 is a key regulator of the cell cycle via FOXO3a/p27 in glioblastoma. Oncotarget *7*, 18.

Paronetto, M.P., Passacantilli, I., and Sette, C. (2016) Alternative splicing and cell survival: from tissue homeostasis to disease. Cell Death Differ. *23*, 1919–1929.

Pelisch, F., Gerez, J., Druker, J., Schor, I.E., Muñoz, M.J., Risso, G., Petrillo, E., Westman, B.J., Lamond, A.I., Arzt, E. and Srebrow, A. (2010). The serine/arginine-rich protein SF2/ASF regulates protein sumoylation. Proc. Natl. Acad. Sci. *107*, 116119–116124.

Pike, A.C., Rellos, P., Niesen, F.H., Turnbull, A., Oliver, A.W., Parker, S.A., Turk, B.E., Pearl, L.H., and Knapp, S. (2008). Activation segment dimerization: a mechanism for kinase autophosphorylation of non-consensus sites. EMBO J. *27*, 704-14.

Plass, M., Agirre, E., Reyes, D., Camara, F., and Eyras, E. (2008). Co-evolution of the branch site and SR proteins in eukaryotes. Trends Genet. *24*, 590-594.

Preussner, M., and Heyd, F. (2018). Temperature-controlled Rhythmic Gene Expression in Endothermic Mammals: All Diurnal Rhythms are Equal, but Some are Circadian. BioEssays *40*, e1700216.

Preussner, M., Goldammer, G., Neumann, A., Haltenhof, T., Rautenstrauch, P., Muller-McNicoll, M., and Heyd, F. (2017). Body Temperature Cycles Control Rhythmic Alternative Splicing in Mammals. Mol. Cell *67*, 433-446.

Preussner, M., Wilhelmi, I., Schultz, A.S., Finkernagel, F., Michel, M., Moroy, T., and Heyd, F. (2014). Rhythmic U2af26 alternative splicing controls PERIOD1 stability and the circadian clock in mice. Mol. Cell *54*, 651-662.

Qiang, X., Yang, W.L., Wu, R., Zhou, M., Jacob, A., Dong, W., Kuncewitch, M., Ji, Y., Yang, H., Wang, H., et al. (2013). Cold-inducible RNA-binding protein (CIRP) triggers inflammatory responses in hemorrhagic shock and sepsis. Nat. Med. *19*, 1489-1495.

Quesnel-Vallières, M., Irimia, M., Cordes, S. P., and Blencowe, B. J. (2015). Essential roles for the splicing regulator nSR100/SRRM4 during nervous system development. Genes Dev. *29*, 746–759.

Refinetti, R., and Menaker, M. (1992). The circadian rhythm of body temperature. Physiol. Behav. *51*, 613-637.

Roscigno, R.F., and Garcia-Blanco, M.A. (1995). SR proteins escort the U4/U6·U5 tri-snRNP to the spliceosome. RNA *1*, 692-706.

Rossi, F., Labourier, E., Forne, T., Divita, G., Derancourt, J., Riou, J.F., Antoine, E., Cathala, G., Brunel, C., and Tazi, J. (1996). Specific phosphorylation of SR proteins by mammalian DNA topoisomerase I. Nature *381*, 80–82.

Saini, C., Morf, J., Stratmann, M., Gos, P., and Schibler, U. (2012). Simulated body temperature rhythms reveal the phase-shifting behavior and plasticity of mammalian circadian oscillators. Genes Dev. *26*, 567-580.

Salomonis, N., Nelson, B., Vranizan, K., Pico, A. R., Hanspers, K., Kuchinsky, A., Ta, L., Mercola, M, and Conklin, B. R. (2009). Alternative splicing in the differentiation of human embryonic stem cells into cardiac precursors. PLoS Comput. Biol. *5*, 11.

Sanulli, S., Justin, N., Teissandier, A., Ancelin, K., Portoso, M., Caron, M., Michaud, A., Lombard, B., da Rocha, S. T., Offer, J., Loew, D., Servant, N., Wassef, M., Burlina, F., Gamblin, S. J., Heard, E., and Margueron, R. (2015). Jarid2 methylation via the PRC2 complex regulates H3K27me3 deposition during cell differentiation. Mol. Cell *57*, 769–783.

Sapra A.K., Anko M.L., Grishina I., Lorenz M., Pabis M., Poser I., Rollins J., Weiland E.M., and Neugebauer K.M. (2009). SR protein family members display diverse activities in the formation of nascent and mature mRNPs in vivo. Mol Cell. *34*, 179–190.

Schroeder, A. L., Metzger, K. J., Miller, A., and Rhen, T. (2016). A novel candidate gene for temperature-dependent sex determination in the common snapping turtle. Genetics *203*, 557–571.

Sen, S., Jumaa, H., and Webster, N. J. (2013). Splicing factor SRSF3 is crucial for hepatocyte differentiation and metabolic function. Nat. Comm. *4*, 1336.

Sharma, S., Kohlstaedt, L.A., Damianov, A., Rio, D.C., Black, D.L. (2008). Polypyrimidine tract binding protein controls the transition from exon definition to an intron defined spliceosome. Nat. Struct. Mol. Biol. *15*, 183–191.

Shen, H. and Green, M. R. (2004). A pathway of sequential arginine-serine-rich domain-splicing signal interactions during mammalian spliceosome assembly. Mol. Cell *16*, 363–373.

Shen, H., Kan, J. L., and Green, M. R. (2004). Arginine-serine-rich domains bound at

Shen M., and Mattox W. (2012). Activation and repression functions of an SR splicing regulator depend on exonic versus intronic-binding position. Nucleic Acids Res. *40*, 428–437.

Shi, Y., Reddy, B., and Manley, J.L. (2006). PP1/PP2A phosphatases are required for the second step of Pre-mRNA splicing and target specific snRNP proteins. Mol. Cell *23*, 819–829.

Shin, C., Feng, Y., and Manley, J.L. (2004). Dephosphorylated SRp38 acts as a splicing repressor in response to heat shock. Nature *427*, 553-558.

Sinha, R., Allemand, E., Zhang, Z., Karni, R., Myers, M.P., and Krainer, A.R. (2010). Arginine methylation controls the subcellular localization and functions of the oncoprotein splicing factor SF2/ASF. Mol. Cell. Biol. *30*, 2762–2774.

Spector, D. L., and Lamond, A. I. (2011). Nuclear speckles. CSH Perspect. Biol. *3*(2), a000646.

Su, C. H., Dhananjaya, D., and Tarn, W. Y. (2018). Alternative Splicing in Neurogenesis and Brain Development. Front. Mol. Biosci. *5*, 12.

Sundgren-Andersson, A.K., Ostlund, P., and Bartfai, T. (1998). Simultaneous measurement of brain and core temperature in the rat during fever, hyperthermia, hypothermia and sleep. Neuroimmunomodulation *5*, 241–247.

Takano, M., Koyama, Y., Ito, H., Hoshino, S., Onogi, H., Hagiwara, M., Furukawa, K. and Horigome, T. (2004). Regulation of binding of lamin B receptor to chromatin by SR protein kinase and cdc2 kinase in Xenopus egg extracts. J. Biol. Chem. *279*, 13265–13271.

Taliaferro, J.M., Lambert, N.J., Sudmant, P.H., Dominguez, D., Merkin, J.J., Alexis, M.S., Bazile, C.A., and Burge, C.B. (2016). RNA Sequence Context Effects Measured In Vitro Predict In Vivo Protein Binding and Regulation. Mol. Cell *64*, 294–306.

Tan, P.L., and Katsanis, N. (2009). Thermosensory and mechanosensory perception in human genetic disease. Hum. Mol. Genet. *18*, R146-R155.

Taylor, S.S., and Radzio-Andzelm, E. (1994). Three protein kinase structures define a common motif. Structure *2*, 345-355.

Tazi, J., Bakkour, N., and Stamm, S. (2009). Alternative splicing and disease. Biochim. Biophys. Acta *1792*, 14–26.

Thompson, M.C., Barad, B.A., Wolff, A.M., Sun Cho, H., Schotte, F., Schwarz, D.M.C., Anfinrud, P., and Fraser, J.S., (2019) Temperature-jump solution X-ray scattering reveals distinct motions in a dynamic enzyme. Nat. Chem. *11*, 1058–1066

Tintaru, A. M., Hautbergue, G. M., Hounslow, A. M., Hung, M. L., Lian, L. Y., Craven, C. J., and Wilson, S. A. (2007). Structural and functional analysis of RNA and TAP binding to SF2/ASF. EMBO Rep. 8, 8.

Twyffels, L., Gueydan, C., and Kruys, V. (2011). Shuttling SR proteins: more than splicing factors. FEBS J. *278*, 3246-3255.

Velazquez-Dones, A., Hagopian, J.C., Ma, C.T., Zhong, X.Y., Zhou, H., Ghosh, G., Fu, X.D., and Adams, J.A. (2005). Mass spectrometric and kinetic analysis of ASF/SF2 phosphorylation by SRPK1 and Clk/Sty. J. Biol. Chem. *280*, 41761–41768.

Wahl, M.C., Will, C.L., and Lührmann, R. (2009). The spliceosome: design principles of a dynamic RNP machine. Cell 136, 701-718

Wang, E.T., Sandberg, R., Luo, S., Khrebtukova, I., Zhang, L., Mayr, C., Kingsmore, S.F., Schroth, G.P., and Burge, C.B. (2008). Alternative isoform regulation in human tissue transcriptomes. Nature *456*, 470-476.

Wang, J., Xiao, S.H. and Manley J.L. (1998). Genetic analysis of the SR protein ASF/SF2: interchangeability of RS domains and negative control of splicing. Genes Dev. *12*, 2222–2233.

Wetsel, W.C. (2011). Sensing hot and cold with TRP channels. Int. J. Hyperthermia *27*, 388-398.

Wheeler, G. L., Miranda-Saavedra, D., and Barton, G. J. (2008). Genome analysis of the unicellular green alga *Chlamydomonas reinhardtii* indicates an ancient evolutionary origin for key pattern recognition and cell-signaling protein families. Genetics 179, 193–197.

Will, C. L., and Lührmann, R. (2011). Spliceosome structure and function. CSH Perspect. Biol. *3*, 7.

Wong, R., Balachandran, A., Mao, A. Y., Dobson, W., Gray-Owen, S., and Cochrane, A. (2011). Differential effect of CLK SR Kinases on HIV-1 gene expression: potential novel targets for therapy. Retrovirology *8*, 47.

Wu, J.Y. and Maniatis, T. (1993). Specific interactions between proteins implicated in splice site selection and regulated alternative splicing. Cell 75, 1061-1070.

Xiao, S.H., and Manley, J.L. (1998). Phosphorylation-dephosphorylation differentially affects activities of splicing factor ASF/SF2. EMBO J.*17*, 6359–6367.

Yang, C., and Carrier, F. (2001). The UV-inducible RNA-binding protein A18 (A18 hnRNP) plays a protective role in the genotoxic stress response. J. Biol. Chem. *276*, 47277–47284.

Yarmolenko, P. S., Moon, E. J., Landon, C., Manzoor, A., Hochman, D. W., Viglianti, B. L., & Dewhirst, M. W. (2011). Thresholds for thermal damage to normal tissues: an update. Int. J. Hyperthermia *27*, 320–343.

Yeakley, J.M., Tronche` re, H., Olesen, J., Dyck, J.A., Wang, H.Y., and Fu, X.D. (1999). Phosphorylation regulates in vivo interaction and molecular targeting of serine/arginine-rich pre-mRNA splicing factors. J. Cell Biol. *145*, 447–455.

Yoon, H.S., Hackett, J.D., Ciniglia, C., Pinto, G., and Bhattacharya, D. (2004). A molecular timeline for the origin of photosynthetic eukaryotes. Mol. Biol. Evol. *21*, 809–818

Yun, B., Farkas, R., Lee, K., and Rabinow, L. (1994). The Doa locus encodes a member of a new protein kinase family and is essential for eye and embryonic development in Drosophila melanogaster. Genes Dev. *8*, 1160–1173.

Yun, C.Y., Velazquez-Dones, A.L., Lyman, S.K., and Fu, X.D. (2003). Phosphorylation-dependent and -independent nuclear import of RS domain-containing splicing factors and regulators. J. Biol. Chem. *278*, 18050–18055.

Zhang, X., Chen, M.H., Wu, X., Kodani, A., Fan, J., Doan, R., Ozawa, M., Ma, J., Yoshida, N., Reiter, J.F., Black, D.L., Kharchenko, P.V., Sharp, P.A., and Walsh, C.A. (2016). Cell-

Type-Specific Alternative Splicing Governs Cell Fate in the Developing Cerebral Cortex. Cell. *166*, 1147-1162.

Zhang, Z. and Krainer, A.R. (2004). Involvement of SR proteins in mRNA surveillance. Mol. Cell *16*, 597–607.

Zhong, X.Y., Wang, P., Han, J., Rosenfeld, M.G., and Fu, X.-D. (2009). SR Proteins in Vertical Integration of Gene Expression from Transcription to RNA Processing to Translation. Mol. Cell *35*, 1-10.

Zhou, Z., and Fu, X. D. (2013). Regulation of splicing by SR proteins and SR protein-specific kinases. Chromosoma 1*22*, 191–207.

Zhu, J., Mayeda, A., and Krainer, A.R. (2001). Exon identity established through differential antagonism between exonic splicing silencer-bound hnRNP A1 and enhancer-bound SR proteins. Mol. Cell *8*, 1351–1361.

List of Figures

Abbreviations

Å	Ångström
ss	splice site
A	adenine
AS	alternative splicing
bp	base pairs
BP	branch point
C	cytosine
CBT	core body temperature
CD	Circular dichroism
CLK	Cdc2-like kinase
CRISPR	Clustered Regularly Interspaced Short Palindromic Repeats
DMSO	Dimethyl sulfoxide
DNA	deoxyribonucleic acid
Doa	darkener of apricot
DYRK	dual-specificity tyrosine phosphorylation-regulated kinase
E	exon
ESE	exonic splicing enhancer
ESS	exonic splicing silencer
FPT	female producing temperature
G	guanine
hnRNP	heterogeneous nuclear ribonucleoprotein particle
KD	kinase domain
LIK	LAMMER-like kinase
IR	intron retention
ISE	intronic splicing enhancer
ISS	intronic splicing silencer
kDa	kilo Dalton
m7G	7-methylguanosine cap
MAPK	mitogen-activated protein kinase
MPT	male producing temperature
mRNA	messenger ribonucleic acid
NLS	nuclear localization signal
NMR	nuclear magnetic resonance
OA	ocadaic acid
PKA	protein kinase A

PKB	protein kinase B
PKC	protein kinase C
Pol II	RNA polymerase II
PP1	protein phosphatase 1
PP2A	protein phosphatase 2 A
PRC2	polycomb repressive complex 2
PSI	percent spliced in
RBP	RNA-binding protein
RNA	ribonucleic acid
RNAPII	RNA polymerase II
RRM	RNA recognition motif
RS	serine-arginine rich
RT-PCR	Reverse transcriptase PCR
SAXS	Small-angle X-ray scattering
SD	standard deviation
SF	splicing factor
siRNA	small interfering RNA
snRNP	small nuclear ribonucleoprotein particle
SRE	splicing regulatory element
SRPK	Serine/arginine-rich protein-specific kinases
SRSF	Serine/arginine-rich splicing factor
Tbp	TATA-binding protein
TSD	temperature-dependent sex determination
U2AF	U2 auxiliary factor
U	uracil
UTR	untranslated region
UV	ultraviolet
WAXS	Wide-angle X-ray scattering
wt	wild

Publications

Publication I

Marco Preußner, Gesine Goldammer, Alexander Neumann, Tom Haltenhof, Pia Rautenstrauch, Michaela Müller-McNicoll, and Florian Heyd (2017). Body Temperature Cycles Control Rhythmic Alternative Splicing in Mammals. Mol Cell. 3;67(3):433-446.

https://doi.org/10.1016/j.molcel.2017.06.006

Publication II

A conserved kinase-based body temperature sensor globally controls alternative splicing and gene expression

Tom Haltenhof[1], Ana Kotte[1], Francesca de Bortoli[1], Samira Schiefer[1], Stefan Meinke[1], Ann-Kathrin Emmerichs[1], Kristina Katrin Petermann[1], Bernd Timmermann[4], Andreas Franz[1,2], Markus C. Wahl[2], Petra Imhof[3], Marco Preußner[1], Florian Heyd[1]

[1]Freie Universität Berlin, Institute of Chemistry and Biochemistry, Laboratory of RNA Biochemistry, Takustrasse 6, 14195 Berlin, Germany.

[2]Freie Universität Berlin, Institute of Chemistry and Biochemistry, Laboratory of Structural Biochemistry, Takustrasse 6, 14195 Berlin, Germany.

[3]Freie Universität Berlin, Institute of Theoretical Physics, Arnimallee 14, 14195 Berlin, Germany.

[4]Sequencing Core Facility, Max-Planck-Institute for Molecular Genetics, Ihnestraße 63-73, Berlin 14195, Germany

[*]Corresponding author / lead contact:

florian.heyd@fu-berlin.de

Phone: +49 30 83862938

FAX: +49 30 838-4-62938

Summary (150 words)

Homoeothermic organisms maintain their core body temperature in a narrow, tightly controlled range. Whether and how subtle circadian oscillations or disease-associated changes in core body temperature are sensed and integrated in gene expression programs remains elusive. Furthermore, a thermo-sensor capable of sensing the small temperature differentials leading to temperature-dependent sex determination (TSD) in poikilothermic reptiles has not been identified. Here we show that the activity of CDC-like kinases (CLKs) is highly responsive to physiological temperature changes, which is conferred by structural rearrangements within the kinase activation loop. Lower body temperature activates CLKs resulting in strongly increased phosphorylation of SR-proteins *in vitro* and *in vivo*. This globally controls temperature-dependent alternative splicing and gene expression, with wide implications in circadian, tissue-specific and disease-associated settings. This temperature sensor is conserved across evolution and adapted to growth temperatures of diverse poikilotherms. The dynamic temperature range of reptilian CLK homologs suggests a role in TSD.

Keywords

Body temperature, temperature sensing, alternative splicing, CLK kinase, SR proteins, CIRBP, sex determination

Highlights (up to 4, 85 characters)

- CLK kinases are thermo-sensors reactive to subtle body temperature changes
- Body temperature globally controls splicing and gene expression through CLKs
- CLK homologs are evolutionarily adapted to diverse body/growth temperatures
- Wide functionality of CLKs: from TSD in reptiles to circadian biology in mammals

Introduction

The environmental temperature has a strong influence on all three domains of life. Examples include daily changes in temperature that serve as Zeitgeber for the circadian clock, seasonal changes in temperature that are linked to hibernation and temperature-dependent sex determination in some reptiles (Buhr et al., 2010; Capel, 2017). In addition, sensing cold and hot temperatures is essential to avoid extreme and potentially dangerous conditions. Therefore, diverse organisms, including humans, have evolved complex thermosensory systems (Tan and Katsanis, 2009). With respect to cold sensing in mammals, two receptors were identified that react to cool (below 26°C) or cold (below 20°C) external temperature, namely Trpm8 and GluK2 (Bautista et al., 2007; Gong et al., 2019). On the other hand, several members of the TRP family have been reported to respond to warm or hot temperature (43°C or above; (Wetsel, 2011)). TRP channels sense changes in environmental temperature and their function is therefore best characterized in skin and primary sensory neurons (Wetsel, 2011). In contrast to the body shell, the core body temperature in homoeothermic organisms is largely independent of the external temperature and kept within a narrow range. Most organs and cells are therefore not exposed to strong ambient temperature changes but rather experience subtle changes in core body temperature. For example, most mammals display a body temperature of around 37°C that shows circadian (~24-hour) oscillation within a range of ~1-4°C (Buhr et al., 2010; Refinetti and Menaker, 1992; Saini et al., 2012). The female hormone cycle and aging also have a mild effect on core body temperature, as have pathological conditions such as hypothermia, fever, or the slightly increased temperature in tumor tissue (Charkoudian et al., 2017; Gautherie and Gros, 1980; Keil et al., 2015). The cellular cold and heat shock responses are triggered below 35°C and above 39°C respectively, and many studies have used even more extreme and unphysiological temperatures, typically 32°C and 42°C, to elicit a full response. Therefore, if and how cells are able to sense and respond to subtle changes in the physiologically relevant range of the core body temperature remains unknown.

Our recent finding that a 1-2°C oscillation of body temperature is sufficient to control alternative splicing (AS) (Preussner et al., 2017) implies the presence of a cellular thermometer that is able to sense very subtle, endogenous changes in the physiological temperature range. Rhythmic AS is regulated through altered SR protein phosphorylation with higher phosphorylation levels at lower body temperature. SR protein phosphorylation is controlled by two classes of kinases, SRPKs (SR protein kinases, SRPK1-3) and CLKs (CLK1-4) (Dominguez et al., 2016; Ghosh and Adams, 2011). SRPKs phosphorylate SR proteins in the cytoplasm triggering nuclear import and localization in speckles (Zhou and Fu, 2013). Further SRPK-assisted nuclear phosphorylation by CLKs (Aubol et al., 2016) mobilizes SR proteins (Colwill et al., 1996), which then control transcription and all further (pre-)mRNA processing

events, from splicing, to nuclear export, translation and degradation (Long and Caceres, 2009; Muller-McNicoll et al., 2016). Knock down and inhibitor experiments suggested an involvement of the close homologs CLK1 and CLK4 in the temperature-dependent control of SR protein phosphorylation (Preussner et al., 2017). Although so far no enzymes have been described whose activity substantially changes within the narrow range of core body temperature, we hypothesized that this could be the case for CLK activity. This would define a new class of cellular temperature sensors that are, in contrast to TRP channels that react mainly to changes in ambient temperature, able to sense changes in the internal body temperature.

In line with this hypothesis, we show here that body temperature controls the activities of CLKs, resulting in dramatically altered SR protein phosphorylation within the physiological temperature range. CLK activity is more than 5-fold higher at 35°C than at 38°C, which contradicts the Q_{10} rule and thus has to be actively regulated, and matches corresponding changes in endogenous SR protein phosphorylation (Preussner et al., 2017). We furthermore show a global impact of body-temperature changes on AS and gene expression in human cells, which is predominantly controlled by CLK activity. This includes identification of a CLK-dependent AS event in the cold-induced RNA-binding protein (CIRBP) regulating its cold-induced gene expression. We thus define a cellular thermo-sensor that integrates subtle changes in the endogenous core body temperature into gene expression programs. The extreme temperature sensitivity is based on reversible temperature-induced structural rearrangements in the activation loop, representing an inherent feature of the protein itself that does not require additional regulators, thus providing a new paradigm for the regulation of enzymatic activity in the physiological temperature range. CLK temperature-sensitivity is conserved across evolution and adapted to growth temperatures of diverse poikilotherms. The dynamic temperature range of reptilian CLK homologs suggests a role as molecular thermometer in TSD.

Results

CLK1/4 activity is highly responsive to physiological temperature changes

While rhythmic AS of numerous exons is controlled by oscillating body temperature (Goldammer et al., 2018; Preussner et al., 2017; Preussner and Heyd, 2018), a temperature sensor that connects such small temperature changes with AS remains unknown. As rhythmic AS depends on body temperature controlled SR protein phosphorylation, we hypothesized that the activity of CLK kinases could be directly controlled by body temperature. To address a potential role of CLKs as molecular thermometer, we expressed and purified mouse GST-tagged CLK1 and CLK4 from bacteria (Figure 1A and S1A). Both kinases are widely expressed across different tissues and show 91/97% homology to the human variants. We used purified CLK proteins in *in vitro* kinase assays with auto- and SR-repeat-phosphorylation as read out. In a temperature gradient from 33-40°C, we find the activity of both CLKs to be strongly temperature-dependent with higher activity at lower temperature, matching the phosphorylation state of SR proteins *in vivo* (Preussner et al., 2017) (Figure 1B, C). For both auto- and SR-repeat-phosphorylation, we find CLK1/4 to be almost completely inactive at 38°C, whereas they show considerable activity at 35°C (50-80% of the activity at 33°C), representing a more than 5-fold change (Figure 1C). This substantial change in activity occurred through a change of 3°C, between 35°C and 38°C, precisely in the range in which circadian body temperature oscillations occur (Buhr et al., 2010; Preussner et al., 2017; Saini et al., 2012). As the *in vitro* kinase reactions contain only purified protein and substrate, temperature sensitivity is independent of additional interaction partners or posttranslational modifications, thus representing an inherent feature of the kinases itself.

CLKs consist of an unstructured N-terminal region and the C-terminal kinase domain (Ghosh and Adams, 2011) (Figure 1A). To investigate which part of the protein mediates temperature sensitivity, we purified the kinase domains alone. Mouse and human CLK1/4 kinase domains showed strong temperature-dependence in both auto- and SR-peptide phosphorylation (Figure 1D, 1E, see Figure S1B for the human variants and comparison between mouse and human), showing that the CLK kinase domain is itself temperature-sensitive and that this feature is conserved across mammals. However, as the activity profiles differ slightly between the f.l. proteins and the kinase domains (Figure S1C), the precise temperature range is partially set by the unstructured N-terminus. CLK-mediated phosphorylation is specific for the SR substrate, as GST alone is not phosphorylated, and is not affected by (potentially temperature-induced) differences in the pH between 6.9 and 7.6 (Figure S1D and S1E). For further experiments we have used the respective kinase domains, as they recapitulate temperature sensitivity and can be produced as pure and stable proteins (Figure S1F-I).

Body temperature sensitivity is specific for CLKs and depends on reversible inactivation

To start addressing the molecular basis for higher CLK activity at lower temperatures and to investigate whether related kinases show a similar behavior, we purified a member of the other family of SR protein kinases, namely SRPK1. We then compared temperature-activity profiles of CLKs and SRPK1 in a wider temperature range between 16°C and 56°C. As before, the activity of CLKs was strongly reduced between 32°C and 36°C, with CLK1 activity starting to decrease at 28°C already (Figure 2A). In contrast to the CLKs, SRPK1 activity was constant between 16°C and 52°C with a loss of activity at 56°C, confirming that temperature sensitivity in the physiological temperature range is not a general feature of all protein kinases (Thomas and Scopes, 1998). The wide temperature range of almost unchanged SRPK1 activity is an interesting feature, suggesting that SRPK1 is intrinsically temperature-compensated. The inactivation temperature of SRPK1 at 56°C is close to the median denaturing temperature of human proteins (~60°C) (Leuenberger et al., 2017) and loss of activity likely represents global and irreversible denaturation, as SRPK1 activity was not restored by shifting reactions back to 40°C (Figure 2B). This is in stark contrast to the inactivation of CLKs at 38°C, which was quickly reversible when reducing the temperature from 38°C back to 34°C (Figure 2C, 2D). Additionally, we did not observe substantial changes in CD spectra of the human CLK1 kinase domain at 25°C, 34°C and 38°C, showing that the overall secondary structure remains intact at 38°C (Figure 2E). This observation is in line with a model in which increasing temperature first leads to subtle reversible changes in protein conformation (as in CLK1), followed by irreversible denaturation at higher temperature (as in SRPK1) (Thomas and Scopes, 1998). In summary, these *in vitro* data define CLK kinase domains as a new class of molecular thermometer that is able to measure small changes in core body temperature to mediate downstream changes in (post-transcriptional) gene expression. In contrast to TRP channels that are involved in sensing changes in external temperature mainly outside of the body temperature range (Wetsel, 2011), CLKs respond to endogenous temperature changes and are broadly expressed in diverse tissues, which could globally synchronize the body to changes in core temperature, e.g. in the circadian cycle.

CLK1/4 act as molecular thermometer that connects physiological temperature changes with SR protein phosphorylation and AS in human cells

To confirm the role of CLK1/4 as molecular thermometer in living cells and to validate altered temperature-dependent SR protein phosphorylation as consequence, we used heat shock in human HEK293 cells as model system. A heat shock is known to induce hypophosphorylation of SR proteins (Shin et al., 2004), and shifting cells back to 35°C leads to rapid re-phosphorylation as assessed by the phospho-SR specific 1H4 antibody (Figures 3A and 3B).

We then performed heat shock recovery in the presence of the CLK1/4 inhibitor TG003 (Ninomiya et al., 2011), and indeed find that inhibition of CLK1/4 almost completely abolished re-phosphorylation of several SR proteins, including SRSF5 and SRSF6, when cells were shifted from 42°C to 35°C (Figures 3A and 3B). These data confirm that CLK1/4 are the main kinases controlling temperature-dependent SR protein phosphorylation, as all temperature-dependent, 1H4 reactive bands (phosphorylated SR proteins) are also sensitive to TG003.

We then used RNA-Seq to investigate temperature-sensitive AS in HEK293 cells as a downstream effect of altered SR protein phosphorylation. We obtained RNA-Seq data from three independent samples per conditions and, using stringent filtering conditions, identified around 1750 cassette exons (see Table S1) that react to a temperature change from 35°C to 39°C, corresponding to the temperature of fever and mild hypothermia. While temperature-dependent AS has been investigated before, previous studies have used rather unphysiological conditions, e.g. 32°C or 42°C (Liu et al., 2013; Shalgi et al., 2014), and our data thus shed first light on global AS controlled by changes within the core body temperature range. Remarkably, adding the CLK1/4 inhibitor TG003 almost quantitatively blocked temperature-dependent AS, as the 35°C TG003 sample essentially matched the splicing pattern of the DMSO 39°C sample (Figure 3C, see also Figure S2A for unsupervised clustering of replicate samples). To obtain a quantitative measure for this observation, we focused on cold-induced exons, which represent around 80% of the body temperature-sensitive exons (Figure 3D). This analysis revealed a strongly reduced median percent spliced in (PSI) change in TG003-treated cells (DMSO: 30% (39°C) to 63% (35°C), TG003: 15% (39°C) to 33% (35°C)). This demonstrates first, that TG003 further increases the effect of warm temperature, likely through inhibiting residual CLK activity at 39°C; second, that at 35°C TG003 abolishes exon inclusion above the level that is observed at 39°C in DMSO treated samples; and finally, that the temperature response (the ΔPSI between 35°C and 39°C) is strongly reduced upon inhibition of CLK1/4. Similar results were obtained for intron retention events (Table S2, Figure S2B and S2C). Using splicing-sensitive RT-PCRs, the global trend was confirmed for 4 out of 4 tested targets (Figure 3E-F and Figure S2D-E). These data demonstrate that almost every exon that is sensitive to changes in the body temperature range also reacts to the inhibition of CLK1/4, which strongly argues that CLK1/4 are the dominant temperature sensors that connect body temperature with AS.

CLK1/4 play a major role in controlling temperature-sensitive gene expression

As discussed above, SR proteins control every aspect of (pre-)mRNA processing, from transcription to degradation. We therefore also analyzed temperature-dependent changes in whole transcripts in our RNA-Seq dataset. We identified more than 1000 mRNAs whose abundance changed between 35°C and 39°C (Figure 4A, Table S3), which further underlines

the global impact of physiological temperature changes on the cellular gene expression program. Notably, around 50% of these mRNAs lose temperature sensitivity in TG003-treated cells (boxed in Figure 4A, see also Figure 4B for examples with abolished temperature-dependent gene expression, Table S3). These data confirm that CLK1/4 are the dominant thermo-sensors that sense changes in the physiologically relevant temperature range to then control AS and gene expression.

One of the mRNAs that is strongly temperature-responsive only in control cells encodes for the cold-induced RNA-binding protein (CIRBP) (Figure 4B). Cold-induced expression of CIRBP has been suggested to provide a link between the circadian clock, sleep and body temperature (Hoekstra et al., 2019; Morf et al., 2012). CIRBP also plays an important role in hypothermia, cancer and inflammation (Lujan et al., 2018; Qiang et al., 2013) and has been implicated in TSD in turtles (Schroeder et al., 2016). Despite the central importance of cold-induced CIRBP expression it remains unclear how a reduction in temperature increases CIRBP expression mechanistically. Given our finding that cold-induced CIRPB expression is completely abrogated in TG003-treated cells (Figure 4B), we chose CIRBP for a more detailed analysis. Interestingly, our splicing analysis revealed an alternative 3'-end in the *Cirbp* mRNA, which is strongly promoted by higher temperature in the DMSO control but almost temperature-insensitive in TG003-treated cells (Figure 4C). In this warm-induced isoform, instead of the canonical last exon 7a an alternative exon 7b is used, which is coupled to exon 8 inclusion (Figure 4C, red). We observe strong evolutionary conservation downstream of the canonical polyadenylation site including the 3' splice site of exon 7b in all vertebrates (Figure 4C, bottom, and Figure S3A), including turtles and alligators (see below). Consistent with an evolutionarily conserved mechanism and function, we also observed warm-induced generation of the exon 7b isoform in primary mouse hepatocytes (Figure S3B). Additionally, we found that young mice exposed to a lower ambient temperature, resulting in decreased body temperature (see (Preussner et al., 2017)), show reduced exon 7b inclusion in liver, which correlates with increased total *Cirbp* expression (Figure 4D, as in hepatocytes Figure S3C), thus confirming regulation *in vivo*. To mechanistically link this splicing event with the temperature-regulated differences in gene expression, we made use of CRISPR/Cas9 and generated cell lines lacking exons 7b to 8 in human HEK293 cells (Figure 4E). These cells show increased *Cirbp* mRNA levels and a decreased response to temperature (Figures 4F). Some residual temperature dependence could be mediated via altered general splicing efficiency (Gotic et al., 2016) or warm-induced retention of intron 6, which interestingly is also directly responsive to changes in body temperature (Horii et al., 2019). Together, these data are consistent with a model, in which warm-induced inclusion of exon 7b results in an mRNA with reduced stability and therefore reduced total gene expression. An analogous mechanism could be globally responsible for the observed temperature and TG003-dependent differences in gene

expression, which would actually reflect splicing changes that control mRNA stability, e.g. through inducing nonsense mediated decay (NMD), to eventually control gene expression. However, other mechanisms to control mRNA abundance through altering the phosphorylation status of SR proteins likely contribute to the regulation of temperature-dependent gene expression.

Mechanistic and structural basis for temperature controlled CLK1/4 activity

The general structure of the CLK and SRPK kinase domains is similar (Bullock et al., 2009), providing a well-suited system to identify mechanistic and structural details of the CLK-specific thermo-sensor. Based on published structures of human CLK1, we initially performed molecular dynamics (MD) simulations at 20°C and 40°C, the temperatures that experimentally show maximal and completely lost CLK1 activity, respectively (Figure 2A). During MD simulations, the overall structure of the KD remained unchanged at the two temperatures (Figure S4A), which is in agreement with our CD spectroscopy data and consistent with subtle and reversible structural changes mediating temperature sensitivity. However, the CLK, but not the SRPK, activation segment shows higher flexibility and an altered conformation at 40°C (Figure S4A, movies S1 and S2). The activation segment is an essential and kinase-specific (Eswaran et al., 2008; Taylor and Radzio-Andzelm, 1994) ~25 residue region (Bullock et al., 2009; Nolen et al., 2004) whose conformation in the active center of the kinase determines kinase activity. As no other region within the CLK1 kinase domain showed substantial temperature-dependent differences (Figure S4A), we hypothesized that the CLK activation segment could act as thermo-sensor. To test this idea, we created chimeric kinases with exchanged activation segments (Figure 5A). Indeed, CLK1 containing the SRPK1 activation segment lost all temperature sensitivity and SRPK1 containing the CLK1/4 activation segment became temperature sensitive in a range similar to CLK1 itself (Figure 5B and S4B-E). Therefore, the CLK activation segment is necessary and sufficient to mediate sensitivity to changes in the physiological temperature range. Additionally, the activation segment is 100% conserved between mouse and human CLK1 and CLK4, suggesting a conserved and essential function.

To further address the molecular basis for temperature sensitivity, we performed an Alanine scan of the activation segment in the context of the kinase domain (Figure S5A). While most active mutants displayed a temperature-activity profile as the wt kinase, mutations of two neighboring amino acid residues, R342 and H343, showed a shift towards a higher inactivation temperature (Figure 5C and S5B). This was especially pronounced for the H343A mutant, which remained fully active at 36°C, a temperature where the activity of the wt enzyme is already below 20% (Figure 5C, S5A and S5B). In our MD simulations, these two residues are found in close proximity to one another and to the ATP in the active center of the kinase only at 40°C (movies S1 and S2), whereas especially H343 is far away from the active center at

20°C (Figure S5C). We then modeled a substrate into the active center of CLK1 at 20°C and 40°C. This clearly showed that at 40°C R342 and H343 clash with the substrate, especially around the target Serine, suggesting that these two residues could block substrate access to the active center at higher temperature (Figure 5D). Our data suggest that a conformational change in H343 pushes R342 towards the substrate binding groove, which is consistent with the increased distance between R343 and ATP that we observe in MD simulations of the H344A mutant at 40°C (Figure S5D). The Histidine residue is conserved in all temperature-sensitive CLKs tested, whereas it is replaced by a Glutamine in the temperature-insensitive SRPK1 (Figure S5E and see below). Remarkably, a H343Q mutation in f.l. CLK1 is sufficient to abolish temperature sensitivity altogether (Figure 5E, S6A and S6B), thus validating our MD simulations and confirming a crucial role of a single amino acid residue in mediating temperature sensitivity.

To address whether this holds true in living cells, we overexpressed either wt CLK1 or the H343Q mutant in HEK293 cells and indeed observed that heat induced exon skipping is abolished by overexpression of the temperature insensitive H343Q mutant (Figure S6C-E), confirming that the *in vitro* mutagenesis data is applicable to living cells. Our results thus suggest a mechanistic basis for body temperature-controlled kinase activity at atomic resolution. In addition, the finding that a single residue exchange can completely abolish temperature sensitivity (H343Q) or shift the temperature optima (R342A, H343A) opens the possibility to engineer designer kinases with a defined temperature-activity profile.

CLK1/4 activity is evolutionarily adapted to the growth temperature of poikilotherms

In contrast to homoeotherms, poikilotherms adapt to the ambient temperature and thus experience stronger variations in body temperature. To address whether the CLK-based temperature-sensing mechanism is evolutionarily conserved and adapted to the respective growth temperatures, we tested the temperature-activity profiles of CLK homologs from three poikilothermic species. We chose two reptilian species, alligator and turtle, and the fly, *D. melanogaster*, as a model organism that has separated from reptiles ~1 billion years ago. For all three organisms we find that the activity of the CLK homologs are switched off at the upper limit of the physiologically relevant temperature ranges (Figures 6A-C and Figures S7A-C), which matches our observation for mammalian CLKs. Of note, the reptilian CLK temperature-activity profiles are markedly different from the mouse version in this temperature range, confirming species-specificity (Figure S7D). These temperature-activity profiles with higher activity in the lower range of the physiologically relevant temperature of diverse organisms show that the mechanism and regulatory principle is conserved across evolution, but that the enzymes have adapted to the respective physiological temperature range. This furthermore indicates a conserved and evolutionarily-adapted function of CLKs in adapting gene expression to the changes in body temperature experienced by the respective organisms.

Interestingly, in diverse reptiles sex determination is controlled by the temperature at which eggs are incubated (Capel, 2017); for example, for the American alligator incubating eggs below 30°C will result in females whereas temperatures between 30°C and 34°C will yield mostly male offspring (Ferguson and Joanen, 1982). While this has been known for decades, the thermo-sensor that initiates sex determination has remained elusive (Georges and Holleley, 2018). Notably, the temperature-activity profile of the alligator CLK4 falls exactly within the range of temperature-dependent sex determination (Figures 6A, 6D and 6E, see also Figures S7E and S7F for f.l. CLK4). Similarly, for the turtle f.l. CLK1 we observe full activity below 26°C and a strong reduction, around 10% remaining activity, above 31°C, basically representing an on-off switch in the temperature range of sex determination (Figures 6B, 6F and 6G). The regulated activity of CLK kinases from two independent reptilian species, exactly in the temperature range for sex determination, suggest that CLK enzymes may represent a temperature sensor for TSD in reptiles. Recent studies have associated temperature-dependent AS, in this case intron retention events in Jumonji histone deacetylases, with TSD (Deveson et al., 2017; Ge et al., 2018). To investigate whether these AS events are CLK dependent, we used cell lines from two different turtle species (Red eared slider turtle and common box turtle). We first confirmed temperature-dependent intron retention of intron 18 in Jarid2, a Jumonji-domain containing chromatin-modifier, which is involved in TSD (Deveson et al., 2017). As in the *in vivo* situation, we find substantially increased intron retention at the male-producing, lower temperature (26°C) than at the female-producing 31.5°C in both cell lines (Figure 6H). We then repeated the experiment in the presence of the CLK1/4 inhibitor TG003 (which was active in inhibiting the turtle kinase *in vitro*, Figures S7G and S7H). TG003 had little effect on Jarid2 intron retention at 31.5°C, where the turtle CLK1 is not active (Figure 6H). However, TG003 prevented the increased intron retention in Jarid2 at colder temperature, providing evidence that a TSD-associated AS event is controlled by temperature-dependent CLK activity. Our combined data show that body temperature-mediated control of CLK activity is conserved across evolution and adapted to the respective temperature range of diverse organisms and implicate cold-induced CLK activity in TSD in reptiles.

Discussion

Here we describe the activity of CLKs to be controlled by subtle changes in (body) temperature. This extreme temperature sensitivity is an inherent feature of the kinases, as it is observed in recombinant proteins purified from bacteria. It does not require allosteric modulators, posttranslational modifications or interaction partners, thus representing a new concept for the regulation of enzymatic activity. Various studies have shown that phosphorylation within the activation segment is crucial for the activity of many kinases, as it induces an ordered

conformation essential for activity (Goldberg et al., 1996; Huse and Kuriyan, 2002; Johnson et al., 1996). However, in the CLK1/3 crystal structure the activation segment is not phosphorylated but has an ordered, active conformation (Bullock et al., 2009), suggesting that for CLKs, and potentially other kinases or enzymes in general, temperature-controlled conformational changes may play a similar role. This kinase-based thermo-sensor represents a new class of cellular thermometers that, in contrast to TRP channels which are mainly reacting to external temperature, reacts to endogenous core body temperature changes.

The direct consequence is altered SR protein phosphorylation, which is involved in all (pre-)mRNA processing events, from transcription to splicing, nuclear export, translation and stability (Long and Caceres, 2009; Maslon et al., 2014; Muller-McNicoll et al., 2016; Zhong et al., 2009). The example of CIRBP highlights how a temperature-controlled AS event can also generate temperature-dependent differences in gene expression. Many more temperature and TG003-dependent mRNAs could be controlled by a similar splicing-based mechanism. This could be achieved through temperature-dependent splicing isoforms with reduced stability, e.g. due to a shorter 3'UTR or containing premature stop codons inducing NMD.

This cellular thermometer has far-reaching functional implications in diverse physiological and pathophysiological conditions. For example, our work directly connects circadian changes in body temperature with posttranscriptional control of gene expression, which will have a substantial impact on diverse aspects of physiology. As core body temperature decreases with ageing (Keil et al., 2015), we also provide a possible mechanism that controls AS and gene expression in general in the ageing population. Given the sensitivity and the quick reaction to small temperature changes, CLK activity is likely to also impact on gene expression in pathological conditions such as hypothermia, septic shock, fever or in the slightly warmer tumor microenvironment. Similarly, processing of viral transcripts, such as HIV or influenza pre-mRNA has been shown to be dependent on CLKs and host SR proteins (Artarini et al., 2019; Wong et al., 2013) and may thus be controlled through body temperature.

In addition, our data from poikilotherms indicate an evolutionarily conserved and adapted function in temperature sensing with fundamental importance, as our analysis suggests an involvement in reptilian sex determination. It is interesting to note that lower temperature induces an intron retention isoform of Jumonji-domain encoding mRNAs (Jarid2 and Kdm6b) in turtle and alligator, whereas intron retention isoforms are induced by warmer temperatures in the bearded dragon *Pogona vitticeps* (Deveson et al., 2017). We suggest that cold-induced CLK activity controls SR protein phosphorylation, which then regulates intron retention. As the binding position of SR proteins relative to the regulated intron/exon determines the effect on splicing (Erkelenz et al., 2013), exclusion or inclusion, we suggest that this accounts for the opposite effects of temperature on intron retention in different species. Formation of the intron retention isoforms is associated with sex determination, but the functionality of the resulting

proteins and a potential role in initiating or stabilizing sex determination remains to be shown. Of note, we find an intron retention event in human Kdm6b to be temperature and TG003-sensitive (Table S2), suggesting wide evolutionary conservation.

As is it plausible to assume that a fundamental decision such as sex determination requires input from more than one signaling pathway, e.g. separate signals for initiation and stabilization, we suggest that CLKs are one, but not necessarily the only, molecular thermometer contributing to TSD. Interestingly, temperature-dependent *Cirbp* expression has also been linked to TSD in turtles (Schroeder et al., 2016). As we show that cold-induced *Cirpb* expression is also dependent on alternative splicing and CLK activity, our data provide evidence that CLKs control at least two independent events, intron retention in chromatin modifiers and *Cirpb* expression, that are implicated in TSD. As CIRBP has been hypothesized to control expression of Kdm6b (Georges and Holleley, 2018), these pathways may eventually interact, to increase expression of the intron-retained Kdm6b isoform at colder temperature (in turtles), which has been suggested to be a crucial event in TSD (Ge et al., 2018).

Finally, our mechanistic analysis reveals individual amino acid residues that are crucial to set the temperature range in which CLKs are inactivated. This opens the possibility to engineer kinases with defined temperature-activity profiles. Such kinases may be used as reversible on-off switches in cell culture, in gene therapeutic applications and potentially to alter temperature sensing of whole organisms, which may become especially relevant in the light of global warming.

Author Contributions

TH, AK and MP performed most experiments with help from FDB, AF and SS; protein purifications were done in MCW's lab. AKE, KKP and SM generated and characterized *Cirbp*-edited cell lines. MP performed bioinformatics analysis. BT performed RNA sequencing. PI performed MD simulations. TH, MP and FH designed the study, planed experiments, analyzed data and wrote the manuscript, with input from PI and MCW. FH conceived and supervised the work.

Acknowledgments

The authors would like to thank Jan Driller (FU Berlin) for providing SRPK1 protein, Ana Rita Lima Fernandes and Dorian Mikolajczak from the AG Koksch (FU Berlin) for help with CD spectroscopy, Sutapa Chakrabarti (FU Berlin) for discussion and members of the Heyd lab for comments on the manuscript. We thank Dr. Matthias Lenk from the Friedrich-Loeffler-Institut (Greifswald, Germany) for providing turtle cell lines. Computational resources provided by the North-German Supercomputing Alliance (HLRN) are gratefully acknowledged. PI thanks Philip

Ulrich for help with vmd/tcl scripting. FH thanks Jan Medenbach (Regensburg University) for discussing sex determination in reptiles. This work was funded through DFG grants HE5398/4 and HE5398/4-2 to FH; additional funding was provided by the DFG grant 278001972 - TRR 186 to FH and MCW. MP is funded by a post-doc stipend of the Peter and Traudl Engelhorn Foundation.

References

Artarini, A., Meyer, M., Shin, Y.J., Huber, K., Hilz, N., Bracher, F., Eros, D., Orfi, L., Keri, G., Goedert, S.*, et al.* (2019). Regulation of influenza A virus mRNA splicing by CLK1. Antiviral research *168*, 187-196.

Aubol, Brandon E., Wu, G., Keshwani, Malik M., Movassat, M., Fattet, L., Hertel, Klemens J., Fu, X.-D., and Adams, Joseph A. (2016). Release of SR Proteins from CLK1 by SRPK1: A Symbiotic Kinase System for Phosphorylation Control of Pre-mRNA Splicing. Molecular cell *63*, 218-228.

Bautista, D.M., Siemens, J., Glazer, J.M., Tsuruda, P.R., Basbaum, A.I., Stucky, C.L., Jordt, S.E., and Julius, D. (2007). The menthol receptor TRPM8 is the principal detector of environmental cold. Nature *448*, 204-208.

Best, R.B., Zhu, X., Shim, J., Lopes, P.E.M., Mittal, J., Feig, M., and MacKerell, A.D. (2012). Optimization of the Additive CHARMM All-Atom Protein Force Field Targeting Improved Sampling of the Backbone ϕ, ψ and Side-Chain χ1 and χ2 Dihedral Angles. Journal of chemical theory and computation *8*, 3257-3273.

Buhr, E.D., Yoo, S.H., and Takahashi, J.S. (2010). Temperature as a universal resetting cue for mammalian circadian oscillators. Science (New York, NY) *330*, 379-385.

Bullock, A.N., Das, S., Debreczeni, J.E., Rellos, P., Fedorov, O., Niesen, F.H., Guo, K., Papagrigoriou, E., Amos, A.L., Cho, S.*, et al.* (2009). Kinase domain insertions define distinct roles of CLK kinases in SR protein phosphorylation. Structure (London, England : 1993) *17*, 352-362.

Bussi, G., Donadio, D., and Parrinello, M. (2007). Canonical sampling through velocity rescaling. J Chem Phys *126*, 014101.

Capel, B. (2017). Vertebrate sex determination: evolutionary plasticity of a fundamental switch. Nature reviews Genetics *18*, 675-689.

Charkoudian, N., Hart, E.C.J., Barnes, J.N., and Joyner, M.J. (2017). Autonomic control of body temperature and blood pressure: influences of female sex hormones. Clinical autonomic research : official journal of the Clinical Autonomic Research Society *27*, 149-155.

Colwill, K., Pawson, T., Andrews, B., Prasad, J., Manley, J.L., Bell, J.C., and Duncan, P.I. (1996). The Clk/Sty protein kinase phosphorylates SR splicing factors and regulates their intranuclear distribution. The EMBO journal *15*, 265-275.

Czerwinski, M., Natarajan, A., Barske, L., Looger, L.L., and Capel, B. (2016). A timecourse analysis of systemic and gonadal effects of temperature on sexual development of the red-eared slider turtle Trachemys scripta elegans. Developmental biology *420*, 166-177.

Deveson, I.W., Holleley, C.E., Blackburn, J., Marshall Graves, J.A., Mattick, J.S., Waters, P.D., and Georges, A. (2017). Differential intron retention in Jumonji chromatin modifier genes is implicated in reptile temperature-dependent sex determination. Science Advances *3*.

Dominguez, D., Tsai, Y.H., Weatheritt, R., Wang, Y., Blencowe, B.J., and Wang, Z. (2016). An extensive program of periodic alternative splicing linked to cell cycle progression. eLife *5*.

Erkelenz, S., Mueller, W.F., Evans, M.S., Busch, A., Schoneweis, K., Hertel, K.J., and Schaal, H. (2013). Position-dependent splicing activation and repression by SR and hnRNP proteins rely on common mechanisms. RNA (New York, NY) *19*, 96-102.

Eswaran, J., Bernad, A., Ligos, J.M., Guinea, B., Debreczeni, J.E., Sobott, F., Parker, S.A., Najmanovich, R., Turk, B.E., and Knapp, S. (2008). Structure of the human protein kinase MPSK1 reveals an atypical activation loop architecture. Structure (London, England : 1993) *16*, 115-124.

Ferguson, M.W., and Joanen, T. (1982). Temperature of egg incubation determines sex in Alligator mississippiensis. Nature *296*, 850-853.

Gautherie, M., and Gros, C.M. (1980). Breast thermography and cancer risk prediction. Cancer *45*, 51-56.

Ge, C., Ye, J., Weber, C., Sun, W., Zhang, H., Zhou, Y., Cai, C., Qian, G., and Capel, B. (2018). The histone demethylase KDM6B regulates temperature-dependent sex determination in a turtle species. Science (New York, NY) *360*, 645-648.

Georges, A., and Holleley, C.E. (2018). How does temperature determine sex? Science (New York, NY) *360*, 601-602.

Ghosh, G., and Adams, J.A. (2011). Phosphorylation mechanism and structure of serine-arginine protein kinases. The FEBS Journal *278*, 587-597.

Goldammer, G., Neumann, A., Strauch, M., Muller-McNicoll, M., Heyd, F., and Preussner, M. (2018). Characterization of cis-acting elements that control oscillating alternative splicing. RNA biology *15*, 1081-1092.

Goldberg, J., Nairn, A.C., and Kuriyan, J. (1996). Structural Basis for the Autoinhibition of Calcium/Calmodulin-Dependent Protein Kinase I. Cell *84*, 875-887.

Gong, J., Liu, J., Ronan, E.A., He, F., Cai, W., Fatima, M., Zhang, W., Lee, H., Li, Z., Kim, G.H.*, et al.* (2019). A Cold-Sensing Receptor Encoded by a Glutamate Receptor Gene. Cell *178*, 1375-1386.e1311.

Gotic, I., Omidi, S., Fleury-Olela, F., Molina, N., Naef, F., and Schibler, U. (2016). Temperature regulates splicing efficiency of the cold-inducible RNA-binding protein gene Cirbp. Genes & development *30*, 2005-2017.

Hess, B. (2008). P-LINCS: A Parallel Linear Constraint Solver for Molecular Simulation. Journal of chemical theory and computation *4*, 116-122.

Hess, B., Kutzner, C., van der Spoel, D., and Lindahl, E. (2008). GROMACS 4: Algorithms for Highly Efficient, Load-Balanced, and Scalable Molecular Simulation. Journal of chemical theory and computation *4*, 435-447.

Hoekstra, M.M., Emmenegger, Y., Hubbard, J., and Franken, P. (2019). Cold-inducible RNA-binding protein (CIRBP) adjusts clock-gene expression and REM-sleep recovery following sleep deprivation. eLife *8*.

Horii, Y., Shiina, T., Uehara, S., Nomura, K., Shimaoka, H., Horii, K., and Shimizu, Y. (2019). Hypothermia induces changes in the alternative splicing pattern of cold-inducible RNA-binding protein transcripts in a non-hibernator, the mouse. Biomedical research (Tokyo, Japan) *40*, 153-161.

Humphrey, W., Dalke, A., and Schulten, K. (1996). VMD: Visual molecular dynamics. Journal of Molecular Graphics *14*, 33-38.

Hunter, J.D. (2007). Matplotlib: A 2D Graphics Environment. Computing in Science & Engineering *9*, 90-95.

Huse, M., and Kuriyan, J. (2002). The Conformational Plasticity of Protein Kinases. Cell *109*, 275-282.

Isshiki, Y., Kohchi, Y., Iikura, H., Matsubara, Y., Asoh, K., Murata, T., Kohchi, M., Mizuguchi, E., Tsujii, S., Hattori, K.*, et al.* (2011). Design and synthesis of novel allosteric MEK inhibitor CH4987655 as an orally available anticancer agent. Bioorganic & medicinal chemistry letters *21*, 1795-1801.

Johnson, L.N., Noble, M.E.M., and Owen, D.J. (1996). Active and Inactive Protein Kinases: Structural Basis for Regulation. Cell *85*, 149-158.

Jorgensen, W.L., Chandrasekhar, J., Madura, J.D., Impey, R.W., and Klein, M.L. (1983). Comparison of simple potential functions for simulating liquid water. The Journal of Chemical Physics *79*, 926-935.

Keil, G., Cummings, E., and de Magalhães, J.P. (2015). Being cool: how body temperature influences ageing and longevity. Biogerontology *16*, 383-397.

Leuenberger, P., Ganscha, S., Kahraman, A., Cappelletti, V., Boersema, P.J., von Mering, C., Claassen, M., and Picotti, P. (2017). Cell-wide analysis of protein thermal unfolding reveals determinants of thermostability. Science (New York, NY) *355*.

Liu, Y., Hu, W., Murakawa, Y., Yin, J., Wang, G., Landthaler, M., and Yan, J. (2013). Cold-induced RNA-binding proteins regulate circadian gene expression by controlling alternative polyadenylation. Scientific reports *3*, 2054.

Long, J.C., and Caceres, J.F. (2009). The SR protein family of splicing factors: master regulators of gene expression. The Biochemical journal *417*, 15-27.

Lujan, D.A., Ochoa, J.L., and Hartley, R.S. (2018). Cold-inducible RNA binding protein in cancer and inflammation. Wiley Interdiscip Rev RNA *9*.

Mallajosyula, S.S., Guvench, O., Hatcher, E., and Mackerell, A.D., Jr. (2012). CHARMM Additive All-Atom Force Field for Phosphate and Sulfate Linked to Carbohydrates. Journal of chemical theory and computation *8*, 759-776.

Maslon, M.M., Heras, S.R., Bellora, N., Eyras, E., and Caceres, J.F. (2014). The translational landscape of the splicing factor SRSF1 and its role in mitosis. eLife, e02028.

Morf, J., Rey, G., Schneider, K., Stratmann, M., Fujita, J., Naef, F., and Schibler, U. (2012). Cold-inducible RNA-binding protein modulates circadian gene expression posttranscriptionally. Science (New York, NY) *338*, 379-383.

Muller-McNicoll, M., Botti, V., de Jesus Domingues, A.M., Brandl, H., Schwich, O.D., Steiner, M.C., Curk, T., Poser, I., Zarnack, K., and Neugebauer, K.M. (2016). SR proteins are NXF1 adaptors that link alternative RNA processing to mRNA export. Genes & development *30*, 553-566.

Ngo, J.C., Chakrabarti, S., Ding, J.H., Velazquez-Dones, A., Nolen, B., Aubol, B.E., Adams, J.A., Fu, X.D., and Ghosh, G. (2005). Interplay between SRPK and Clk/Sty kinases in phosphorylation of the splicing factor ASF/SF2 is regulated by a docking motif in ASF/SF2. Molecular cell *20*, 77-89.

Ninomiya, K., Kataoka, N., and Hagiwara, M. (2011). Stress-responsive maturation of Clk1/4 pre-mRNAs promotes phosphorylation of SR splicing factor. The Journal of cell biology *195*, 27-40.

Nolen, B., Taylor, S., and Ghosh, G. (2004). Regulation of Protein Kinases: Controlling Activity through Activation Segment Conformation. Molecular cell *15*, 661-675.

Preussner, M., Goldammer, G., Neumann, A., Haltenhof, T., Rautenstrauch, P., Muller-McNicoll, M., and Heyd, F. (2017). Body Temperature Cycles Control Rhythmic Alternative Splicing in Mammals. Molecular cell *67*, 433-446.e434.

Preussner, M., and Heyd, F. (2018). Temperature-controlled Rhythmic Gene Expression in Endothermic Mammals: All Diurnal Rhythms are Equal, but Some are Circadian. BioEssays : news and reviews in molecular, cellular and developmental biology *40*, e1700216.

Preussner, M., Wilhelmi, I., Schultz, A.S., Finkernagel, F., Michel, M., Moroy, T., and Heyd, F. (2014). Rhythmic U2af26 alternative splicing controls PERIOD1 stability and the circadian clock in mice. Molecular cell *54*, 651-662.

Qiang, X., Yang, W.L., Wu, R., Zhou, M., Jacob, A., Dong, W., Kuncewitch, M., Ji, Y., Yang, H., Wang, H.*, et al.* (2013). Cold-inducible RNA-binding protein (CIRP) triggers inflammatory responses in hemorrhagic shock and sepsis. Nature medicine *19*, 1489-1495.

Ran, F.A., Hsu, P.D., Wright, J., Agarwala, V., Scott, D.A., and Zhang, F. (2013). Genome engineering using the CRISPR-Cas9 system. Nature protocols *8*, 2281-2308.

Refinetti, R., and Menaker, M. (1992). The circadian rhythm of body temperature. Physiology & behavior *51*, 613-637.

Saini, C., Morf, J., Stratmann, M., Gos, P., and Schibler, U. (2012). Simulated body temperature rhythms reveal the phase-shifting behavior and plasticity of mammalian circadian oscillators. Genes & development *26*, 567-580.

Sali, A., and Blundell, T.L. (1993). Comparative protein modelling by satisfaction of spatial restraints. Journal of molecular biology *234*, 779-815.

Schroeder, A.L., Metzger, K.J., Miller, A., and Rhen, T. (2016). A Novel Candidate Gene for Temperature-Dependent Sex Determination in the Common Snapping Turtle. Genetics *203*, 557-571.

Shalgi, R., Hurt, J.A., Lindquist, S., and Burge, C.B. (2014). Widespread inhibition of posttranscriptional splicing shapes the cellular transcriptome following heat shock. Cell reports *7*, 1362-1370.

Shin, C., Feng, Y., and Manley, J.L. (2004). Dephosphorylated SRp38 acts as a splicing repressor in response to heat shock. Nature *427*, 553-558.

Sterne-Weiler, T., Weatheritt, R.J., Best, A.J., Ha, K.C.H., and Blencowe, B.J. (2018). Efficient and Accurate Quantitative Profiling of Alternative Splicing Patterns of Any Complexity on a Laptop. Molecular cell *72*, 187-200.e186.

Studier, F.W. (2005). Protein production by auto-induction in high density shaking cultures. Protein expression and purification *41*, 207-234.

Tan, P.L., and Katsanis, N. (2009). Thermosensory and mechanosensory perception in human genetic disease. Human molecular genetics *18*, R146-R155.

Taylor, S.S., and Radzio-Andzelm, E. (1994). Three protein kinase structures define a common motif. Structure (London, England : 1993) *2*, 345-355.

Thomas, T.M., and Scopes, R.K. (1998). The effects of temperature on the kinetics and stability of mesophilic and thermophilic 3-phosphoglycerate kinases. The Biochemical journal *330 (Pt 3)*, 1087-1095.

Van Der Spoel, D., Lindahl, E., Hess, B., Groenhof, G., Mark, A.E., and Berendsen, H.J. (2005). GROMACS: fast, flexible, and free. Journal of computational chemistry *26*, 1701-1718.

Walt, S.v.d., Colbert, S.C., and Varoquaux, G. (2011). The NumPy Array: A Structure for Efficient Numerical Computation. Computing in Science & Engineering *13*, 22-30.

Wetsel, W.C. (2011). Sensing hot and cold with TRP channels. International journal of hyperthermia : the official journal of European Society for Hyperthermic Oncology, North American Hyperthermia Group *27*, 388-398.

Wong, R.W., Balachandran, A., Ostrowski, M.A., and Cochrane, A. (2013). Digoxin suppresses HIV-1 replication by altering viral RNA processing. PLoS pathogens *9*, e1003241.

Zhong, X.-Y., Wang, P., Han, J., Rosenfeld, M.G., and Fu, X.-D. (2009). SR Proteins in Vertical Integration of Gene Expression from Transcription to RNA Processing to Translation. Molecular cell *35*, 1-10.

Zhou, Z., and Fu, X.D. (2013). Regulation of splicing by SR proteins and SR protein-specific kinases. Chromosoma *122*, 191-207.

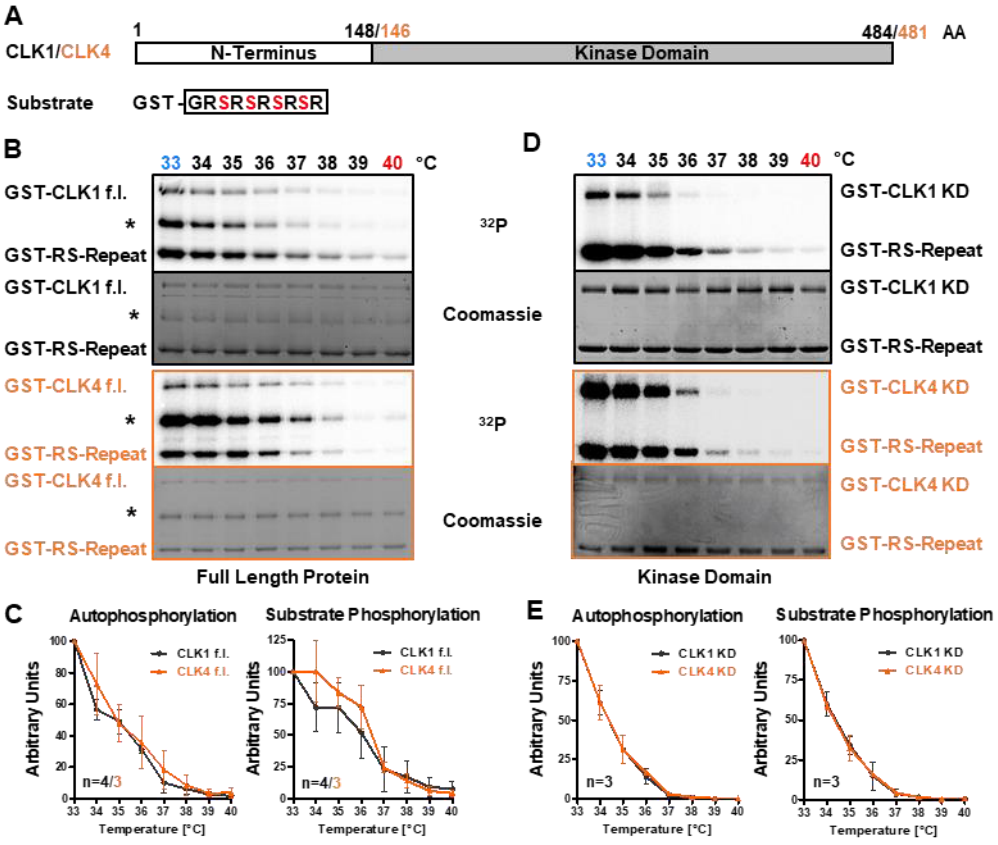

Figure 1. The activity of the CLK1/4 kinase domain is controlled by changes in the physiologically relevant temperature range

(A) Schematics of CLK1/4 kinases and an arginine/serine (RS) peptide substrate. Borders in CLK1 and CLK4 domain organization are highlighted in black or orange, respectively.

(B) *In vitro* kinase assay with full length (f.l.) kinases. CLK1 (top, black) and CLK4 (bottom, orange) were purified from bacteria and coupled to glutathione beads, incubated with GST-RS and ^{32}P-γ-ATP at the indicated temperatures. After SDS-PAGE, phosphorylation was investigated by autoradiography (top, ^{32}P), equal loading was confirmed by Coomassie staining (bottom). The asterisks likely represent

extended kinase domains (KD), which lost the GST units due to cleavage in the unstructured N-termini by residual proteases, and which are also phosphorylated in a temperature-dependent manner.
(C) Quantification of auto- and substrate phosphorylation experiments as in (B) relative to the highest activity (n=3 for CLK4, n=4 for CLK1).
(D) *In vitro* kinase assays as in (B) with purified kinase domains.
(E) Quantification of experiments as in (D) (n=3). In (C) and (E) data represent means +/- standard deviations (SD).
See also Figure S1.

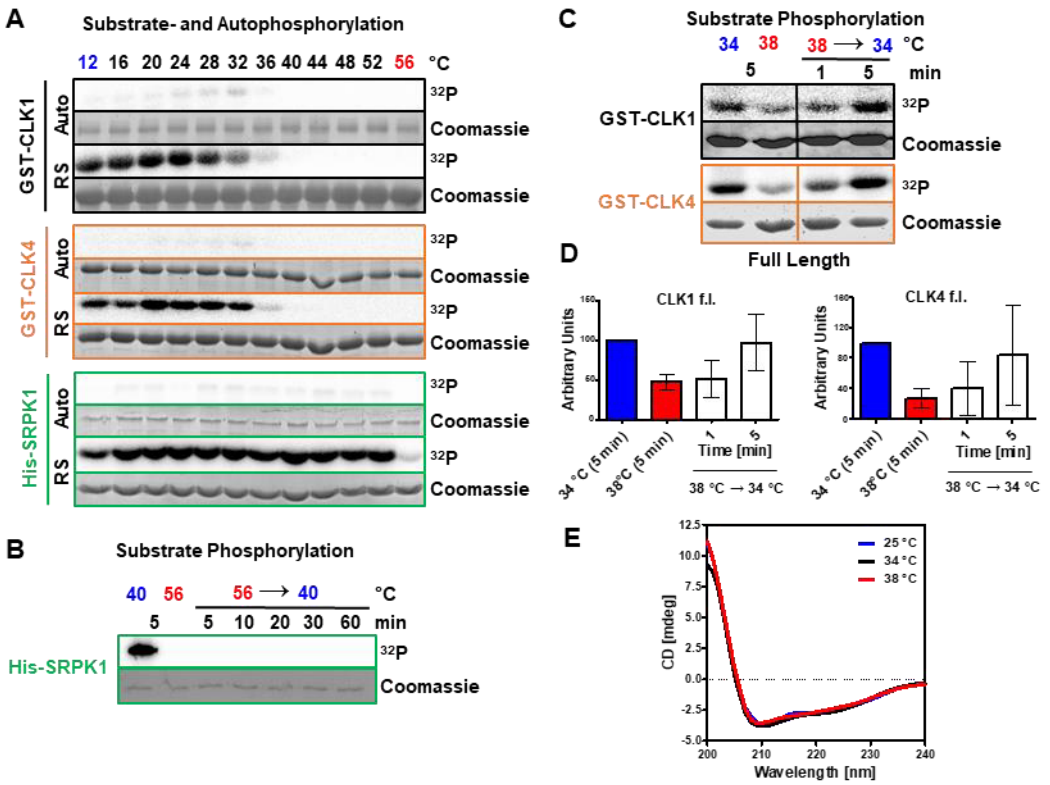

Figure 2. Temperature-dependent SR protein phosphorylation is specifically mediated by CLK1/4 and the inactivation at high temperature is reversible

(A) Kinase activity was investigated as in Figure 1B in a larger temperature range (indicated on top) for CLK1 (black), CLK4 (orange), and the SR protein kinase SRPK1 (green).

(B) Heat-induced inactivation of SRPK1 is irreversible. Substrate phosphorylation was investigated after incubation for 5 min at 56°C and then shifting the reactions back to 40°C for the indicated times.

(C, D) Reversible inactivation of CLK1/4. Substrate phosphorylation was investigated after incubation at 38°C and shifting the reactions back to 34°C for the indicated times. Quantifications of experiments as in (C) are shown in (D) (n=3, mean +/- SD).

(E) CD spectroscopy of the CLK1 kinase domain at 25°C (blue) 34°C (black) and 38°C (red). Data represent the mean of three recorded spectra.

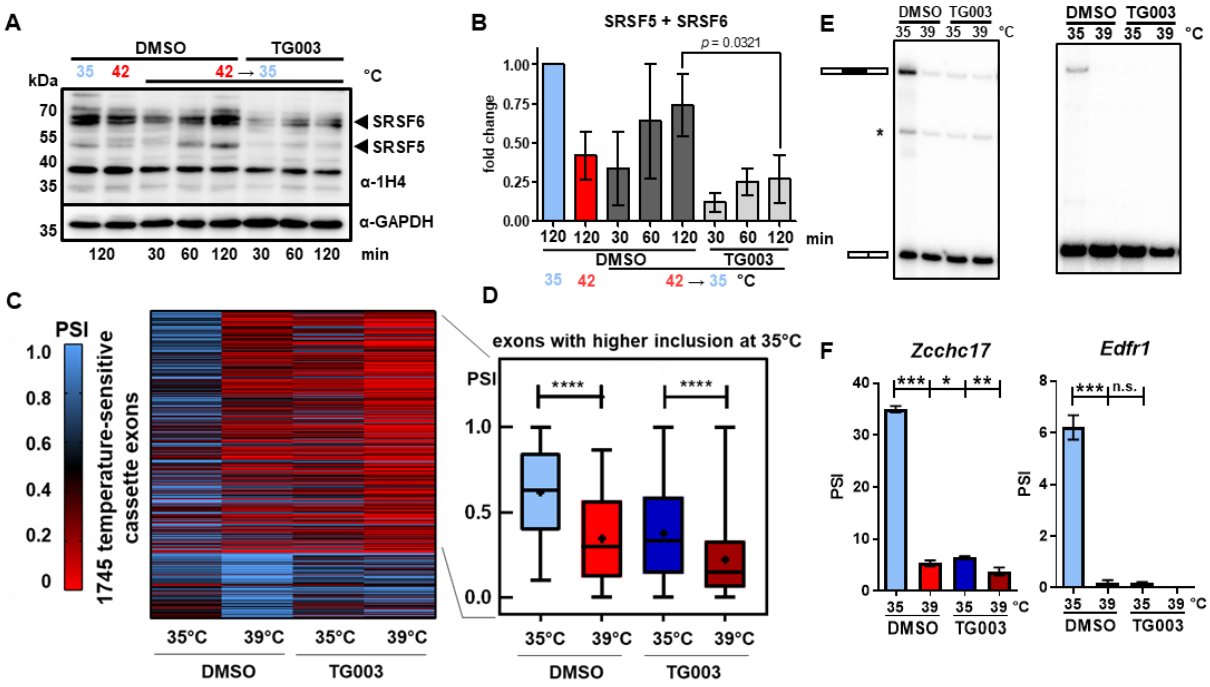

Figure 3. CLK activity controls body temperature dependent SR protein phosphorylation and AS in vivo

(A) HEK293 cells were incubated at 35°C overnight, then placed at 42°C for 120 min, treated with TG003 or DMSO and shifted back to 35°C for 30, 60 or 120 min respectively. A representative Western Blot using the Phospho-SR-specific antibody 1H4 is shown. GAPDH served as loading control.

(B) Quantification of Western Blots as in (A). Band intensities at 70 kDa (SRSF6) and at 55 kDa (SRSF5) were quantified and normalized to the GAPDH loading control. Data represent mean of three independent sets +/- SD. Statistical significance was determined by an unpaired t-test.

(C, D) HEK293 cells were pre-entrained to 39°C for 12 hours. After addition of DMSO or TG003 cells were shifted to 35°C (or maintained at 39°C); RNA was extracted after 6 hours and analyzed by RNA-Seq. In (C) a heatmap of percent spliced in (PSI) values of all (1745) skipped exon events that are temperature-dependent in control (DMSO) is shown (n=3). In (D) Box-Whisker-Plots of PSI values for exons with higher inclusion at 35°C. The line represents the median PSI, circle represents mean PSI. Statistical significance is determined by 1-way ANOVA (Tukey's multiple comparisons test, ****$p<1x10^{-15}$).

(E-F) AS of *Zcchc17* and *Edfr1* was confirmed by radioactive RT-PCR. Representative gels are shown in (E) and quantified in (F) (n=3, mean+/-SD). Statistical significance was determined by unpaired t-test. For further targets see Figures S2D and S2E.

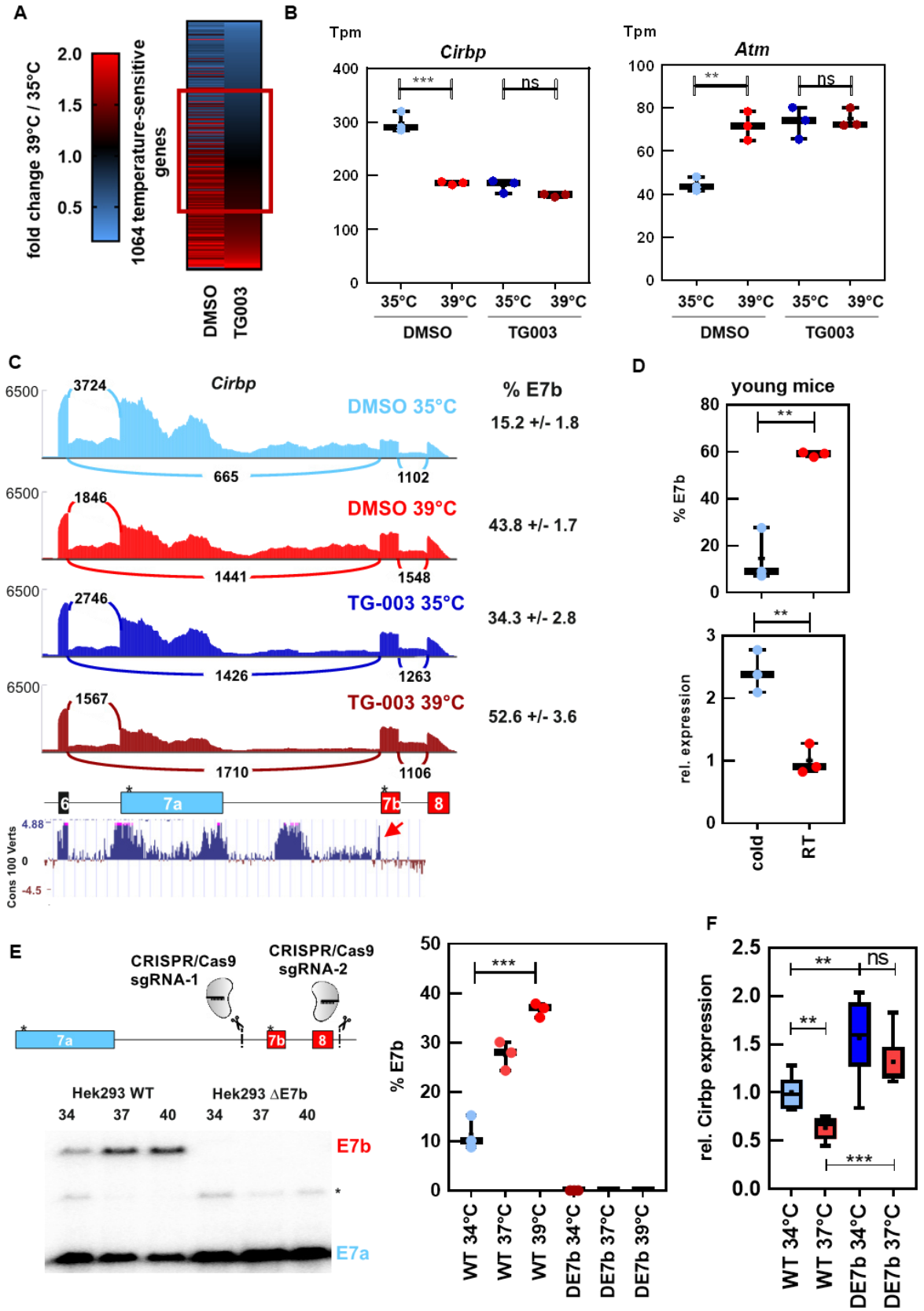

Figure legend on the next page

Figure 4. CLK activity controls body temperature dependent gene expression

(A) Heatmap of 1064 genes with >1.3-fold changed gene expression in DMSO. Genes are sorted by the fold-change in TG003; the red box highlights genes with a fold-change <1.3 in TG003 (n=507).

(B) Examples with abolished temperature-dependent gene expression. Plotted are the transcripts per million (tpm) values. Statistical significance was determined by unpaired t-test. Note that temperature dependent gene expression is basically abolished upon TG003 treatment.
(C) Temperature dependent AS of the *Cirbp* 3'-end. A sashimi blots shows the read distribution for the different conditions (y-axis set to 6500 reads per base). The lines indicate junction reads. Percentage of the E7b isoform was calculated in the triplicate samples, mean and standard deviation are depicted on the right. Below, Exon/Intron structure of the pre-mRNA. Exons are depicted by boxes, introns by lines, the asterisks indicate stop codons. At the bottom Basewise comparison across 100 vertebrates by PhyloP from the UCSC genome browser is shown. The red arrowhead marks the conserved 3' splice site of exon 7b. See also Figure S3A.
(D) *Cirbp* splicing and gene expression in the liver of young mice (12-13 days) kept at room temperature (RT) or at 18°C for 2 hours (cold, see (Preussner et al., 2014) for post mortem temperatures). Splicing was analyzed by splicing sensitive RT-PCR with a forward primer in exon 6 and two reverse primers in exons 7a and 7b, gene expression was analyzed by qRT-PCR and is shown normalized to *Hprt* and RT (n=3). Statistical significance was determined by unpaired t-tests, **p<0.01.
(E) Depletion of exons 7b-8 using CRISPR/Cas9 in Hek293 cells (top: position of guide RNAs), below a radioactive RT-PCR investigating *Cirbp* AS at the indicated temperatures is shown and quantified (right, n=3, mean +/-SD). Statistical significance was determined by unpaired t-tests, ***p<0.001.
(F) Increased and less temperature dependent *Cirbp* expression in cells lacking the temperature dependent exon 7b. *Cirbp* expression was investigated after 12 hours at the indicated temperatures by RT-qPCR (relative to *Gapdh*, n>5, statistical significance was determined by unpaired t-tests, **p<0.01, ***p<0.001).
See also Figure S3.

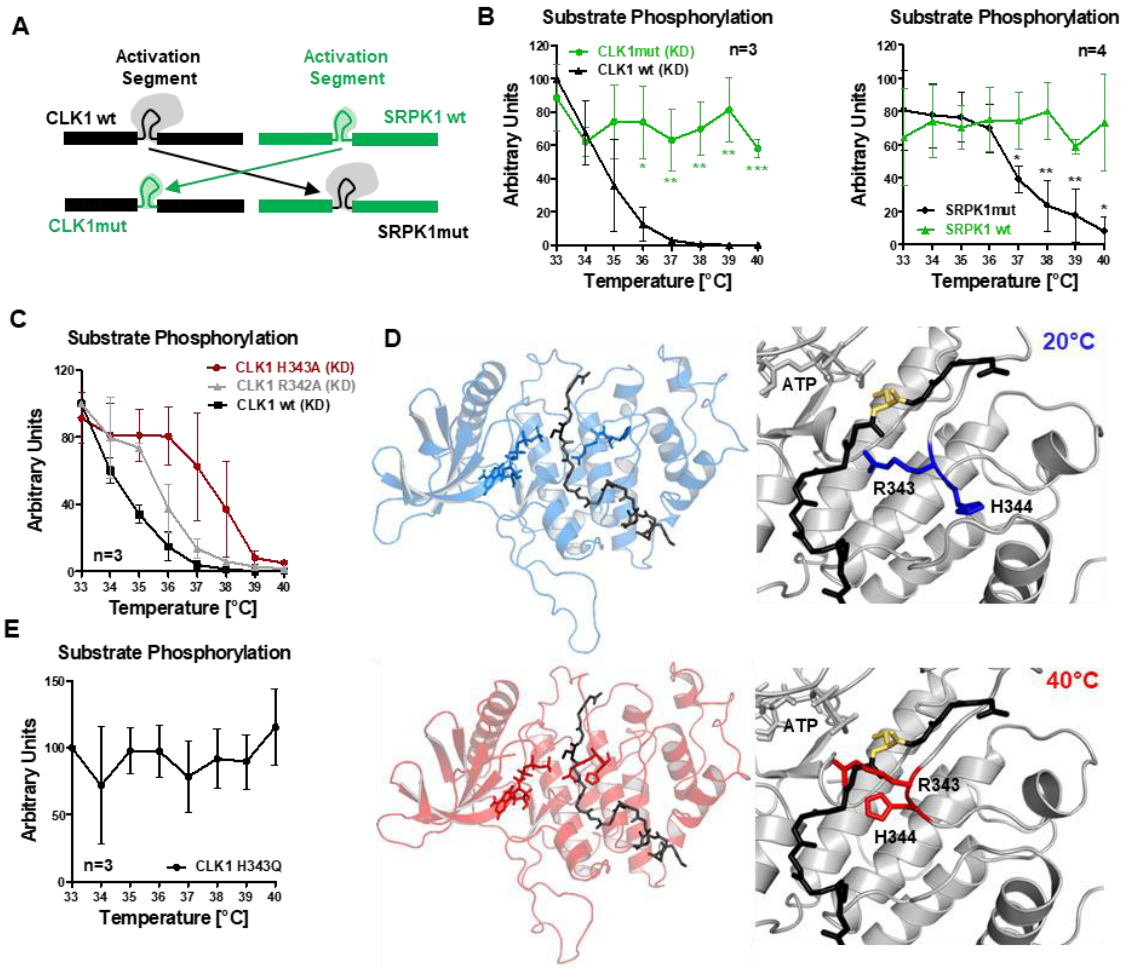

Figure 5. Temperature-sensitivity of CLK activity is mediated through a conserved His residue in the activation segment

(A, B) Generation of activation segment switch hybrids (A) transfers loss and gain of temperature sensitivity (B; n=3, mean +/- SD). Activation segment mutants are based on MD simulations (Figure S4A). Temperature-dependent activity was determined as in Figure 1B. See also Figure S4B-E for gel images and quantification of autophosphorylation.

(C) Quantification of CLK1 kinase domain (KD) wt, R342A and H343A activities. R342A and H343A represent the mutants with the strongest effect on the temperature profile, see Figure S5A and S5B for the full Alanine scan.

(D) Structures of the CLK1 kinase domain at 20°C (top) and 40°C (bottom) as modelled by MD simulations, the substrate (modelled from PDB:1JBP) is shown in black. Critical residues R343 and H344, as well as the ATP are highlighted. At high temperature R343 and H344 adapt a conformation that interferes with substrate binding. Right panel: Zoom into the substrate binding groove. The Serine, which becomes phosphorylated, is shown in yellow.

(E) His343 is required for temperature sensitivity. Kinase assay with the CLK1 H343Q mutant as in B (n=3, mean +/- SD, also see Fig. S6A and S6B for gel images and autophosphorylation).

See also Figure S4, S5 and S6.

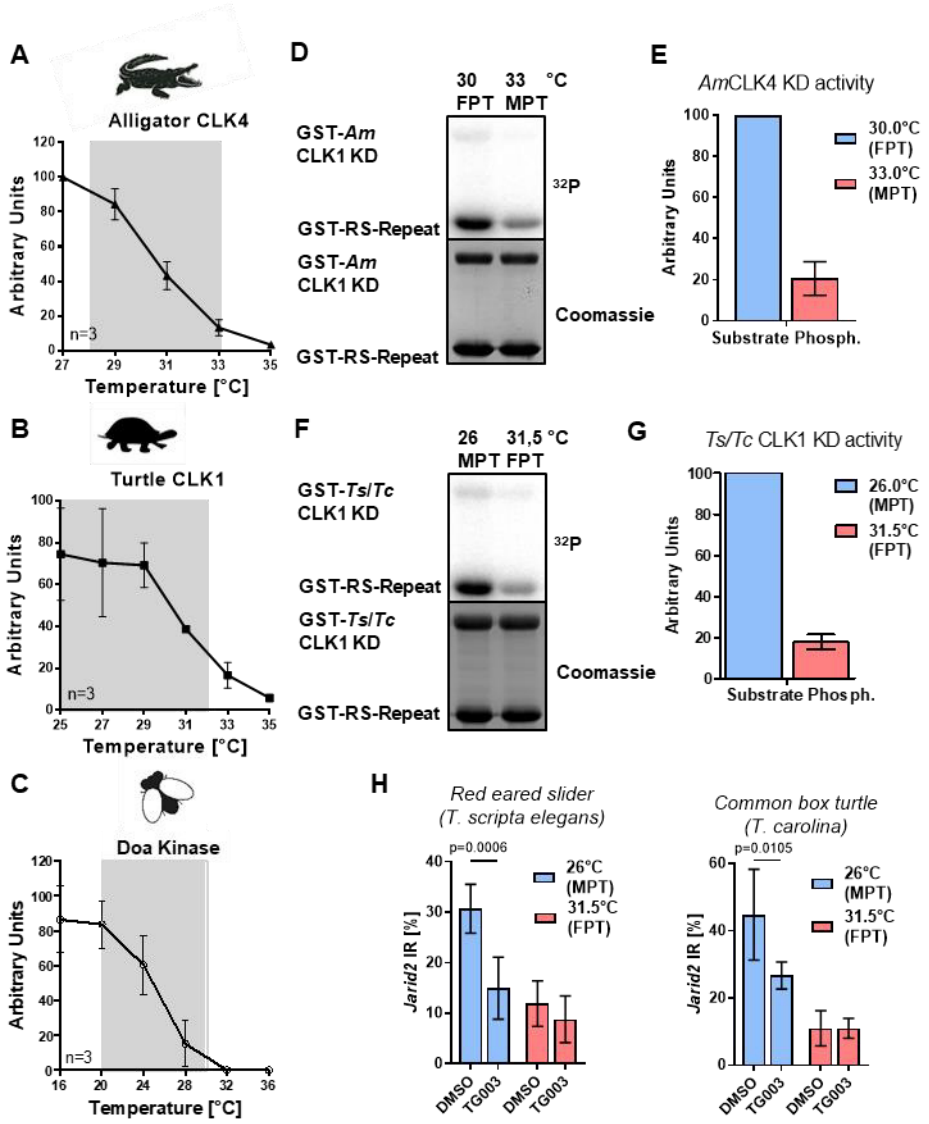

Figure 6. Temperature-dependent activity of poikilothermic CLK homologs is evolutionarily adapted

(A-C) Temperature sensitivity of alligator (A), turtle (B) and fly (C) CLK homologs falls into the range of preferred living temperatures (grey boxes). For gel images see Figures S7A-C.

(D, E) The activity of the alligator CLK4 was investigated at female producing temperature (FPT, 30°C) or male producing temperature (MPT, 33°C). Representative gel is shown in (D), quantifications of substrate phosphorylation in (E, n=3, mean +/- SD).

(F, G) The activity of the turtle CLK1 kinase domain (identical in *T. scripta* and *T. carolina*) was investigated at MPT (26°C) FPT (31.5°C, (Czerwinski et al., 2016)). Representative gel is shown in (F), quantifications of substrate phosphorylation in (G, n=3, mean +/- SD).

(H) Quantification of an intron retention event involved in TSD in two independent turtle cell lines (*T. carolina* and *T. scripta*, cell lines established from heart and spleen tissue, respectively) at MPT or FPT with or without the CLK inhibitor TG003, using RT-qPCR. Data represent mean +/- SD of three independent experiments. Statistical significance was determined by unpaired t-tests. See also Figure S7.

STAR methods

Contact for Reagent and Resource Sharing

Please contact F.H. (florian.heyd@fu-berlin.de) for reagents and resources generated in this study.

Method Details

Cloning and Protein purifications

For overexpression of CLK1-4 f.l. and kinase domain, inserts were amplified from mouse or human cDNA and cloned into the pGEX-6P1 bacterial expression vector. Ts/Tc CLK1f.l., amCLK4 f.l. or kinase domain or *D. melanogaster* darker of apricot (DOA) kinase domain were amplified from turtle RNA or ordered as a synthetic gene (MWG), respectively. A DNA fragment encoding the substrate GST-GRSRSRSRS was cloned into pGEX-6P1 by synthetic oligonucleotides, harboring restriction sites. The expression construct for human SRPK1 was kindly provided by Gourisankar Ghosh (UCSD). For activation segment hybrid mutants, SRPK1 was shuttled into pGEX-6P1. Hybrid mutants and point mutants were generated by 2-step PCRs and conventional cloning. All constructs were validated by sequencing. Constructs were expressed in the *E. coli* strain BL21 (DE3) by induction with 0.2 mM IPTG at 18°C overnight. Cells were lysed by sonication and cleared by centrifugation, followed by GSH-sepharose affinity chromatography. The protein was eluted with 3 column volumes (CVs) of lysis buffer (for CLK1 f.l. and kinase domain: 50 mM HEPES (pH 7.5), 500 mM NaCl, 5% glycerol, 50 mM L-glutamic acid, 50 mM L-arginine; for CLK4 f.l. and kinase domain and the RS containing substrate: 50 mM Tris (pH 8.4), 300 mM NaCl, 1 mM DTT) supplemented with 20 mM gluthathione, followed by dialysis in 3 l lysis Buffer. F.l. proteins and RS-substrate were used after dialysis. Where indicated, CLK1/4 kinase domain was cleaved with Prescission protease, recycled over GSH-beads and further purified by size exclusion chromatography (SD75 10/300). Aliquots were flash frozen in liquid nitrogen and stored at -80°C until use. His-tagged SRPK1 (used in Figure 2) was expressed in *Escherichia coli* BL21 Rosetta 2 cells in ZYM auto-induction medium (Studier, 2005). Cells were lysed by sonication (Sonopuls HD 3100, Bandelin) in buffer (400 mM NaCl, 40 mM Tris/HCl, pH 7.5, 5% (v/v) glycerol, 1 mM DTT) and purified by NiNTA affinity chromatography (Macherey Nagel) and ion exchange chromatography (High Trap QXL, GE Healthcare) according to the manufacturer's protocol, and a final purification was done by size exclusion chromatography (SEC) on Superdex S200 10/300 Increase columns (GE Healthcare) in SEC buffer (200 mM NaCl, 20 mM Tris/HCl, pH 7.5, 5 % (v/v) glycerol, 1 mM DTT). Purified proteins were concentrated to 10-20 mg/ml and flash frozen in liquid nitrogen.

Kinase assay

Reaction mixtures contained the respective kinase, GST-RS substrate, kinase buffer (10X: 700 mM Tris-HCl (pH 7.6), 100 mM MgCl2, 50 mM DTT) and ~2mM [γ-^{32}P]ATP (~0.025 Ci mmol^{-1}) in a final volume of 15 µl. Proteins were affinity purified as described above (for one assay, an OD equivalent of 80 from bacteria culture was used), but not eluted. Bead slurry with bound kinases and substrate were mixed 1:1 and washed 5 times with lysis buffer. After the final wash, 14 µl 1X kinase buffer was added. Reaction mixtures were pre-incubated without [γ-^{32}P]ATP for 20 min at indicated temperatures, then 1µl [γ-^{32}P]ATP (2mM final concentration) was added followed by another 5 min incubation step (for Figure 4B CLKwt and CLKmut 1 hour). For temperature shift experiments, samples were pre-incubated at indicated temperatures for 20 min. After adding [γ-^{32}P]ATP, samples were shifted back to colder temperatures and incubated for 1-60 min. Reactions were stopped by adding 6X SDS-loading dye, samples were heated to 95°C for 5 min and analyzed on a 12% or 15% SDS PAGE. Gels were stained with Coomassie and imaged. Afterwards, they were transferred onto filter papers and dried for 1 hour in a gel drier. The dried gels were exposed to phosphoscreens overnight. Detection was carried out with a Phosphoimager and ImageQuant TL software.

Cell culture, RNA extraction, RT-PCRs, Transfection and Western blot

HEK293T cells were cultured in DMEM High glucose (Biowest) containing 10% FCS (Biochrom) and 1% Penicillin/Streptomycin (Biowest). Temperature shifts and RT-PCRs were performed as previously described (Preussner et al., 2017). Briefly, RNA was extracted using RNATri (Bio&Sell) and 1µg RNA was used in a gene-specific RT-reaction. Low-cycle PCR with a ^{32}P-labeled forward primer was performed, products were separated by denaturing PAGE and quantified using a Phosphoimager and ImageQuantTL software. Results of endogenous AS represent the mean value of at least three independent experiments with the according SD. *Trachemys scripta elegans* and *Terrapene carolina* cell lines were obtained from the Friedrich-Loeffler-Institut (Greifswald, Germany). Cell culture was performed at 26°C in a humidified atmosphere with 2.5% CO_2. *Trachemys scripta elegans* cell line (derived from spleen of a juvenile) was cultured w/o antibiotics in a 1:1 mixture of Ham´s F-12 Nutrient Mix (Thermo Scientific) and Iscove´s Modified Dulbecco´s Medium (Thermo Scientific) with 10% (v/v) fetal bovine serum. The *Terrapene carolina* cell line (explant culture from heart) was cultured in DMEM High glucose (Biowest). For temperature shift experiments cells were either kept at 26°C or 31.5°C for 4h.

For qRT-PCR, gene-specific primers for *Gapdh* and a reverse primer within intron 15 and a reverse primer within exon 16 of *Jarid2* (for intron retention in turtle cell lines) were combined in one RT reaction. qPCR was then performed in 96 well format using the ABsolute QPCR SYBR Green Mix (Thermo Fisher) on a Stratagene Mx3000P instrument. qPCRs were performed in technical duplicates, mean values were used to normalize expression to mRNA

of *gapdh* (ΔCT) and Δ(ΔCT)s were calculated for different conditions. For intron retention mean values of intron products were normalized to products of spliced mRNA using primers in flanking exons. Significance was calculated by Student's unpaired t-test and significance is indicated: *p<0.05, **p<0.01, ***p<0.001. Primer sequences are available upon request.

For overexpression experiments, $1.5x10^5$ HEK293T cells in a 12 well plate were transfected with 0.8 µg expression vectors for Flag-tagged CLK1 and CLK1 H343Q. 48 hours after transfection, cells were incubated at 39°C for 12 hours. Samples were then incubated for 6 hours at either 39°C or 35°C and RNA was prepared and analyzed as above.

SDS-PAGE and immunoblotting were performed according to standard protocols. Briefly, to extract proteins, cells were washed with PBS and lysed with 1x RIPA buffer (10 mM Tris (pH 8.0), 1% NP40, 4 mM EDTA, 200 mM NaCl, 5 mg/ml sodium deoxycholate) containing protease and phosphatase inhibitors. Phosphorylation of SR-Proteins was analyzed by SDS PAGE, blotting to a PVDF membrane, and using the Anti-Phosphoepitope SR protein antibody 1H4 (Merck, MABE50) and against GAPDH (GT239, GeneTex) as loading control. Expression of Flag-tagged CLK1wt and CLK1H343Q was analyzed by SDS PAGE, blotting to a PVDF membrane, and using antibodies against the Flag-Tag (Cell Signaling, 2368) and against GAPDH (GT239, GeneTex) as loading control.

Investigation of AS and gene expression by RNA sequencing

To identify CLK-dependent and temperature-regulated AS in human cells, confluent HEK293 cells were incubated at 39°C for 12 hours. Cells were then treated with 50µM TG003 (or DMSO as solvent control) and after further 30 minutes at 39°C, samples were incubated for 6 hours at either 39°C or 35°C. RNA was extracted using RNATri (Bio&Sell) followed by DNaseI digestion. Sequencing libraries were analyzed on a HiSeq4000 instrument yielding ~50 million paired-end 150-bp reads per replicate and condition. Reads were aligned to the hg38 genome and splicing patterns as well as transcripts per million (tpm) values were determined using Whippet version 0.11 (Sterne-Weiler et al., 2018). Events with a minimum PSI difference of 0.15 and a probability above 0.9 between the two temperatures in DMSO control were further investigated. For gene expression, genes were considered temperature dependent in DMSO when first tpm values are > 5 in all 12 samples, second the ∆tpm between the three DMSO35 and DMSO39 is > 5 (with the same directionality and a fold change of at least 1.2), and finally the mean fold-change is >1.3 between DMSO35 and DMSO39. Downstream analyses were performed using Python2 (numpy (numerical operations, (Walt et al., 2011)), Matplotlib (data visualization, (Hunter, 2007)) or GraphPad Prism 7.05.

Generation of CRISPR-Cas9 edited cells and analysis of Cirbp expression

For genome-engineering in Hek293T cells, sequences flanking exon 7b and 8 of *Cirbp* were analyzed for sgRNA candidates *in silico* using the Benchling tool. Upstream and downstream a pair of oligonucleotides for the highest ranked candidate sgRNA (Ran et al., 2013) was synthesized and subcloned into the PX459 vector (kindly provided by Stefan Mundlos). sgRNA sequences: upstream: 5'-ctagcctgagaccttcctag; downstream: 5'-cgcacgagtaggacccgaca. Cells were transfected in 6-well plates using Rotifect following the manufacturer's protocol. 48 hours after transfection, the transfected cells were selected with 1 µg/ml puromycin and clonal cell lines were isolated by dilution (Ran et al., 2013). Genomic DNA was extracted using DNA extraction buffer (200 mM Tris pH 8.3, 500 mM KCl, 5 mM MgCl2, 0.1% gelatin in H_2O) and a PCR was performed to confirm the exon knockout on DNA level. In promising clones the exon knockout was additionally confirmed after RNA isolation by splicing sensitive PCR using one forward primer in exon 6 and two reverse primers in exon 7a or exon 7b, respectively *Cirbp* expression levels were investigated by RT-qPCR as described above (qPCR primers detect both the E7a and E7b isoforms simultaneously).

To analyze *Cirbp* AS and gene expression in mice, we prepared primary hepatocytes from adult mice and incubated them at the indicated temperatures and additionally re-investigated RNA from livers from young mice from different ambient temperatures, as previously described (Preussner et al., 2017). Due to primer design the exon 7b product is larger in human and smaller in mouse than the 7a product.

To investigate *Cirbp* AS in RNA-Seq data we used the –sam tag of Whippet version 0.11 (Sterne-Weiler et al., 2018) to create sam files. These were transferred to bam files, sorted and indexed using samtools. Sashimi blots were created using IGV genome browser, PSI values were manually determined using the junction reads to exons 7a and 7b. Conservation scores across 100 vertebrates are from the '100 vertebrates Basewise Conservation by PhyloP' track from the UCSC Genome browser.

Molecular Dynamics Simulation

The SRPK1 protein was modeled based on crystal structure 1WBP(Ngo et al., 2005). A large loop of residues 238-476 missing in the crystal structure was not modeled. Instead, the first and last resolved residue bordering this loop, 237 and 477, respectively, were capped by neutral termini and positionally restrained. The peptide substrate present in the crystal structure was removed and the ADP molecule was changed to ATP. The missing coordinates of the γ-phosphate and the Mg^{2+} ion were taken from the crystal structure of another kinase-ATP-Mg^{2+} complex, 3OS3 (Isshiki et al., 2011). The kinase domain of the CLK1 protein was modeled based on the crystal structure 1Z57 (Bullock et al., 2009). Residues 307 to 310 and 483 to 494 missing in the crystal structure were modeled by using the Modeller9.19 tool kit (Sali and Blundell, 1993). The 10Z-Hymenialdisine inhibitor bound in the crystal structure was replaced by ATP and a Mg^{2+} ion taken from, and similarly placed as in our SRPK1 model (after

superimposing the active sites of the two proteins). All titratable groups were kept in their standard protonation states. The proteins, ATP, and Mg^{2+} ion were described by the charmm36 force field (Best et al., 2012; Mallajosyula et al., 2012). The protein-ATP-Mg^{2+} models were immersed in a periodic cubic box (side length of 11 nm) with TIP3P water (Jorgensen et al., 1983) (~130,000 atoms in total). Van der Waals and short-range electrostatic interactions were truncated after 1.4 nm, long-range electrostatic interactions were treated with the particle mesh Ewald method and a 0.16 nm Fourier grid spacing. After an initial minimization, a first equilibration at 300 K for 1 ns with positional restraints on all heavy atoms was performed, followed by another round of equilibrations, again at 300 K and for 1 ns, with positional restraints only on the ATP molecule and the Mg^{2+} ion. After equilibration, three individual 500-ns production simulations were performed for each model system, starting with different initial velocities, at either 293K or 313K. All covalent bonds to hydrogen atoms were constrained by the LINCS algorithm (Hess et al., 2008), allowing an integration time step of 2 fs. The V-rescale thermostat (Bussi et al., 2007) was employed to control temperature at 293K or 313K. All simulations were performed with the gromacs package, version 4.6.7 (Hess, 2008; Van Der Spoel et al., 2005). Analyses were carried out with tools provided by the gromacs package. Only the last 400 ns of each simulation were analyzed, considering the first 100 ns as further equilibration time. Values reported are averages over the three individual simulations of each model system and errors are estimated as SDs. Graphics were prepared by using VMD (Humphrey et al., 1996) and the python library matplotlib (Hunter, 2007). The kinase substrate was modelled into the modelled CLK structures from 20°C and 40°C in PyMOL using the crystal structure of the catalytic subunit of the cAMP-dependent protein kinase complexed with a substrate peptide (PDB: 1JBP) for the position of the substrate.

The H344A mutant was generated from the equilibrated wild type structures by in silico replacing H344 with alanine. After re-equilibration at 313K, the mutant model was subjected to one 200 ns long production run with the same settings as for the simulations of the wild-type systems.

CD-spectroscopy

CD-spectroscopy was performed with 0.015 mg/ml hCLK1 kinase domain in kinase buffer as used for *in vitro* kinase assays (see kinase assay) in a JASCO J-715 Spectropolarimeter. CD spectra were recorded from 200 to 250 nm at 25°C, 34°C and 38°C after an initial incubation at the given temperatures for 5 min. For each temperature 3 spectra were recorded and averaged.

Quantification and statistical analysis

All data are represented as mean +/- standard deviation (SD). Figure legends contain information on repetitions and statistical tests used.

Data and Software Availability

Full gel images and raw data files will be deposited as Mendeley Data.

Supplemental information

Supplementary Figures S1-S7
Table S1. Skipped Exon Events
Table S2. Intron Retention Events
Table S3. Gene Expression
Supplemental movie 1 and 2

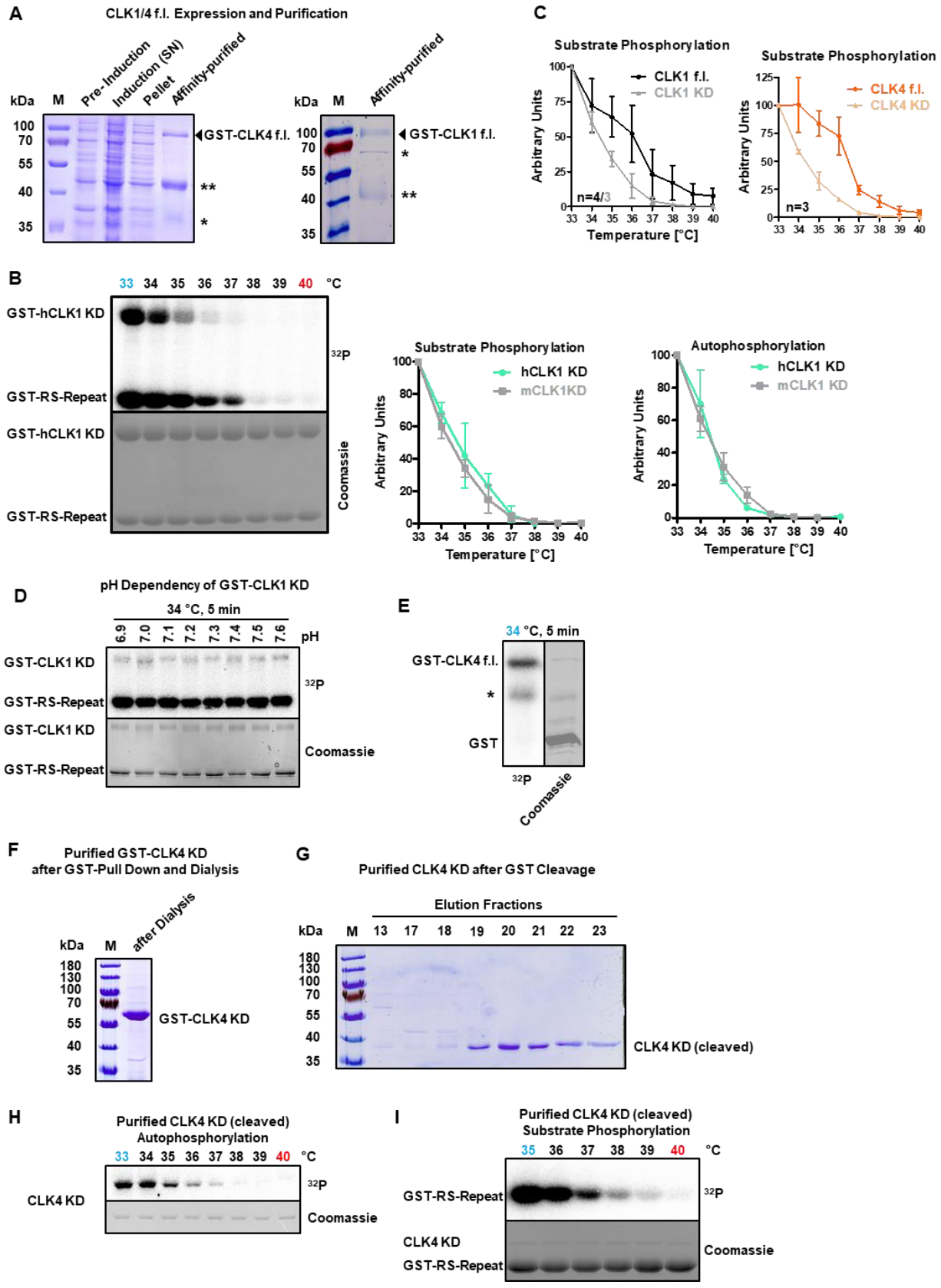

Figure legend on the next page

Figure S1. The activity of the CLK1/4 kinase domain is controlled by changes in the physiologically relevant temperature range

(A) Purification of f.l. GST-CLK1/4. Coomassie-stained gels after purification are shown. Asterisks indicate degradation products. ** likely represents an N-terminally extended kinase domain (KD), resulting from loss of the GST-tag with most of the unstructured N-terminus.
(B) Human (h) and mouse (m) CLK1 (91% identity, CLK4s are 97% identical) show identical temperature response curves. For hCLK1 KD a representative gel is shown. On the right, quantifications of substrate and autophosphorylation relative to mCLK1 kinase domain (from Figure 1) are shown (n=3, mean +/- SD).
(C) The CLK1/4 N-terminus shifts the temperature optimum. Comparison of the temperature response profiles of the f.l. kinase or the kinase domain lacking the N-terminus for CLK1 (left) and CLK4 (right). Data from Figure 1.
(D) CLK1/4 kinase activity is not pH-dependent. To rule out secondary effects of temperature-mediated differences in pH, we confirmed lack of pH sensitivity of CLK1 kinase domain activity at 34°C in the pH range between 6.9 and 7.6.
(E) CLK4 specifically phosphorylates RS peptides. To rule out unspecific phosphorylation of GST, we incubated CLK4 f.l. kinase with a large excess of GST. In contrast to autophosphorylation, we did not observe any phosphorylation of GST alone. The asterisk indicates a degradation product of CLK4 (see above), which is also phosphorylated.
(F) Coomassie-stained gel showing essentially pure GST-CLK4 kinase domain (KD).
(G) Coomassie-stained gel showing purified CLK4 kinase domain after cleavage of GST.
(H, I) Purified CLK4 kinase domain – after cleavage of the GST-tag – shows temperature-dependent autophosphorylation (H) and substrate phosphorylation (I). Due to the similar size and stronger signal for substrate phosphorylation, autophosphorylation is not visible in (I). These controls validate the use of GST-tagged proteins for in vitro kinase assays.

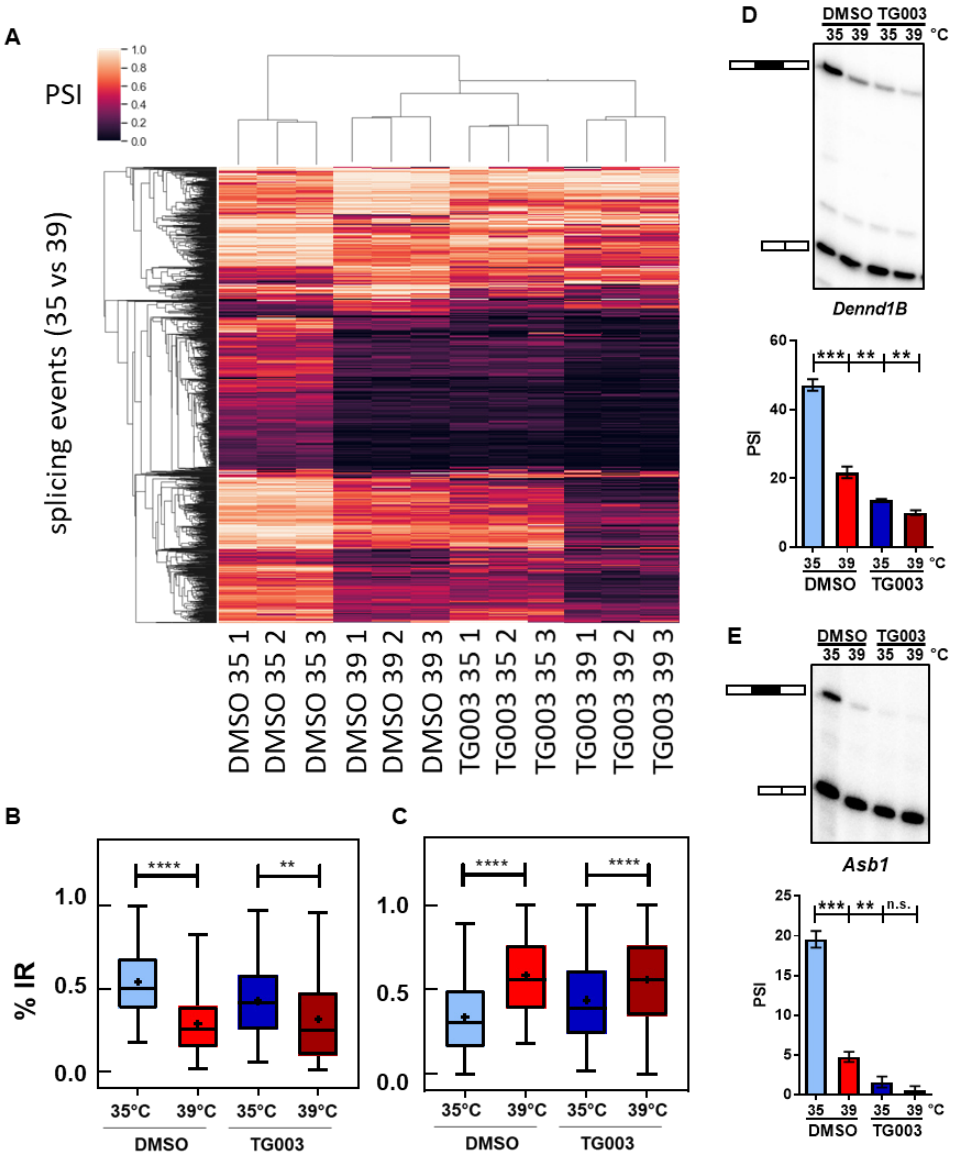

Figure S2. CLK activity controls body temperature dependent SR protein phosphorylation and AS in vivo

(A) Unsupervised clustering of percent spliced in values for temperature-dependent exons presented in Figure 3C. Note the high similarity of the triplicate samples and the clear clustering of DMSO 39°C and TG003 35°C samples.

(B, C) Box-Whisker-Plots of intron retention (IR) events with higher IR at 35°C (B, n=101) or at 39°C (C, n=531). Note the reduced ΔPSI in TG003-treated samples, where the 35°C sample shows a reduced response when compared with the DMSO control. The line represents the median PSI, circle represents mean PSI. Statistical significance was determined by 1-way ANOVA (Tukey's multiple comparisons test, **p<0.01, ****p<1x10^{-15}).

(D-E) Representative gels and quantifications for additional splicing targets, *Dennd1b* (D) and *Asb1* (E). Statistical significance was determined by unpaired t-test.

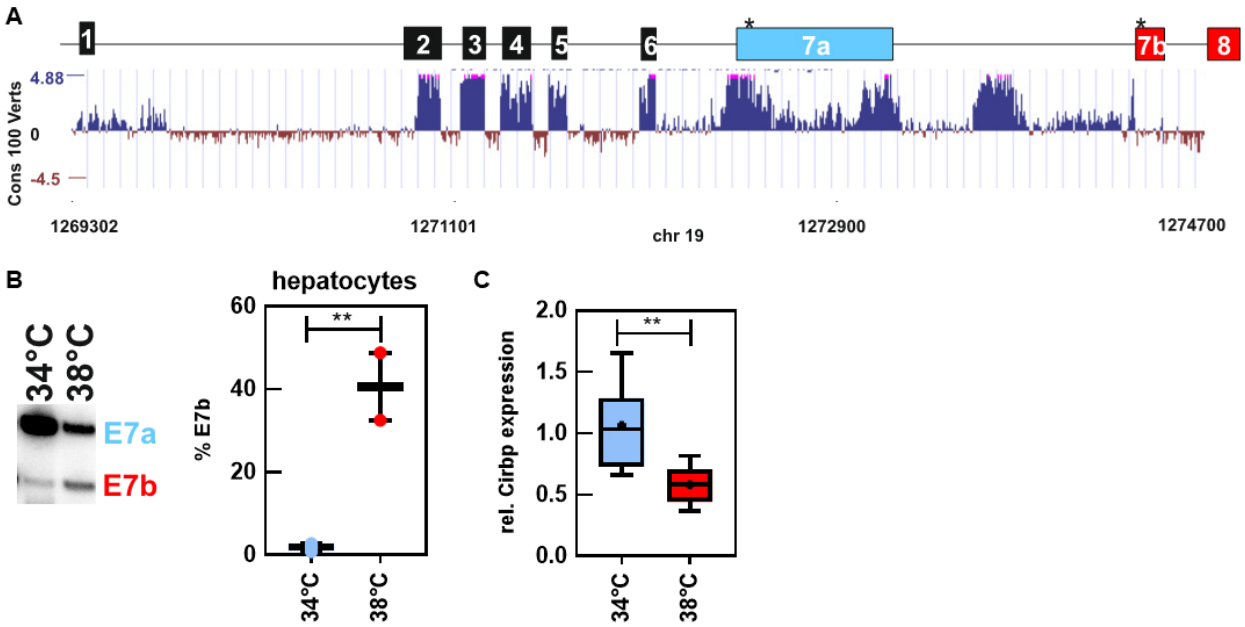

Figure S3. CLK activity controls body temperature dependent gene expression

(A) Evolutionary conservation across the whole *Cirbp* gene locus as shown in Figure 4D. Top: Exon/Intron structure of the whole *Cirbp* pre-mRNA. Exons are depicted by boxes, introns by lines, the asterisks indicate stop codons. Below the Basewise comparison across 100 vertebrates by PhyloP track from the UCSC genome browser is shown. Values above zero show high conservation. Note that sequences downstream of exon 7a and at the 3' splice site of exon7b are as conserved as exonic protein coding sequences.

(B, C) *Cirbp* splicing (B) and gene expression (C) in mouse hepatocytes. Purified primary hepatocytes were incubated at 34 or 38°C. After 12 hours the temperature was switched and after further 8 hours *Cirbp* AS was investigated by radioactive RT-PCR (B). A representative gel is shown on the left and quantification of E7b inclusion is shown on the right (n>2, unpaired t-test derived p-value **p<0.01). Gene expression was analyzed by qRT-PCR and is shown normalized to *Gapdh* (n=8, unpaired t-test derived p-value **p<0.01).

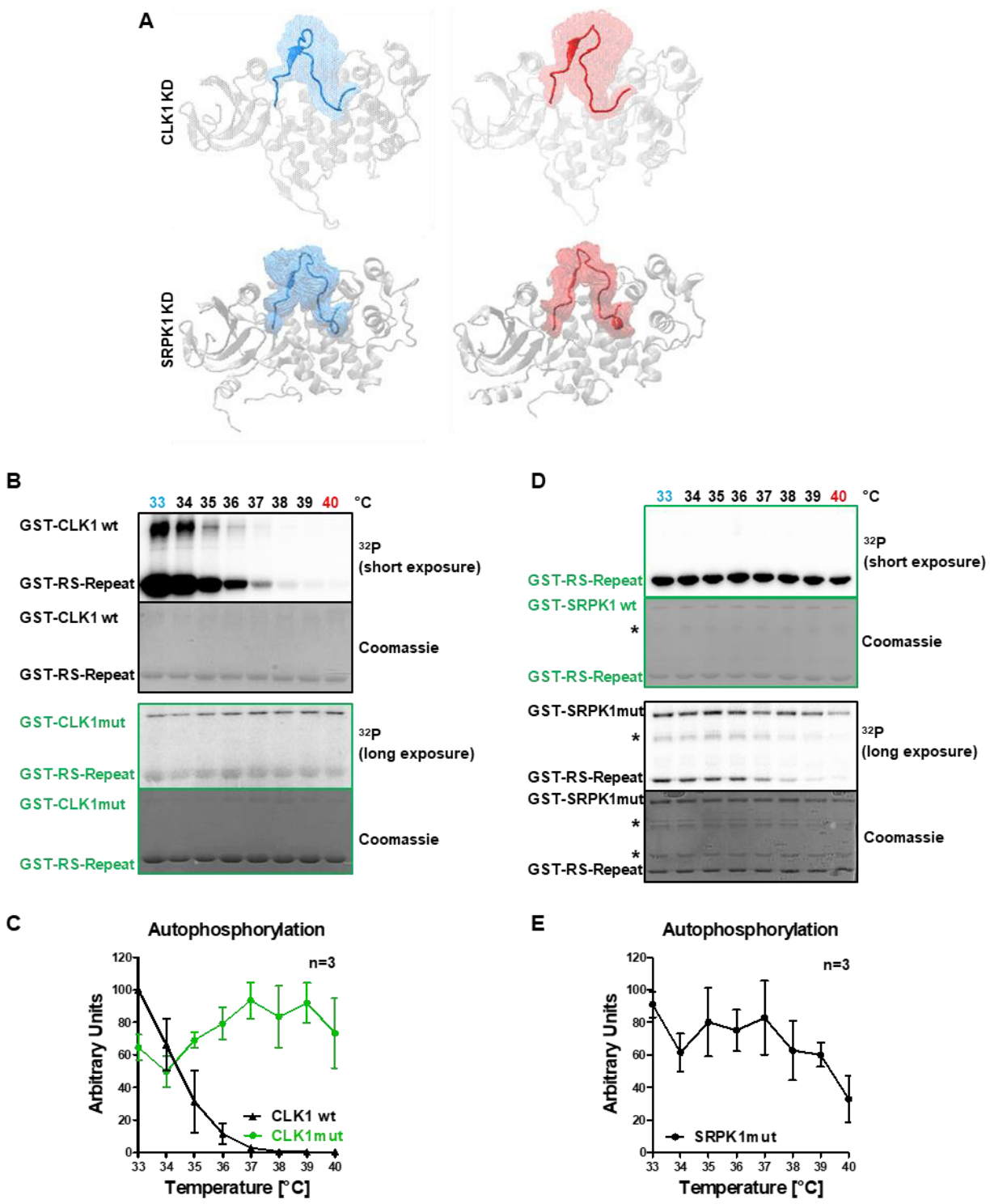

Figure S4. Temperature-sensitivity of CLK activity is mediated through the activation segment

(A) Temperature-dependent molecular dynamics (MD) simulations were performed with the kinase domains (KDs) of CLK1 (top, PDB: 1Z57) and SRPK1 (bottom, PDB: 1WBP) at 20°C (blue) and at 40°C (red). These temperatures represent maximal and completely lost activity, see Figure 2A. No global structural differences are visible comparing 20°C and 40°C. The shaded areas represent the volumes in which the activation segments were observed during the MD simulations. Note that the CLK1 activation segment (top) shows higher flexibility (larger shaded area) at 40°C.

(B, C) Introducing the SRPK1 activation segment into the CLK1 kinase domain abolishes temperature sensitivity. CLK1 kinase domain wt (black) and a mutant (mut) containing the SRPK1 activation segment (green) were investigated as in Figure 1B (longer incubation time, see methods). Representative gel images are shown in (B). Quantification of substrate phosphorylation is shown in Figure 5B. The quantification in (C) illustrates that the mutant with the SRPK1 activation segment in the CLK1 kinase domain lost temperature-sensitive autophosphorylation (n=3, mean +/- SD).
(D, E) Introducing the CLK1 activation segment into SRPK1 creates temperature sensitivity. SRPK1 wt (green) and a mutant containing the CLK1/4 activation segment (black) were investigated as in Figure 1B. The asterisks indicate SRPK1 degradation products. Representative gel images are shown in (D). Quantification of substrate phosphorylation is shown in Figure 5B. The quantification in (E) illustrates that the SRPK mutant bearing the CLK activation segment gained temperature-sensitive autophosphorylation (n=3, mean +/- SD). Due to lower kinase activity of the mutant kinases a longer exposure of the gels is shown.

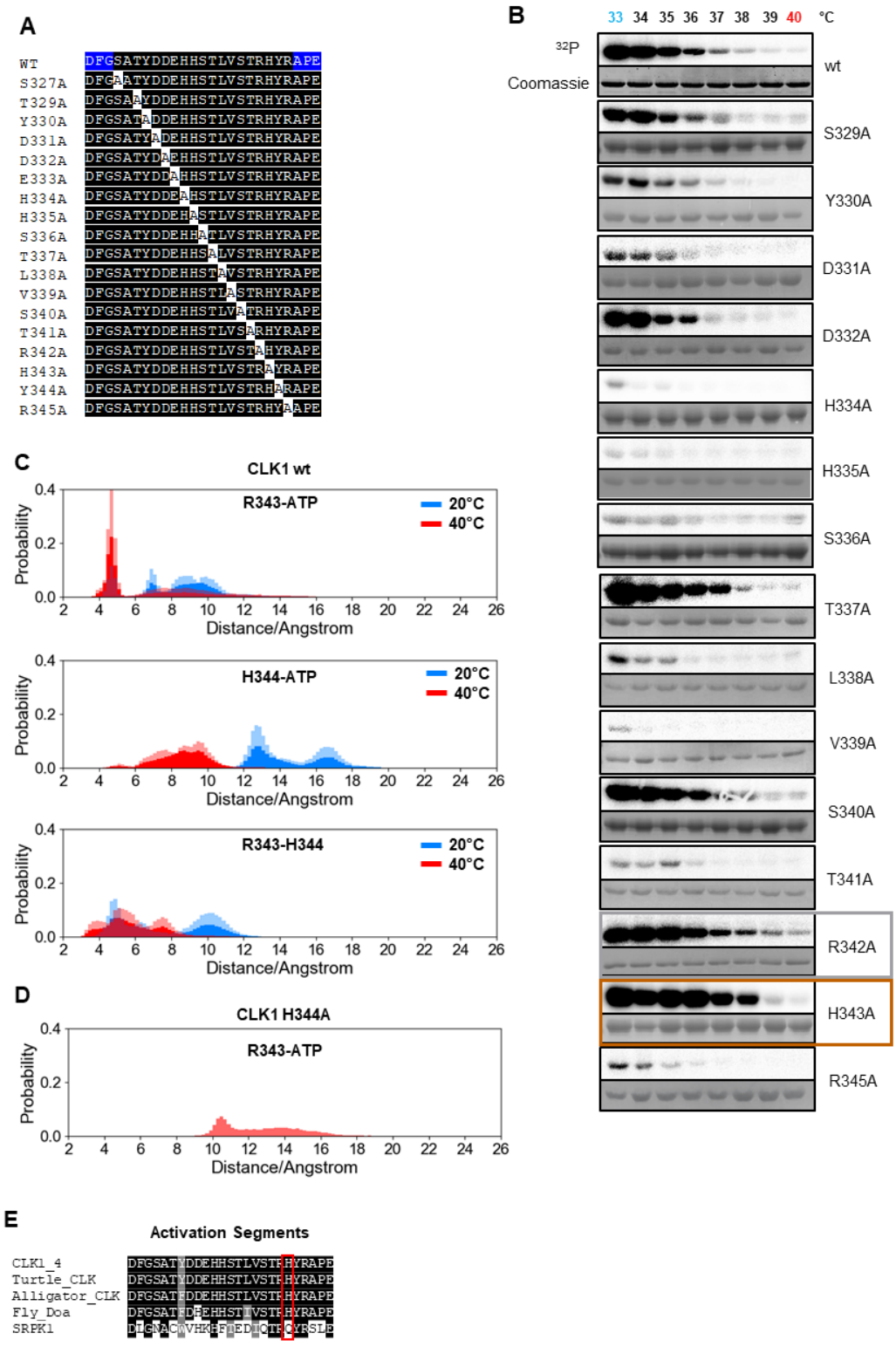

Figure S5. Temperature-sensitivity of CLK activity is mediated through specific residues in the activation segment

(A) Schematics of the Alanine Scan of the CLK1 activation segment. Blue residues were not mutated. The Alanine scan has been performed with the mouse CLK1 kinase domain. Numbers of residues are shifted -1 compared to the human variant.

(B) In vitro kinase assay with CLK1 wt and mutants. Mutants S327A, E333A and Y344A were not expressed. All variants were purified from bacteria and coupled to glutathione beads, incubated with

GST-RS and 32P-γ-ATP at the indicated temperatures. After SDS-PAGE, phosphorylation was investigated by autoradiography (for each variant top, ^{32}P), equal loading was confirmed by Coomassie staining (bottom). For simplification only substrate phosphorylation of each variant is shown. Variants shifting the temperature optimum towards a higher temperature are boxed grey and brown, respectively.
(C) MD simulations confirm residue crucial for setting the inactivation temperature. Depicted are the distances between human CLK1 activation segment residue R343 (guanidino group) and ATP (top), H344 and ATP (middle) and between R343 and H344 as observed in MD simulations at 20°C and 40°C. Distances and probabilities are shown as mean +/- SD from three simulations.
(D) Distances between R343 and ATP in the CLK1 H344A mutant were investigated by MD simulations. At 40°C we do not observe close R343-ATP proximity as in the wt, suggesting that the H343 conformational change is instrumental to reposition R343 at higher temperature in the wt kinase.
(E) Alignment of activation segments of temperature sensitive CLK1/4 homologs and temperature insensitive SRPK1. Highlighted is CLK His343 (red box).

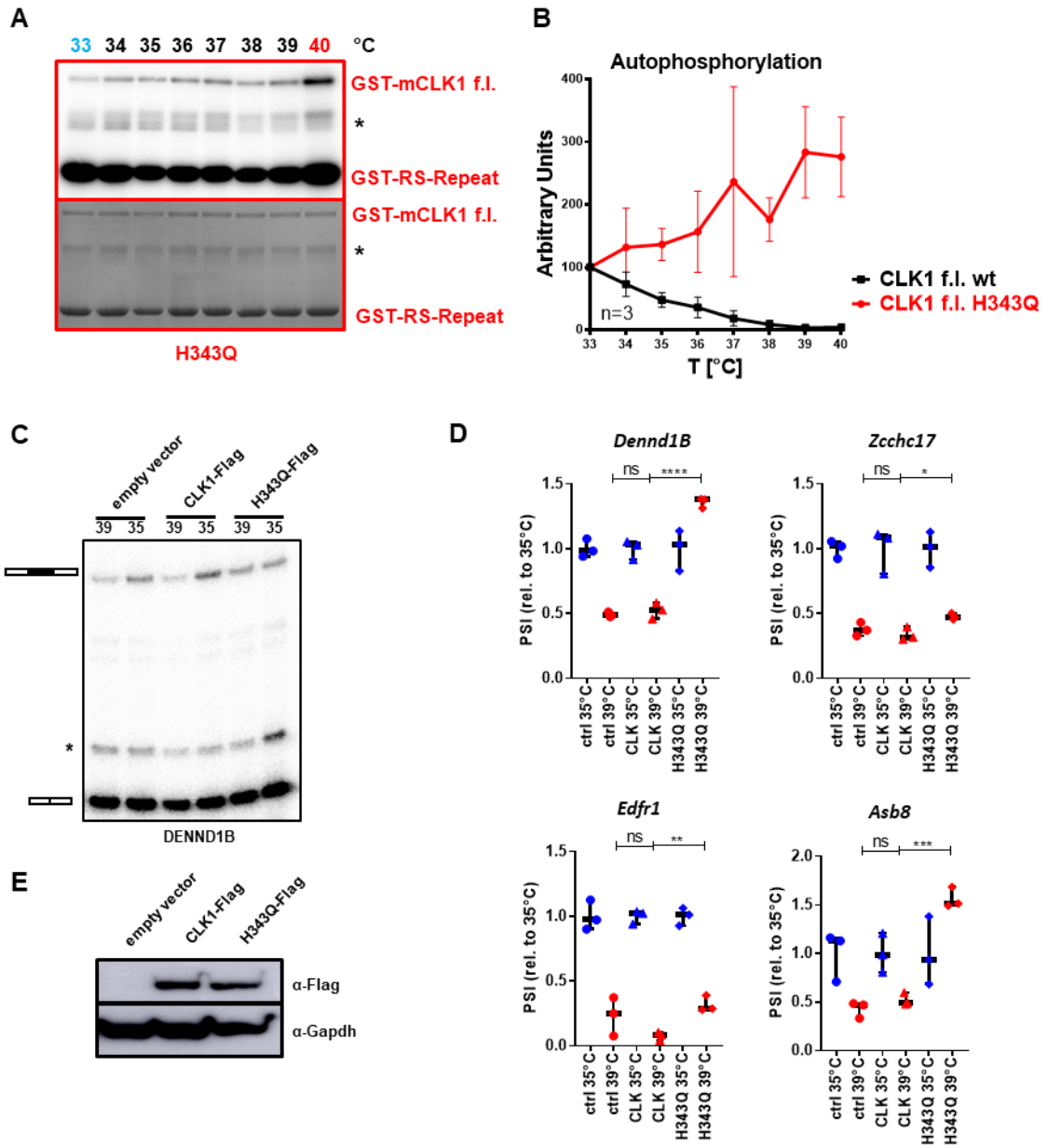

Figure S6. A single amino acid substitution renders CLK1 activity temperature insensitive

(A) *In vitro* kinase assay with f.l. CLK1 H343Q. The mutant kinase was purified from bacteria and coupled to glutathione beads, incubated with GST-RS and ^{32}P-γ-ATP at the indicated physiological temperatures. After SDS-PAGE, phosphorylation was investigated by autoradiography (top, ^{32}P), equal loading was confirmed by Coomassie staining (bottom). The asterisks likely represent extended kinase domains, which lost the GST units due to cleavage in the unstructured N-termini by residual proteases and which are also not phosphorylated in a temperature-dependent manner.

(B) Quantification of auto-phosphorylation from experiments as in (A) relative to 33°C (n=3). Quantification of f.l. CLK1 wt from Figure 1. Data represent means +/- standard deviations (SD).

(C, D) Representative gel and quantification of splicing sensitive, radioactive RT-PCRs for targets shown in Figure 3E-F and S2D-E, in control cells, or in cells overexpressing CLK1-Flag (CLK1) or CLK1H343Q-Flag (H343Q). Shown is the fold change (PSI) relative to 35°C. Note that *Dennd1B* and *Asb8* lose warm-induced exon skipping upon H343Q overexpression. *Zcchc17* and *Edfr1* show a similar trend. Statistical significance was determined by unpaired t-tests.

(E) Western Blot confirming similar levels of CLK1-Flag and H343Q-Flag overexpression, GAPDH served as loading control.

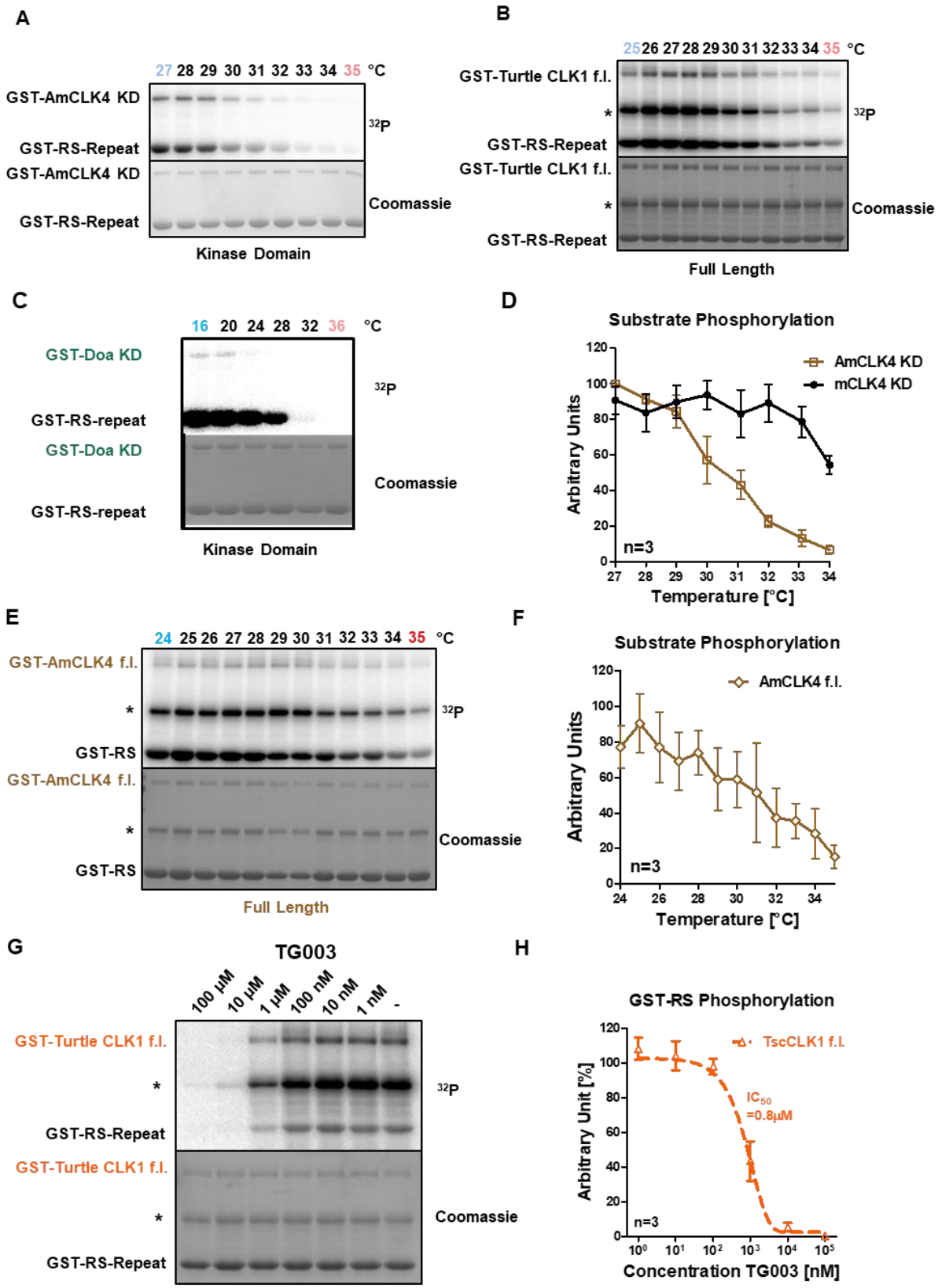

Figure S7. Temperature-dependent activity of poikilothermic CLK homologs is evolutionarily adapted

(A-C) Representative gels of alligator (A), turtle (B) and fly (C) CLK homologs as in Figure 6A-C.

(D) Comparison of mouse (black) and alligator (brown) CLK4 kinase domain (KD) in the temperature range of alligator sex determination (n=3, mean +/- SD).

(E, F) Temperature-dependent activity of full length alligator CLK4 in the sex determining temperature range. Quantification of f.l. alligator CLK4 activity as in (E). Data represent mean +/- SD (n=3).
(G, H) f.l. turtle CLK1 is inhibited by the CLK inhibitor TG003 in a concentration range comparable to mammalian CLKs. Data in (H) represents mean +/- SD (n=3).